THE UNIVERSITY OF QUEENSLAND

Simulation of Acoustic Pressure Field
Generated by Ultrasonic Transducer

Student Name: Muhammad Aliff, AZIZI

Course Code: MECH4501

Supervisor: Associate Professor Martin Veidt

Submission date: 30 May 2019

Faculty of Engineering, Architecture and Information Technology

ABSTRACT

Simulation which incorporates numerical method is practical in investigating the effect of ultrasonic excitations on the acoustic pressure and flow patterns of fluid with arbitrary settings as it can produce reliable results in a relatively short time even for complex cases. This thesis aims to develop efficient simulation of acoustic pressure field generated by ultrasonic transducer using ANSYS Workbench to obtain accurate data of the resulting flow and pressure fields for harmonic ultrasonic excitations. Simulation methodology is developed from reviewing literatures and it is used as a basis to simulate and replicate results from two distinct literatures for validation purpose. An arbitrary simple case is simulated to gauge the effectiveness of simulation made based on the established simulation methodology in investigating acoustic pressure field. Through these processes, the following are concluded:

- Computation effort increases with higher number of degrees of freedom (DOF) of nodes involved in solving process.
- Mesh quality should be decent, and the element size should follow the meshing guidelines to ensure accurate results.
- Appropriate assumption of boundary conditions of experimental setup is important to ensure feasibility of simulation results.
- Simple simulation model is better than complex model in both result accuracy and computation time when there is insufficient information on the case to be simulated.
- Model reduction via plane/axis of symmetry and use of 2D/2.5D models should be prioritised for fast and accurate simulation.

ACKNOWLEDGEMENT

Firstly, I would like to sincerely thank my thesis supervisor, Associate Professor Martin Veidt, for his constant support and guidance throughout the thesis period. I consider myself very fortunate to be under the supervision of such helpful and considerate person.

Next, I am greatly thankful to Mr. Allan Duong, who had assisted me and other students by swiftly rectifying software issues encountered during the thesis period. Without his help, the thesis outcome would be limited.

Lastly, I express my deepest gratitude to my friends and family for their moral supports and advices that gave me the extra push I need to complete the thesis.

Table of Contents

ABSTRACT ... i

ACKNOWLEDGEMENT ... ii

1 INTRODUCTION ... 1

1.1 Background ... 1

1.2 Aim ... 2

1.3 Scope ... 2

2 BACKGROUND THEORY AND LITERATURE REVIEW ... 3

2.1 Background Theory ... 3

2.1.1 Radiation of Ultrasonic Transducer ... 3

2.1.2 Effects of Ultrasonic Waves on Fluid ... 4

2.1.2.1 Acoustic Streaming ... 4

2.1.2.2 Ultrasonic Cavitation ... 5

2.1.3 Acoustic Impedance ... 6

2.2 Literature Review ... 7

2.2.1 Elements for Acoustic Analysis ... 7

2.2.2 Wave Absorption Boundary ... 9

2.2.2.1 Absorbing Boundary Condition (ABC) ... 9

2.2.2.2 Radiation Boundary ... 10

2.2.2.3 Artificially Matched Layers ... 11

2.2.3 Fluid-Structure Interaction (FSI) ... 12

2.2.4 Meshing in Acoustic Analysis ... 15

2.2.5 Model Reduction of Symmetrical Model ... 16

2.2.6 Comparison of 3D Model and 2D Model ... 18

3 SIMULATION METHODOLOGY ... 20

3.1 Methodology Overview ... 20

3.2 Material Identification ... 20

3.3 Model Design ... 22

3.4 Model Reduction 24

3.5 Meshing 26

3.6 Physics Region, Coupling and Boundary Condition 28

3.7 Excitation Source 29

3.8 Solve Model 30

3.9 Post-Processing 31

4 TEST CASE 1: RADIATION OF BAFFLED PISTON 32

4.1 Method and Comparison 33

4.1.1 2D Simulation Methods 33

4.1.2 2.5D Simulation Methods 36

4.2 Results 39

4.2.1 Initial Results 39

4.2.1.1 2D Simulation 39

4.2.1.2 2.5D Simulation 40

4.2.2 Improvements 41

4.2.2.1 Uniform Surface Mesh for 2D Model 41

4.2.2.2 Fixed Support for 2.5D Piezoelectric Piston 43

4.2.2.3 Scaled Excitation Input Value for All 2.5D Models 44

4.2.3 Data Tabulation and Plotting 46

4.3 Discussion and Recommendation 51

5 TEST CASE 2: ULTRASONIC CLEANING TANK 53

5.1 Method and Comparison 54

5.2 Results 59

5.2.1 Initial Results 59

5.2.2 Improvements 60

5.2.2.1 Fixed Support on Edges of Plate 60

5.2.2.2 Reduce Element Size 61

5.2.2.3 Transducer Model and Material Switch 61

5.2.2.4 Cylindrical Support on Lateral Surface of Transducer 64
5.2.2.5 Model Reduction via Plane of Symmetry 64
5.2.3 Data Tabulation and Plotting 67
5.2.3.1 28kHZ Ultrasonic Cleaning Tank Model 67
5.2.3.2 48kHZ Ultrasonic Cleaning Tank Model 72
5.3 Discussion and Recommendation 76
6 CASE STUDY: EFFECT OF PLATE TO ACOUSTIC PRESSURE FIELD 77
6.1 Model Description 78
6.2 Analysis Procedure 80
6.3 Results 81
6.3.1 Near Field Radiation 81
6.3.2 Default Plate Size 82
6.3.3 Plate with Adjusted Length 83
6.3.4 Plate with Adjusted Thickness 87
6.4 Discussion and Recommendation 91
7 CONCLUSION AND RECOMMENDATION 93
7.1 Conclusion 93
7.2 Recommendation for Future Work 94
REFERENCES 95
APPENDIX 99

1 INTRODUCTION

1.1 Background

An ultrasonic transducer is a device that converts electrical energy into mechanical energy or vice versa usually via a piezoelectric material integrated to it [1]. This device can be used to generate or detect ultrasound and it is respectively referred to as a projector or receive. To produce and receive ultrasound effectively, the ultrasonic transducer is designed based on the intended medium of use and frequency range [1]. When designed for underwater use, an ultrasound projector is called immersion transducer and an ultrasound receiver is called hydrophone. These underwater ultrasonic transducers have been adjusted to have good impedance match with water for better sound energy output (into the water) and sound input sensitivity [2].

In investigating the effect of ultrasonic excitations on the acoustic pressure and flow patterns of fluid with arbitrary settings to obtain reliable quantitative data, doing experiments for each arbitrary case is costly and can be impractical. Computer simulation which incorporates numerical method is a more practical approach in achieving this as it can produce results in a relatively short time even for complex cases. With the correct simulation method and assumptions, the complex cases can be simplified further to reduce computation time while still maintaining results accuracy.

This thesis is concerned with the simulation of acoustic pressure field generated by ultrasonic transducer using ANSYS Workbench and validation of simulation methodology by reproducing results from chosen literatures. The simulation methodology is developed from reviewing related literatures aimed to identify method that produces reliable results while taking computation time into consideration. It is hoped that the methodology and findings from this thesis contributes for a more profound simulation in researches involving relatively simple system or even more complicated ones such as ultrasonic-guided drug delivery.

1.2 Aim

The aim of this thesis is to develop efficient simulation of acoustic pressure field generated by ultrasonic transducers using ANSYS Workbench to obtain accurate data of the resulting flow and pressure fields for steady state ultrasonic excitations. The preferred simulation methodology is ones that incorporates techniques that produces results faster than other techniques without affecting the results accuracy. To achieve this, the following sub-goals are established:

- Have adequate understanding of the working principle of an ultrasonic transducer and the effect of its excitation towards fluid.
- Identify essential boundary conditions for modelling an acoustic problem specific to cases that involves ultrasonic excitations.
- Identify and compare simulation techniques to find ones that produces fast and accurate results.
- Establish simulation methodology and validate the methodology by using it as a basis to replicate results from chosen literatures and comparing the results.
- Investigate acoustic pressure field produced by ultrasonic transducer for an arbitrary simple case to gauge effectiveness of simulation.

1.3 Scope

To ensure that the aim can be realistically achieved within the thesis project period, the following scope is set:

- Minimal use of APDL commands. Therefore, APDL commands is not included in the simulation methodology.
- Simulation of only harmonic excitations as mentioned in the aim. Consequently, transient excitation is not considered.
- Only considers commonly used ultrasonic transducer with unidirectional radiation such as piston-shaped and horn-shaped transducer.

2 BACKGROUND THEORY AND LITERATURE REVIEW

This chapter consists of background theory and literature review. Background theory focuses on radiation of ultrasonic transducer, effects of ultrasonic waves on fluid and acoustic impedance which are the essence of the behaviour of an acoustic pressure field generated by ultrasonic excitation. Literature review focuses on optimal methods and the necessary information to understand the methods to simulate said behaviour accurately.

2.1 Background Theory

2.1.1 Radiation of Ultrasonic Transducer

Ultrasonic transducer is a device that uses piezoelectric material to convert electrical energy into mechanical energy and vice versa to produce or receive ultrasonic excitations. The ultrasonic wave produced by the transducer comes from most of the surface of the piezoelectric material (i.e. wave origin points distributed on the surface) rather than a single point [3]. The ultrasonic wave produced by the transducer generates pressure field on the acoustic domain. The radiation field of ultrasonic transducer is often categorised into two and they are near field region and far field region. This is shown in Figure 1 below.

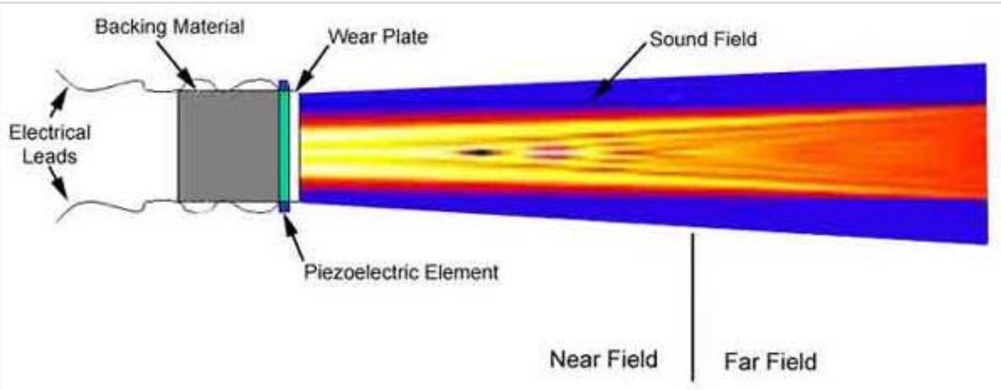

Figure 1: Radiation of ultrasonic transducer [3]

For this figure, intensity of the radiation is indicated by the colour where lighter colour means higher intensity. Since the wave originates from many points on the surface, the near field is heavily influenced by destructive and constructive wave interferences which fluctuates the intensity of the radiation. This is in contrast with far field as the radiation in far field is more predictable and is relatively uniform. Therefore, flaw detection application requires the material of interest to be in the far field of transducer radiation [4].

From the figure, there is a point of high intensity in between the near field and far field and this is called the transition point. The location of maximum radiation intensity is right after the transition point [5]. The formula to find the near field length, N [6] is shown below:

$$N = \frac{D^2}{4\lambda} = \frac{D^2 f}{4V} \tag{1}$$

N : Near field length

D : Diameter of transducer

λ : Wavelength in acoustic medium

f : Operating frequency

V : Velocity of acoustic medium

2.1.2 Effects of Ultrasonic Waves on Fluid

2.1.2.1 Acoustic Streaming

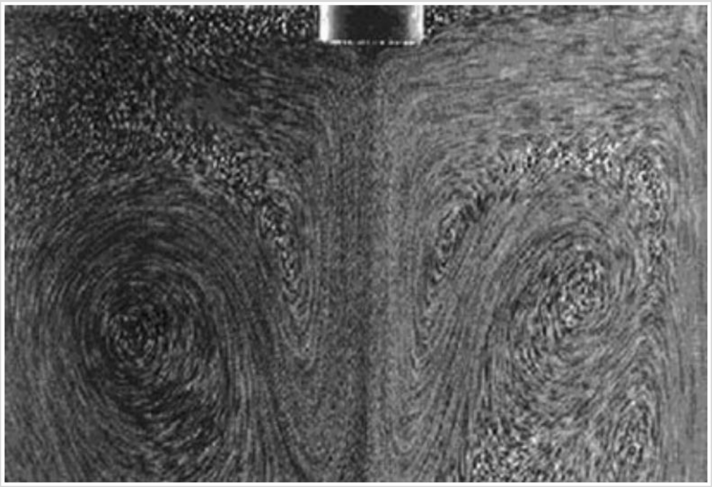

Figure 2: Acoustic streaming generated by ultrasonic transducer [7]

The flow of fluid due to sound propagation is called acoustic streaming [8]. The increase in acoustic streaming is possible by increasing the ultrasound intensity [9]. Due to ultrasonic vibrations and cavitation effect, acoustic streaming induced by ultrasound source is highly turbulent. Therefore, acoustic streaming flow in ultrasonic applications generally consists of steady flow components, small oscillations and large eddies [10]. FEM software should be able to simulate acoustic streaming with proper coupling of acoustic elements.

2.1.2.2 Ultrasonic Cavitation

Propagation of ultrasonic wave in a fluid produces cycles of low and high acoustic pressure due to the rarefaction and compression of the medium [11] .Instantaneous vacuum formed from rarefaction instants may create gas bubble. The creation of bubble by this method is called ultrasonic cavitation [9]. Due to the cyclic behaviour of the wave propagation, the formed bubble would increase and decrease in radius before imploding. Figure 3 below illustrates this phenomenon.

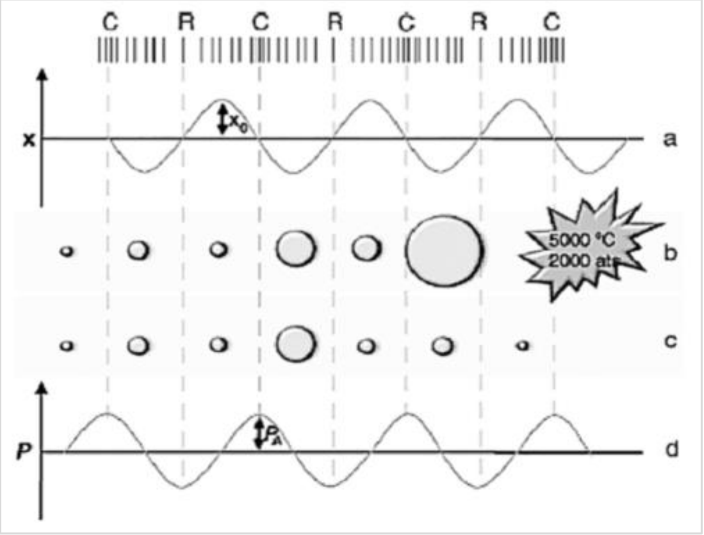

Figure 3: Cavitation phenomenon; (a) displacement, (b) transient cavitation, (c) stable cavitation and (d) pressure [12]

From Figure 3, the bubble increases in radius when the pressure is heading to maximum negative pressure from maximum positive pressure (rarefaction) and decreases in radius when the pressure is heading to maximum positive pressure from maximum negative pressure (compression). Compression of the bubble can cause it to burst (adiabatically) which produces pressure of up to 50MPa and temperature up to 5000K [9]. The bubble may implode after oscillating for a long period of time with large number of cycles or implode before it reaches one cycle [9]. The former is called stable cavitation and the latter is called transient cavitation. Stable cavitation bubbles do not produce light emission or chemical reactions when imploding due to it oscillating for a long period of time. In contrast, the implosion of transient cavitation bubbles produces light emission and/or chemical reactions [13]. Implosion of transient cavitation bubbles is also strong enough that it can potentially damage the surface of a body that is in contact with the bubbles [14]. Generation of bubbles from cavitation effect reduces pressure amplitude within the acoustic field of the fluid domain which attenuates the ultrasonic wave moving into the domain [15]. To put it simply, cavitation bubbles cause reduction of acoustic pressure in the acoustic field and sound speed within the fluid domain.

FEM software is unable to simulate the actual production and implosion of cavitation bubbles while simulating acoustic field generated by ultrasonic transducer. Therefore, the effect of cavitation bubbles should be captured in the simulation instead by considering ultrasound attenuation coefficient and sound speed reduction. Other limitation includes inability to obtain response concerning instantaneous pressure increase from bubble implosions [12].

2.1.3 Acoustic Impedance

Since acoustic impedance depends on the property of the medium, each medium will have different acoustic impedance [16]. Therefore, there is differences in acoustic impedance in a setting where there is more than one medium in contact with each other. The differences in acoustic impedance causes wave transmission and reflection from one medium to the other. Equation for transmission coefficient, T and reflection coefficient, R assumes plane wave normal to plane surface as follows [17].

$$T_{1,2} = \frac{2Z_2}{Z_1+Z_2} \quad (2)$$

$$R_{1,2} = \frac{Z_2-Z_1}{Z_1+Z_2} \quad (3)$$

From equation (2) and (3), there will be full wave transmission when $Z_1 = Z_2$. On the other extreme where $Z_1 \gg Z_2$, there will be full wave reflection with the wave completely out-of-phase from before the wave hits the other medium [18].

2.2 Literature Review

2.2.1 Elements for Acoustic Analysis

In acoustic analysis, acoustics elements based on pressure formulation are used and their characteristics are shown in Table 1 below.

Table 1: Acoustic fluid elements [19] [20]

Element	Dimension	Nodes	Shapes	Degrees of Freedom per Node
FLUID29	2D	4	Default ▪ Quadrilateral Option ▪ Triangle	Uncoupled ▪ Pressure Coupled ▪ Pressure and 2D displacement
FLUID129	2D	2	▪ Line	Pressure
FLUID30	3D	8	Default ▪ Brick Option ▪ Tetrahedral ▪ Wedge ▪ Pyramid	Uncoupled ▪ Pressure Coupled ▪ Pressure and 3D displacement
FLUID130	3D	4 or 8	Default ▪ Quadrilateral Option ▪ Triangle	Pressure
FLUID220	3D	20	Default ▪ Brick Option ▪ Pyramid ▪ Prism	Uncoupled ▪ Pressure Coupled ▪ Pressure and 3D displacement
FLUID221	3D	10	Tetrahedral	Uncoupled ▪ Pressure Coupled ▪ Pressure and 3D displacement

FLUID 129 and FLUID 130 are wave absorbing elements set to the exterior of an acoustic domain to absorb outgoing pressure waves and the other elements are used as the acoustic domain. From the shapes and the nodes in Table 1, FLUID29, FLUID129 and FLUID30 have linear shape function and FLUID220 and FLUID221 have quadratic shape function [20]. FLUID130 shape function depends on the element used for the inner acoustic domain that is paired with it (i.e. linear if paired with FLUID30 and quadratic if paired with FLUID220 or FLUID221) [20]. For elements with linear shape function, pressure through the elements varies linearly. For elements with quadratic shape function, pressure through the elements follows quadratic formula. Figure 4 shows comparison of linear and quadratic shape function to pressure distribution.

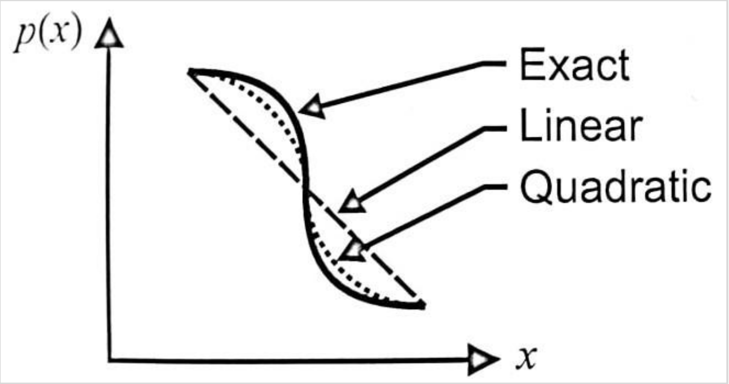

Figure 4: Comparison of linear and quadratic shape function to pressure distribution [20]

From the figure, quadratic shape function is closer to the exact pressure distribution compared to linear shape function. However, elements with quadratic shape function requires more computational resource and computation time since the elements have more nodes [20].

From Table 1, there is uncoupled and coupled variations of the degrees of freedom. This means that these acoustic elements can be coupled with elements with displacement degrees of freedom. The Fluid-Structure Interaction (FSI) section covers this coupling mechanism.

2.2.2 Wave Absorption Boundary

Wave absorption boundary is a boundary set on the exterior of an acoustic body to absorb outgoing waves [21]. This is essential in acoustic simulation as it allows simulation to be closer to real-life application where the distance of the excitation source and the very end of real-life acoustic boundary is substantially large [22]. In short, it allows simulation of infinite acoustic domain.

There are three wave absorption methods in ANSYS. The first method uses wave absorbing elements which are FLUID129 (for 2D acoustic analysis) and FLUID 130 (for 3D acoustic analysis) on the exterior of the acoustic domain. This wave boundary condition is termed as Absorbing Boundary Condition (ABC) [23] [21]. The second wave absorption method uses radiation boundary [21]. The third wave absorption method uses Artificially Matched Layer [24] [21]. Review of these methods are provided in their respective sections.

Without wave absorption boundary, the outgoing waves will be reflected when it hits the outermost surface of acoustic body. An example of real-world case that can be represented without the use of wave absorption boundary is the operation of ultrasonic cleaning tank. Tangsopha, Thongsri and Busayaporn [25] did not set wave absorption boundary on his ultrasonic cleaning tank simulation model to allow reflection of waves on the tank surface. This is because realistically, waves from the water inside the tank would be reflected when it hits the tank due to high impedance difference.

2.2.2.1 Absorbing Boundary Condition (ABC)

For Absorbing Boundary Condition (ABC), absorption element FLUID129 is set on the exterior of a circular acoustic domain (2D) and FLUID130 is set on the exterior of a spherical acoustic domain (3D). This can be done by setting absorption element to the exterior surface. Figure 5 depicts a typical setting of analysis with ABC.

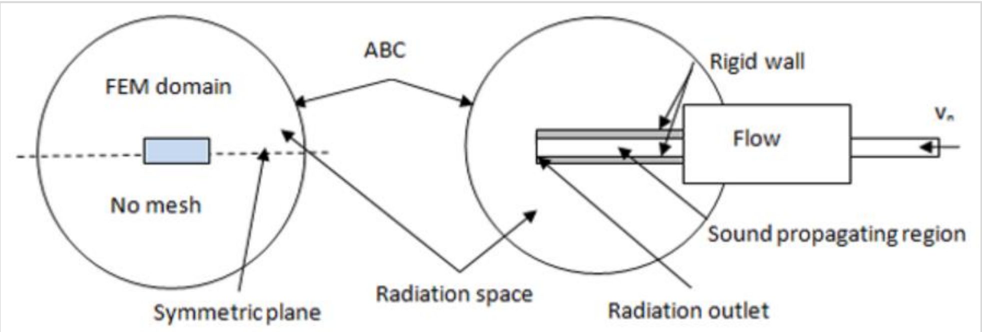

Figure 5: Typical setting of analysis with Absorbing Boundary Condition (ABC) [23]

Figure 5 indicates that circular/spherical FEM domain can be reduced via plane/axis of symmetry. To ensure accurate results, the pressure wave produced in the simulation must comply with Sommerfield radiation condition [23] [21] . This means that acoustic wave in the acoustic domain should only propagate outwards (i.e. there is no wave propagating inwards). If FLUID129/130 is set on non-circular/spherical exterior, some waves will be reflected when it hits the acoustic boundary. The ABC wave absorption method is viable, and this is confirmed from simulation done be Massimino et al [26]. He used FLUID130 as the wave absorption boundary for his simulation which has a quarter hemisphere acoustic domain and obtained satisfactory sound pressure level (SPL) results (Appendix A).

2.2.2.2 Radiation Boundary

Radiation boundary is a wave absorption boundary that is set on exterior surface of an acoustic domain in which it defines the surface impedance of the set surface as follows [21]:

$$Z = \frac{p}{v_n} = \rho_0 c_0 \tag{4}$$

Z : Impedance

p : pressure

v_n : acoustic particle velocity

ρ_0 : density

c_0 : speed of sound

Equation (4) indicates that there is surface impedance on the boundary of the acoustic domain and hence, there is absorption. This boundary condition absorbs waves that propagates normal to the surface. Therefore, it can effectively absorb plane wave. For non-plane wave and angled wave, minor reflections can occur [21].

2.2.2.3 Artificially Matched Layers

Artificially matched layers are set on an enclosing acoustic body (since it is used to absorb wave) that encloses the acoustic domain of interest in which the material of both bodies is the same [24]. When an acoustic body is set as artificially matched layers, the enclosing body will behave as an artificial anisotropic material that absorbs incoming pressure waves [24]. According to Howard and Cazzolato [21], a pressure boundary condition with pressure set to zero must be set on the exterior of the artificially matched layers. However, this is not necessary as artificially matched layers have soft-sound boundary by default where the pressure is zero [24]. This is shown in Figure 6.

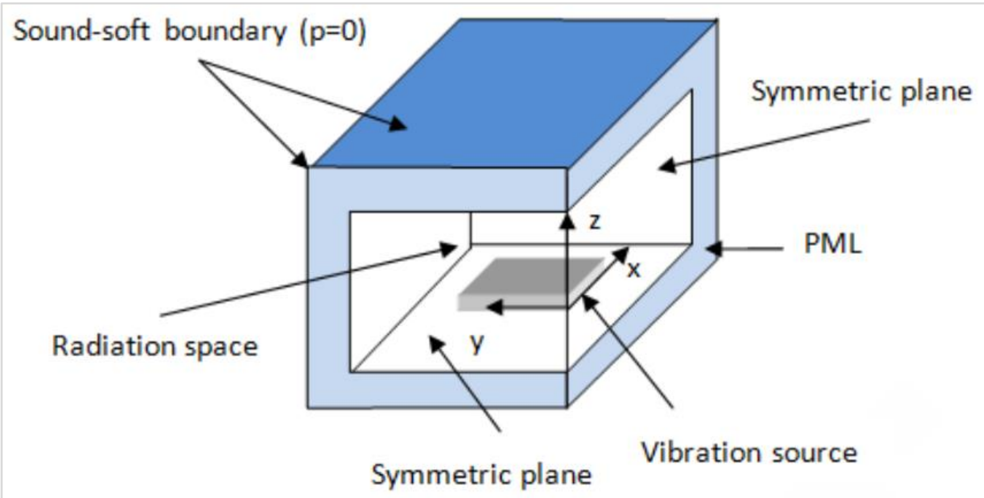

Figure 6: Typical setting of analysis with artificially matched layer [24]

From Figure 6, the artificially matched layers are labelled as PML which stands for perfectly matched layer. PML is a type of artificially matched layers made of brick acoustic elements which are FLUID30 and FLUID220. Another variation of the artificially matched layers is called irregular perfectly matched layer (IPML) which are made of the tetrahedron acoustic element, FLUID221. With this, IPML is not constricted to the shape of the model but it may not absorb wave as effective as PML [24]. According to Nygren [27], PML should have adequate thickness to ensure absorption of waves that is not propagated normal to the surfaces of PML.

2.2.3 Fluid-Structure Interaction (FSI)

Fluid-structure interaction (FSI) is a term for when acoustic and structural body interacts via boundary condition that couples them [28]. One commonly used coupling boundary condition in ANSYS Workbench is fluid solid interface which is set on surface where acoustic body touches the structural body [28]. Another way to enable FSI is by using APDL commands [29]. Figure 7 below shows an example of FSI setting and the degrees of freedom (DOF) involved in a model with FSI.

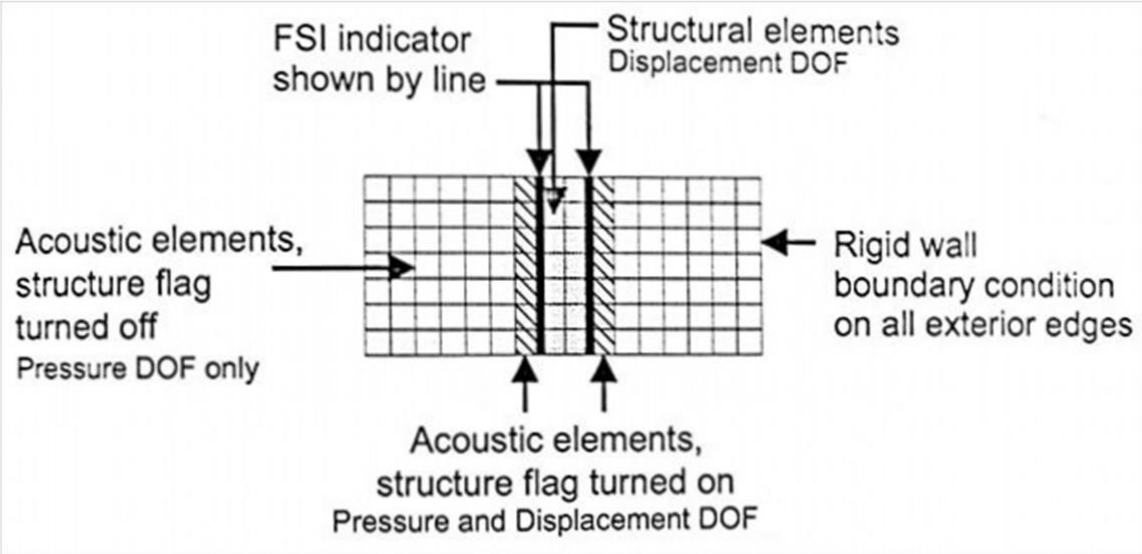

Figure 7: Fluid-Structure Interaction (FSI) [29]

From the figure, structural elements have displacement DOF while acoustic elements only have pressure DOF. This just means that the nodes of the structural elements can only move while the nodes of acoustic elements can only handle acoustic pressure. With FSI, the nodes of the acoustic elements that are shared with the structural elements that is in direct contact with it have both pressure and displacement DOF [28] [29]. This allows the movement of the structure to produce acoustic pressure on the fluid and vice versa. Since the purpose of FSI is to allow proper interaction between acoustic elements with strictly pressure DOF and structural elements with displacement DOF, FSI is viable only for acoustic elements that are based on pressure formulation [29].

It is mentioned in Elements for Acoustic Analysis section that there are six acoustic elements that are based on pressure formulation and they are FLUID29, FLUID129, FLUID30, FLUID130, FLUID220 and FLUID221. Although FLUID129 and FLUID130 are pressure formulated elements, FSI is irrelevant to these elements since they are used for wave absorptions which are set on the exterior of simulation model [29]. The formation of coupled equation of motion for FSI is shown below [29]:

The finite element equation of motion for pressure-formulated acoustic elements is [30]:

$$[\boldsymbol{M_f}]\{\ddot{\boldsymbol{p}}\} + [\boldsymbol{K_f}]\{\boldsymbol{p}\} = \{\boldsymbol{F_f}\} \tag{5}$$

$[\boldsymbol{M_f}]$: Equivalent fluid mass matrix

$\{\ddot{\boldsymbol{p}}\}$: Vector of the second derivative of acoustic pressure with respect to time

$[\boldsymbol{K_f}]$: Equivalent fluid stiffness matrix

$\{\boldsymbol{p}\}$: Vector of unknown nodal acoustic pressures

$\{\boldsymbol{F_f}\}$: Vector of applied fluid loads

The finite element equation of motion for structural elements is:

$$[\boldsymbol{M_s}]\{\ddot{\boldsymbol{U}}\} + [\boldsymbol{K_s}]\{\boldsymbol{U}\} = \{\boldsymbol{F_s}\} \tag{6}$$

$[\boldsymbol{M_s}]$: Equivalent structural mass matrix

$\{\ddot{\boldsymbol{U}}\}$: Vector of the second derivative of displacements with respect to time

$[\boldsymbol{K_s}]$: Equivalent structural stiffness matrix

$\{\boldsymbol{U}\}$: Vector of unknown nodal displacements

$\{\boldsymbol{F_s}\}$: Vector of applied structural loads

Additional terms and coupling matrix, $[\boldsymbol{R}]$ are added to equation (5) and (6) to account for the coupling of structure and fluid.

$$[\boldsymbol{M_f}]\{\ddot{\boldsymbol{p}}\} + [\boldsymbol{K_f}]\{\boldsymbol{p}\} = \{\boldsymbol{F_f}\} + \rho_0[\boldsymbol{R}]^T\{\ddot{\boldsymbol{U}}\} \tag{7}$$

$$[\boldsymbol{M_s}]\{\ddot{\boldsymbol{U}}\} + [\boldsymbol{K_s}]\{\boldsymbol{U}\} = \{\boldsymbol{F_s}\} + [\boldsymbol{R}]\{\boldsymbol{p}\} \tag{8}$$

Matrix equation is then formed from equation (7) and (8) with added structural damping, $[\boldsymbol{C_s}]$ and acoustic damping, $[\boldsymbol{C_f}]$ effects.

$$\begin{bmatrix} \boldsymbol{M_s} & 0 \\ \rho_0 \boldsymbol{R}^T & \boldsymbol{M_f} \end{bmatrix} \begin{Bmatrix} \ddot{\boldsymbol{U}} \\ \ddot{\boldsymbol{p}} \end{Bmatrix} + \begin{bmatrix} \boldsymbol{C_s} & 0 \\ 0 & \boldsymbol{C_f} \end{bmatrix} \begin{Bmatrix} \dot{\boldsymbol{U}} \\ \dot{\boldsymbol{p}} \end{Bmatrix} + \begin{bmatrix} \boldsymbol{K_s} & -\boldsymbol{R} \\ 0 & \boldsymbol{K_f} \end{bmatrix} \begin{Bmatrix} \boldsymbol{U} \\ \boldsymbol{p} \end{Bmatrix} = \begin{Bmatrix} \boldsymbol{F_s} \\ \boldsymbol{F_f} \end{Bmatrix} \quad (9)$$

Equation (9) is then reduced by omitting the differentials.

$$\begin{bmatrix} -\omega^2 \boldsymbol{M_s} + j\omega \boldsymbol{C_s} + \boldsymbol{K_s} & -\boldsymbol{R} \\ -\omega^2 \rho_0 \boldsymbol{R}^T & -\omega^2 \boldsymbol{M_f} + j\omega \boldsymbol{C_f} + \boldsymbol{K_f} \end{bmatrix} \begin{Bmatrix} \boldsymbol{U} \\ \boldsymbol{p} \end{Bmatrix} = \begin{Bmatrix} \boldsymbol{F_s} \\ \boldsymbol{F_f} \end{Bmatrix} \quad (10)$$

Equation (10) is the first variation of coupled equation of motion for FSI. This equation has unsymmetrical matrix on the left-hand side. When solving for nodal displacements and pressures, the unsymmetrical matrix needs to be inverted and this requires substantial amount of computational resource [29].

The symmetrical variation of coupled equation of motion for FSI (equation (12)) incorporates transformation variable for the nodal pressures (equation (11)).

$$\dot{\boldsymbol{q}} = j\omega \boldsymbol{q} = \boldsymbol{p} \quad (11)$$

$$\begin{bmatrix} -\omega^2 \boldsymbol{M_s} + j\omega \boldsymbol{C_s} + \boldsymbol{K_s} & -j\omega \boldsymbol{R} \\ -j\omega \boldsymbol{R}^T & \frac{\omega^2 \boldsymbol{M_f}}{\rho_0} - \frac{j\omega \boldsymbol{C_f}}{\rho_0} - \frac{\boldsymbol{K_f}}{\rho_0} \end{bmatrix} \begin{Bmatrix} \boldsymbol{U} \\ \boldsymbol{q} \end{Bmatrix} = \begin{Bmatrix} \boldsymbol{F_s} \\ \frac{j}{\omega \rho_0} \boldsymbol{F_f} \end{Bmatrix} \quad (12)$$

Howard and Cazzolato [29] demonstrated a harmonic analysis case using both the unsymmetrical matrix and symmetrical matrix version of the equation and found that it produces similar results (Appendix B). In terms of computation time, their simulation model is solved significantly faster when the symmetrical coupled equation of motion is used [29]. The option to choose between the unsymmetrical and symmetrical coupled equation is not available when native acoustic harmonic analysis tool called “harmonic acoustics” is used in ANSYS Workbench. This tool is available on the more recent version of ANSYS such as ANSYS 19.1. It is assumed that “harmonic acoustics” uses symmetrical matrix version of the equation by default since it produces accurate result with less computational time.

2.2.4 Meshing in Acoustic Analysis

Meshing of simulation model for acoustic analysis should be sufficiently fine to capture the mode shapes of the model [31]. The mesh is considered sufficiently fine when the element size is at least 12 times smaller than the wavelength for linear elements [31] [32]. For quadratic elements, the element size should be at least 6 times smaller than the wavelength [31] [32]. The wavelength should be the smallest wavelength in the system [27]. The formula to find suitable element size consists of the wavelength formula, $\lambda = c/f$, where λ is wavelength of acoustic medium, c is speed of sound of acoustic medium and f is excitation frequency [31]. The following are the formula to find suitable element size:

$$element\ size = \frac{\lambda}{EPW} = \frac{c}{EPW \times f} \quad (13)$$

EPW is the recommended number of elements per wavelength (i.e. 12 for linear elements and 6 for quadratic elements). Nygren [27] has tested the validity of the EPW for quadratic elements by doing several iterations on his model. The element size of the model is reduced for each iteration until the element size is smaller than a sixth of the wavelength of the model. Nygren [27] found that for element size close to or less than a sixth of the wavelength, the mean average errors are relatively small (Appendix C). Another test to validate the recommended EPW done by Langer, Maeder, Guist, Krause and Marburg [33] shows promising results (Appendix D). He tested his model using both quadratic and linear elements with EPW of 2, 4, 6, 10 and 20. His results shows that for quadratic element, the error found is less than 0.1% when EPW is set to 6. For linear element, EPW of 10 (which is close to 12) results in less than 1% error. Also shown in the results is that the percentage error decreases with smaller element size.

If PML is used as the wave absorption boundary, sufficient elements for the PML and buffer elements (elements from the radiation source to the inner surface of PML) are necessary to ensure proper wave absorption [24]. This description is illustrated in Figure 8 below:

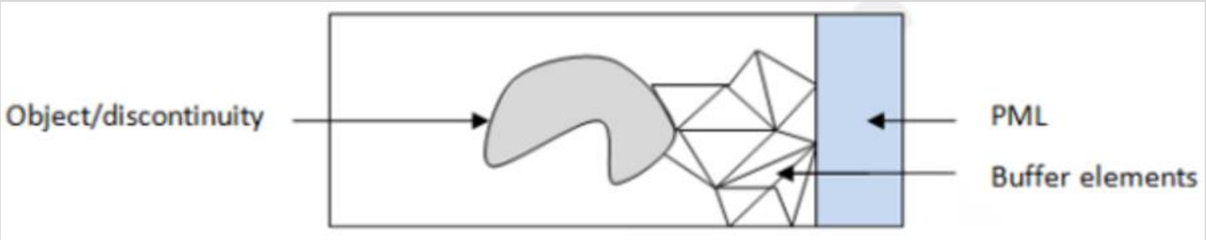

Figure 8: Perfectly Matched Layers (PML) meshing guidelines [24]

The following PML meshing guidelines are recommended to ensure satisfactory results [24]:

- Number of PML elements ≥ 3
- Number of layers of PML ≥ 2
- Number of layers of buffer elements ≥ 2

2.2.5 Model Reduction of Symmetrical Model

Model reduction in acoustic simulation is desirable as it reduces the elements and nodes of the simulation model leading to faster solving time. This is especially relevant to simulation involving frequency in the ultrasonic range since the model would require significantly smaller element size for accurate results compared to acoustic simulation with frequency below ultrasonic [31]. Simulation model can be reduced to half or quarter if the model is symmetrical depending on the number of planes of symmetry [34]. Figure 9 shows an example of model reduction.

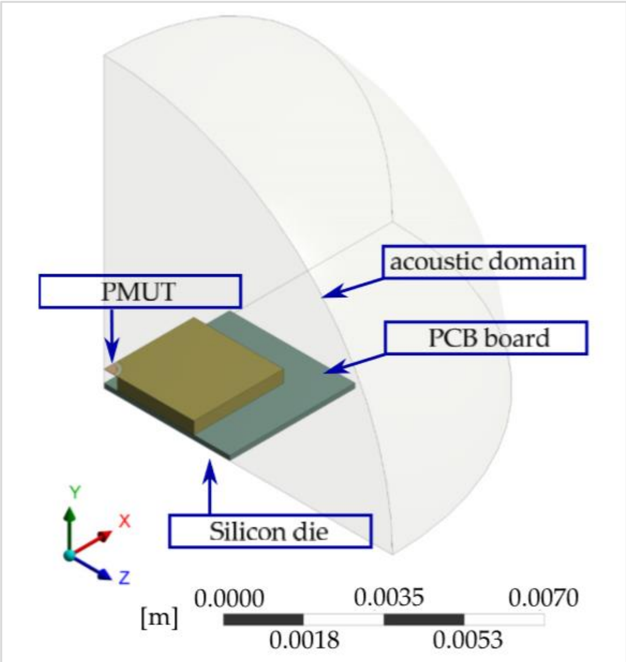

Figure 9: Quarter model of Piezoelectric Micromachined Ultrasonic Transducer (PMUT) in hemispherical acoustic domain [26]

According to Howard and Cazzolato [34], using ANSYS Workbench, symmetry boundary condition can only be set to elements with displacement DOF. This means that it is not possible to set symmetry boundary condition to acoustic elements which mostly only have pressure DOF instead of displacement DOF.

Since there is no way to set symmetry boundary condition to an acoustic body in ANSYS Workbench, the result obtained from acoustic analysis using model that is reduced via its plane of symmetry need to be scaled [34]. The scaling factor is based on the basic pressure formula, $p = F/A$, where p is pressure, F is force and A is area. The following are examples of the formula with scaling factor [34]:

$$p_{half} = \frac{F}{A_{half}} = \frac{2F}{A_{full}} = 2p_{full} \tag{14}$$

$$p_{quarter} = \frac{F}{A_{quarter}} = \frac{4F}{A_{full}} = 4p_{full} \tag{15}$$

Howard and Cazzolato [34] had made a full model and a quarter model of an air-filled duct using ANSYS 14.5 for comparison to prove this. Their result shows that the $p_{quarter}/4$ is identical to p_{full} (Appendix E).

Massimino et al [26] had done a quarter model of piezoelectric micromachined ultrasonic transducer (PMUT) using ANSYS 17.2 as shown in Figure 9. However, he never mentioned any use of scaling factor for his sound pressure level (SPL) results. This indicates that the newer version of ANSYS is capable to set symmetry boundary condition to an acoustic body making result or input scaling for reduced model to match its full model counterpart unnecessary. A simple simulation with arbitrary model size and excitation input is done using ANSYS 19.1 to confirm this and it is found that full model, half model and quarter model produces similar results (Appendix F).

Howard and Cazzolato [34] mentioned that for vibro-acoustic analysis which involves vibrating structure, usage of symmetry can cause complications and it is recommended to model the full system instead. This may be true since Tangsopha et al [25] modelled a symmetrical ultrasonic cleaning tank using ANSYS 17.0 which involves vibrating plate and transducer components without reducing it. However, Massimino et al [26] did not mention any complication for his quarter PMUT model which also involves vibrating structure. Model reduction option for Tangsopha et al [25] tank model is considered in Test Case 2: Ultrasonic Cleaning Tank section.

2.2.6 Comparison of 3D Model and 2D Model

In researches involving the use of finite element simulation, 2D model is preferred over 3D model for its minimal use of computational resource and significantly lower computation time [35]. However, 2D model may produce less accurate result compared to 3D model as it effectively assumes that the model extends infinitely in one axis. For this reason, 3D model and 2D model is often compared with experimental results before proceeding with simulation of case of interest [26] [36]. Figure 10 shows an example of result comparison.

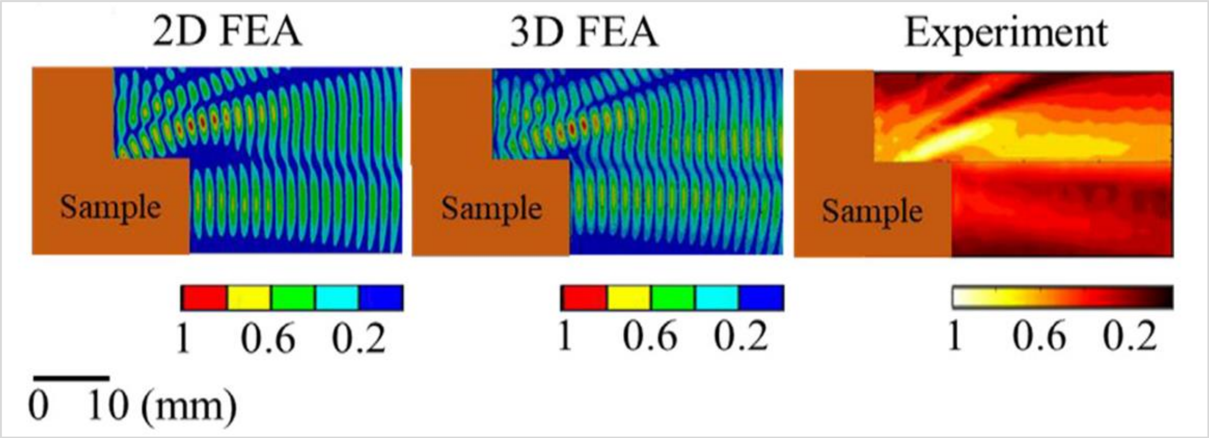

Figure 10: Comparison between result of 2D model, 3D model and experiment [37]

Figure 10 above is a validation test done by Odabaee, Odabaee, Pelekanos, Leinenga and Gotz [37] to ensure viability of 3D and 2D models in simulating ultrasound propagation through layered materials. From the result, both 3D and 2D models shows good agreement with the experimental results.

Massimino et al [26] also obtained satisfactory results when comparing his 3D model and 2D model with experimental results which shows that 2D simulation is feasible (Appendix A). Odabaee et al [37] revealed that her 3D model uses 600GB of computational memory while her 2D model only uses 3GB of computational memory with a substantial decrease in computation time. This confirms that 2D model is better in term of computational resource usage and computation time.

Another option that can be considered is 2.5D model which is 3D model with very small thickness in one axis. ANSYS demonstrated an analysis on piezoelectric flextensional transducer in water using 2D model and 2.5D model [38]. Comparison of the results is in Figure 11 below.

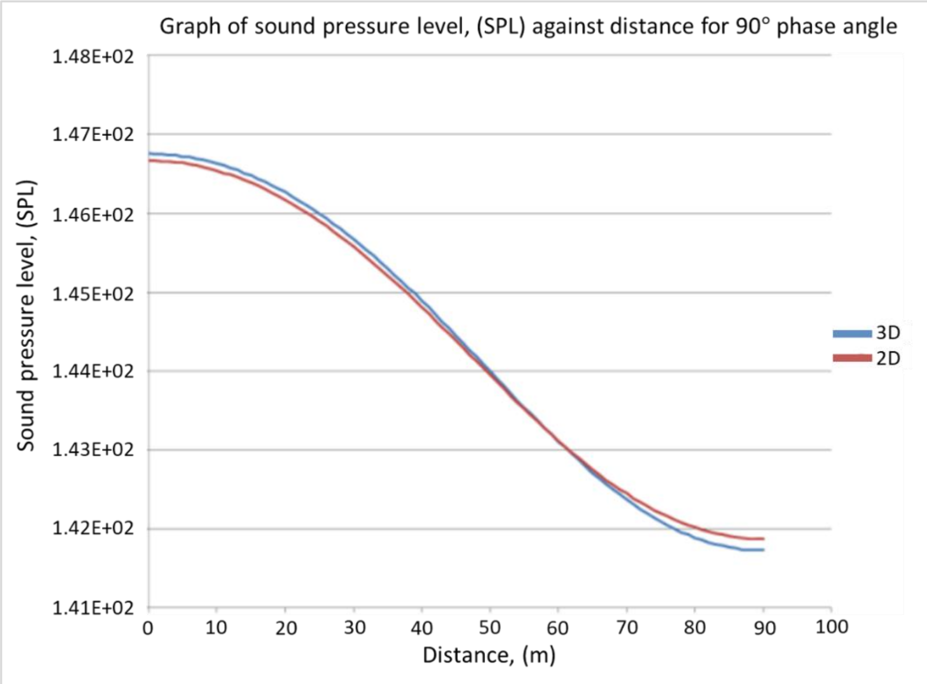

Figure 11: Comparison between result of 2D model and 2.5D model [38]

From the graph, the 2.5D model (shown as 3D as it is technically 3D model) shows good agreement with 2D model. The use of 2.5D and 2D model instead of 3D model is a form of model reduction. In ANSYS, 2.5D and 2D model can be made using ANSYS Workbench. However, 2D model requires APDL commands to set the proper elements, excitations and boundary conditions to the model which can be challenging for new user. Simulation using 2.5D model is considered in Test Case 1: Radiation of Baffled Piston section.

3 SIMULATION METHODOLOGY

This chapter provides the methodology to do simulation of acoustic pressure field produced by ultrasonic transducer using ANSYS workbench. This methodology is made based on methods found in literature review and other finite element analysis methods that can be helpful for the simulation. The importance and reasoning for methods suggested in each stage of the methodology are provided.

3.1 Methodology Overview

Figure 12 shows the stages for simulation of acoustic pressure field produced by ultrasonic transducer. Details for each stage are available in their respective section.

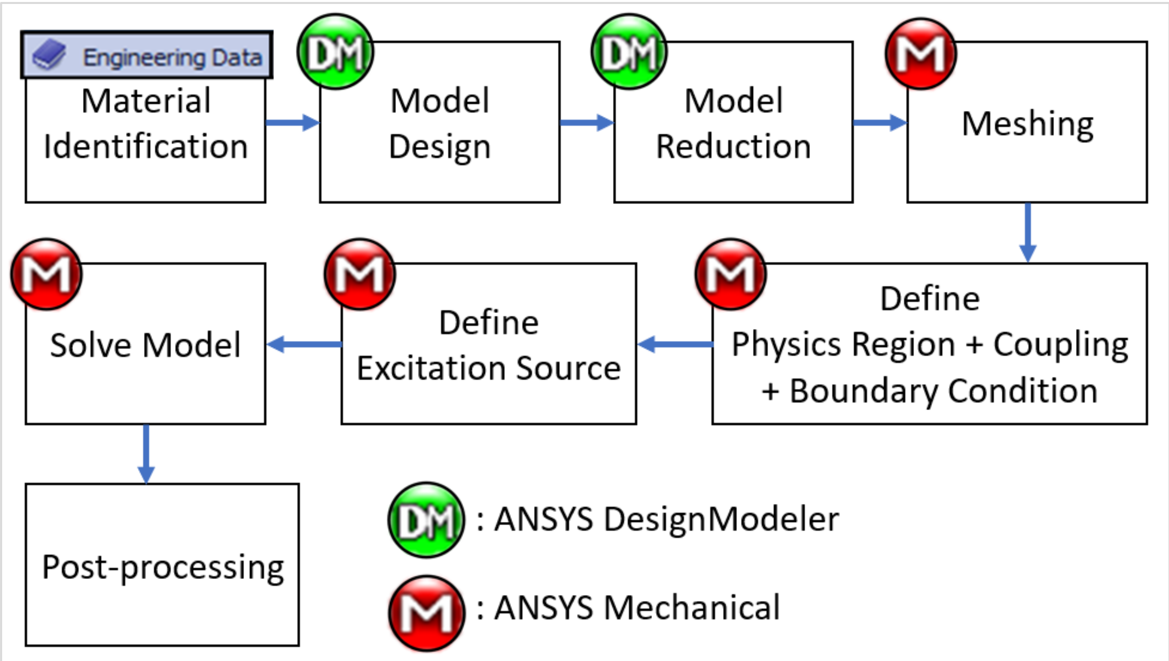

Figure 12: Stages of simulation of acoustic pressure field produced by ultrasonic transducer

3.2 Material Identification

Before proceeding to model design, materials required for the model are identified and cross-checked with ANSYS built-in engineering data sources which have a fair amount of materials. If the material is not available in ANSYS, new material can be added by defining the name and necessary properties of the material using the toolbox provided (Appendix G). When modelling an ultrasonic excitation source, the user may want to consider the orthotropic (a subset of anisotropic) behaviour of a piezoelectric material. This can be done by filling the elastic properties as in Figure 13.

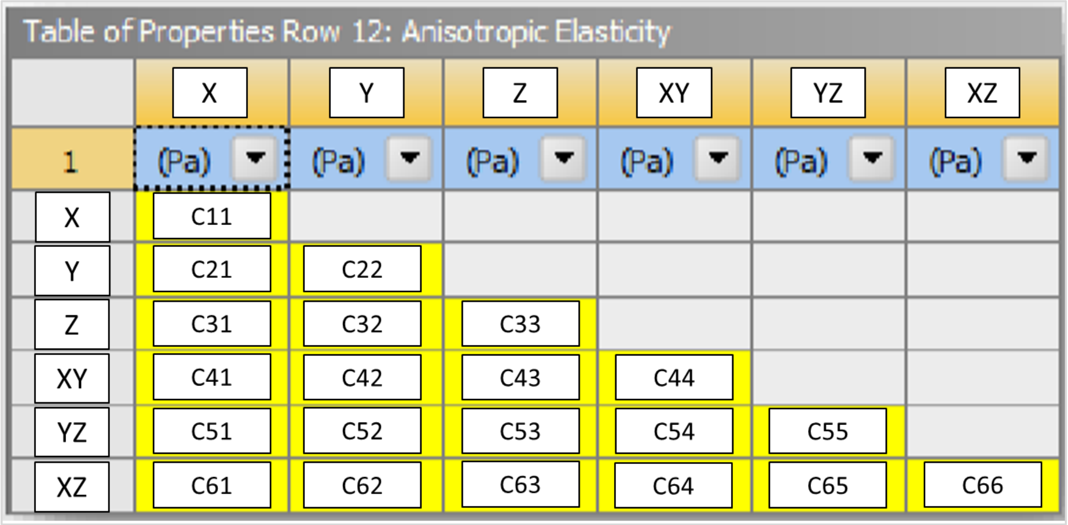

Figure 13: Labelled rows and columns for inputting elastic coefficient value [39]

From the Figure 13 above, the sequence of rows and columns for elasticity coefficient matrix differs from IEEE standards. This is also true for piezoelectric coefficient matrix [39]. The conversion from IEEE standards to ANSYS is shown below:

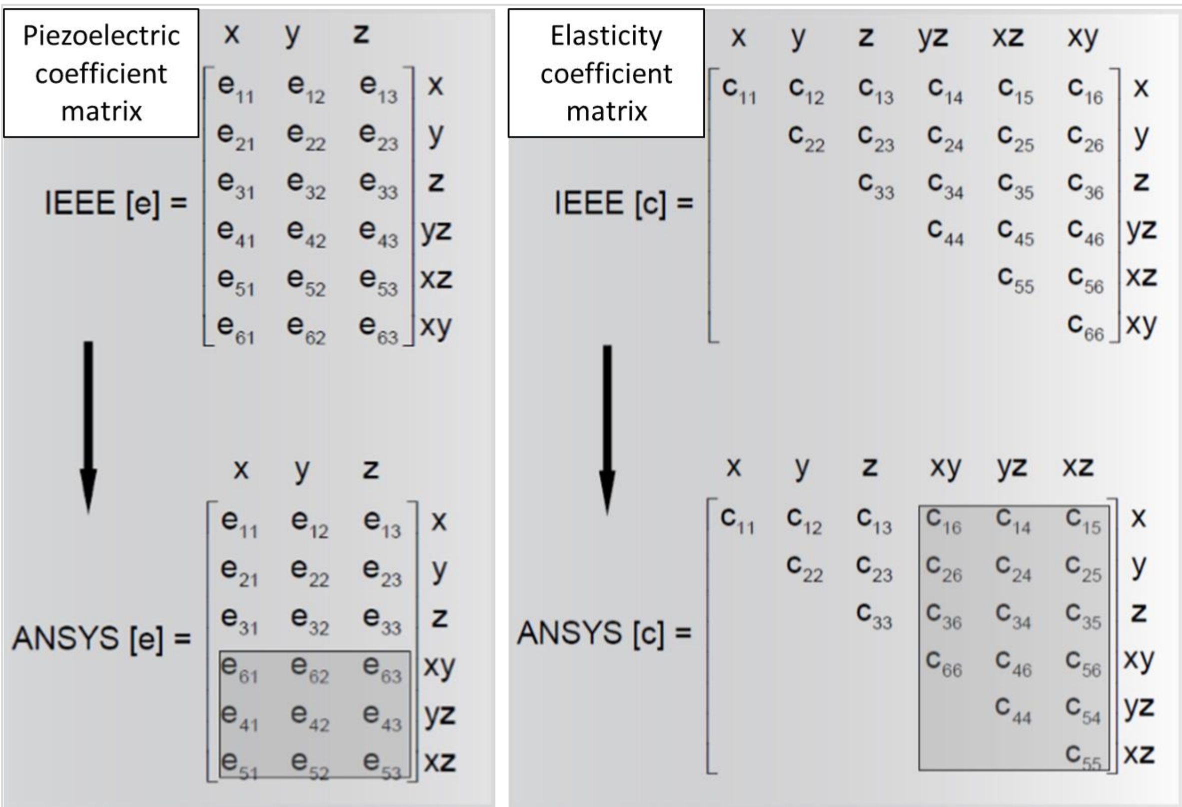

Figure 14: Conversion of piezoelectric and elasticity coefficient matrix from IEEE standards to ANSYS [39]

It is important to know these differences between IEEE standards and ANSYS since most literatures shows these matrices according IEEE standards [39].

3.3 Model Design

Model design can be made using ANSYS built-in modelling software or other modelling software. There are two built-in software available and they are "SpaceClaim" and "DesignModeller". "DesignModeller" is preferred since there are many tutorials on using it compared to the relatively new "SpaceClaim". Model made using other modelling software can be imported into ANSYS. The model for acoustic simulation is categorised into four components as shown in Figure 15.

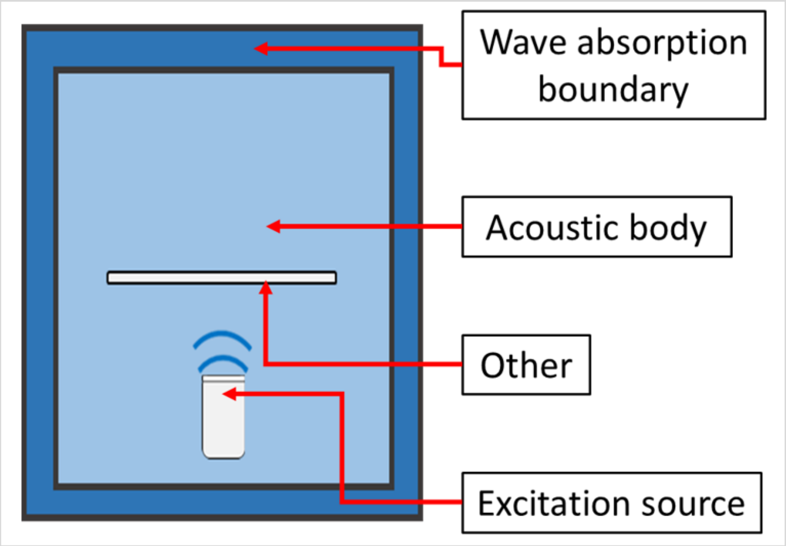

Figure 15: Four components in an acoustic simulation model

Excitation source and acoustic body is a must for acoustic simulation. "Other" in the figure indicates the variation of simulation model as it is based on the case to be simulated. The component that needs more attention in this section is wave absorption boundary as it affects the overall design of the model. To decide on the wave absorption boundary, absorption methods discussed in literature review are summarised and compared in Table 2.

Table 2: Comparison of wave absorption methods

Wave Absorption Method	Description
Perfectly Matched Layer (PML) 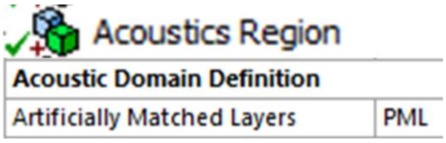	▪ Excellent pressure wave absorption. ▪ Additional layers can help with wave absorption for waves that is not propagated normal to boundary of acoustic domain. ▪ More elements and nodes which may require more computational resources and time compared to the other two methods.
Radiation Boundary 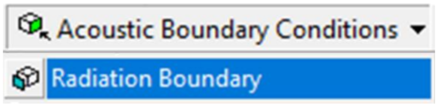	▪ Excellent for plane wave absorption if it is incident normal to a planar surface. ▪ Require less computational resource and time compared to the other two methods. ▪ Not suitable when pressure field is complicated.
Absorbing Boundary Condition (ABC) 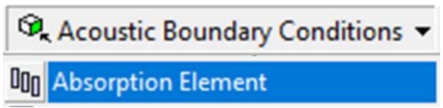	▪ Excellent for outward propagating acoustic pressure waves if Sommerfield radiation condition is fulfilled. ▪ Restricted to spherical/circular acoustic domain which can be larger than actual domain of interest. ▪ PML or radiation boundary that favours quad-shaped models can easily covers just the domain of interest.

From the comparison above, PML is chosen as the main wave absorption method since it can provide excellent wave absorptions even for complicated wave propagations. The computational resource and time can be reduced by modelling only the acoustic domain of interest and by optimizing number of absorption layers. Radiation of piston-shaped and horn-shaped transducer only covers the area in front of it with minimal radiation spread and this is perfect for PML.

On optimising the size of simulation model, the parameter features provided in ANSYS is used to easily change the size of any components in the simulation model. Therefore, there is no need to open ANSYS built-in modelling software to edit the sizing of the model and this makes model editing efficient. This is also useful to study the effect of changing parameter of interest to the simulation results.

3.4 Model Reduction

Model reduction is the term used when a simulation model is made with the model reduced via its plane/axis of symmetry or by simplifying it into a 2.5D (3D model with relatively small thickness in one axis) or 2D model. This is shown in Figure 16.

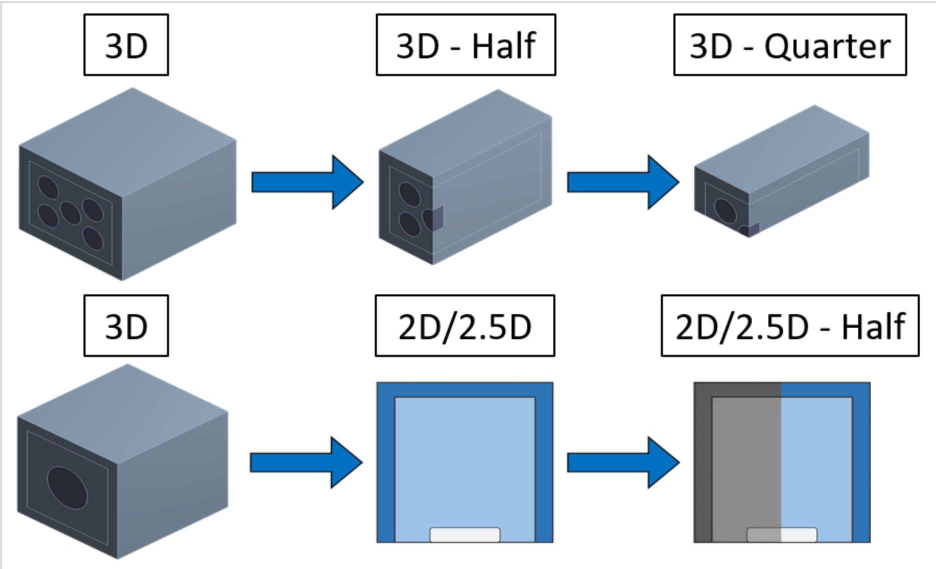

Figure 16: Example of model reduction

Model reduction is done when possible as it significantly reduces computational resource usage and computation time. Comparison between full model, half model and quarter model are not provided in this section as it is found to produce similar results. This may not be true for a more complex (but still symmetrical) model. This is tested in Test Case 1: Ultrasonic Cleaning Tank. Comparison between 3D, 2.5D and 2D model is shown in Table 3.

Table 3: Comparison of 3D model, 2.5D model and 2D model

Simulation Model	Description
3D Model	▪ Produces more accurate result than the other two models especially for complex case. ▪ Able to simulate complex and non-symmetrical experimental setup. ▪ Computational resource and time required to simulate can be very high for a slight increase in accuracy.
2.5D Model	▪ Produces accurate result for relatively simple case. ▪ Substantial decrease in computational resource usage and computation time. ▪ Easier to model than 2D model.
2D Model	▪ Produces result about the same accuracy as 2.5D model. ▪ Less computational resource usage and computational time compared to 2.5D model. ▪ Slightly harder to model than 2.5D model as it requires familiarity with APDL commands.

From the comparison, 2.5D model appears to be the optimal choice when result accuracy, solving time and modelling difficulty are considered.

3.5 Meshing

Meshing is done in ANSYS simulation software called "Mechanical". Before meshing the model, ensure that correct material is set to the model. Meshing guidelines from literature review is summarised and depicted in Figure 17.

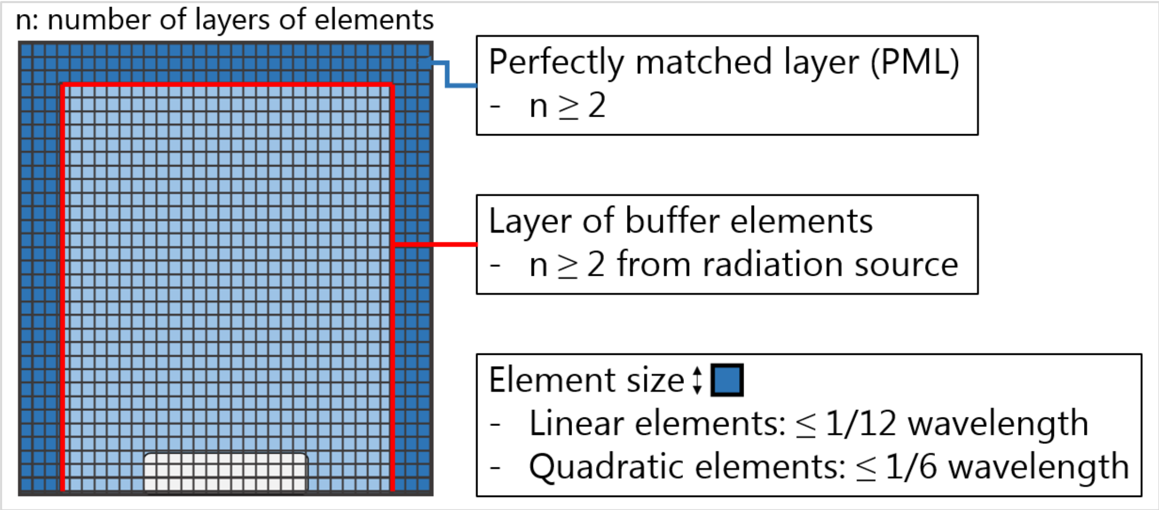

Figure 17: Meshing guidelines

Linear elements are elements with linear shape function and quadratic elements are element with quadratic shape function. For the acoustic domain in Figure17, linear elements refer to FLUID129 and FLUID30 whereas quadratic elements refer to FLUID220 and FLUID230. From literature review, the guidelines provided results in simulation with less use of computational resource and faster computation time while still maintaining good accuracy. The user can deviate from the guideline if the results from the deviation is justifiable (i.e. increase accuracy with tolerable computation time or decrease computation time with tolerable accuracy).

To control the element shape and size, “Method” and “Sizing” under “Mesh Control” is used as shown below.

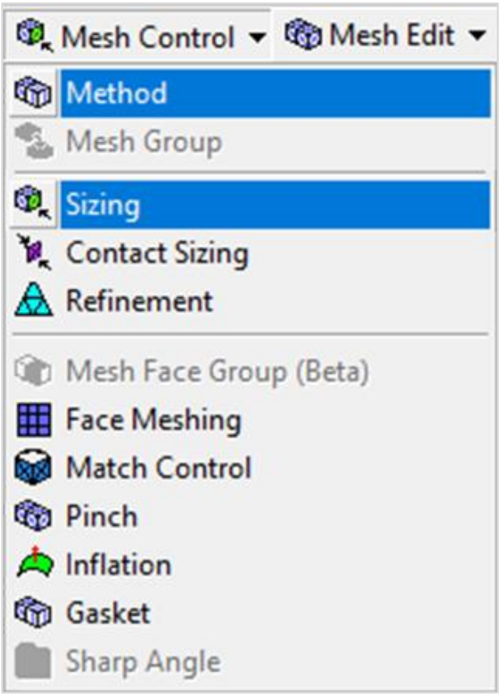

Figure 18: Mesh control

Using Method, the shape of element can be determined, and the element size can be made uniform or incrementally increase/decrease. The shape of element corresponds to the type of element used. For example, when hexahedral is chosen, the element used will be FLUID220 since it is a hexahedron by default. Other shape variation of the same element can be set using APDL commands. Using Sizing, the element size can be set according to preference. After meshing is complete, the mesh quality and size are checked and should be fixed if there is any problem.

3.6 Physics Region, Coupling and Boundary Condition

Physics region and boundary condition is set to represent real-life setup. Figure 19 below shows essential physics region, coupling and boundary condition for acoustic simulation.

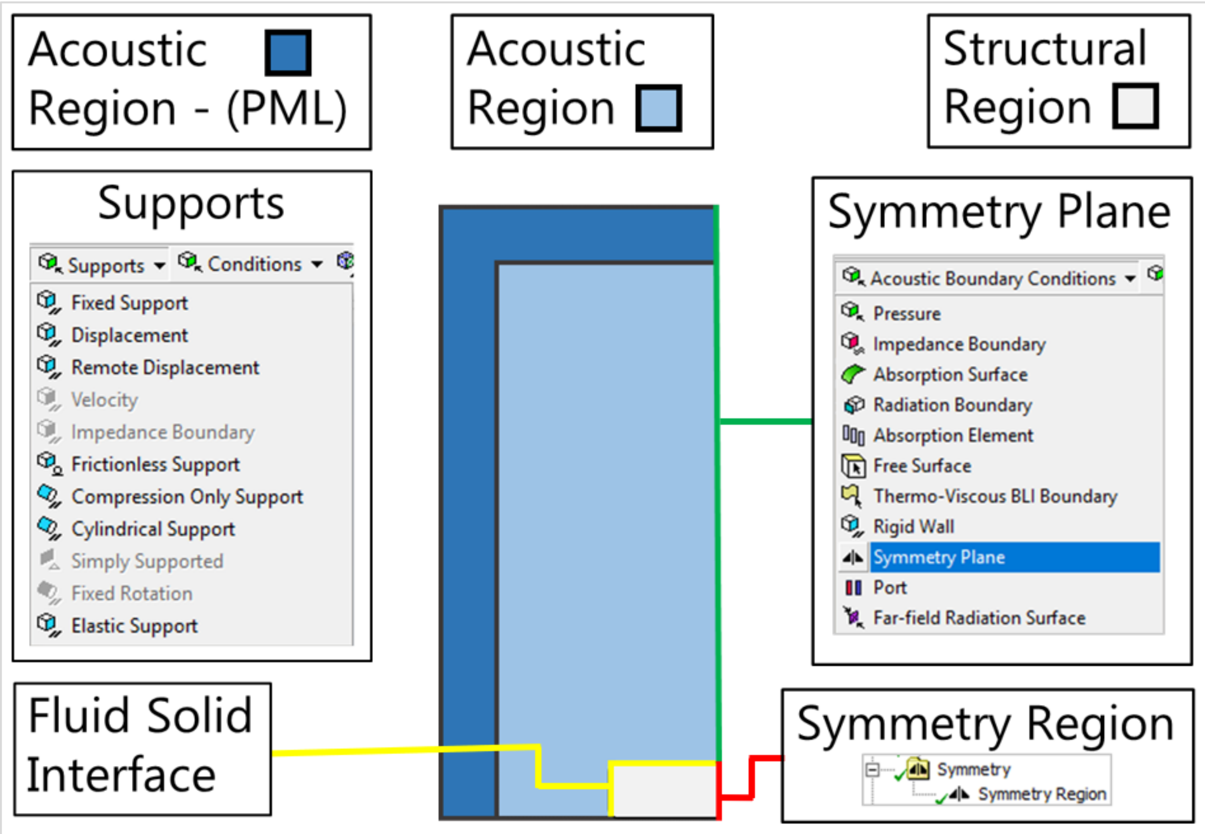

Figure 19: Physics region, coupling and boundary condition for acoustic simulation model

From the figure, there are two physics region and they are acoustic region and structural region. Acoustic region is set to acoustic body and structural region is set to structural body. In ANSYS Workbench, body that is set to acoustic region and structural region will automatically use acoustic fluid elements and structural solid elements respectively. For acoustic region, artificially matched layers option is available.

Fluid solid interface is set on surface of interaction between fluid and solid. This enables fluid structure interaction (FSI) between the fluid and solid which couples it. Suitable supports are placed based on assumptions of real-life setup. Symmetry region can only be set on structural body and symmetry plane can only be set on acoustic body. If model is reduced via plane/axis of symmetry, symmetry region and symmetry plane boundary condition is set on the cut surface of structural body and acoustic body respectively to ensure that the solver considers usage of symmetry.

3.7 Excitation Source

The methods to produce excitations are categorised into three as shown in Figure 20.

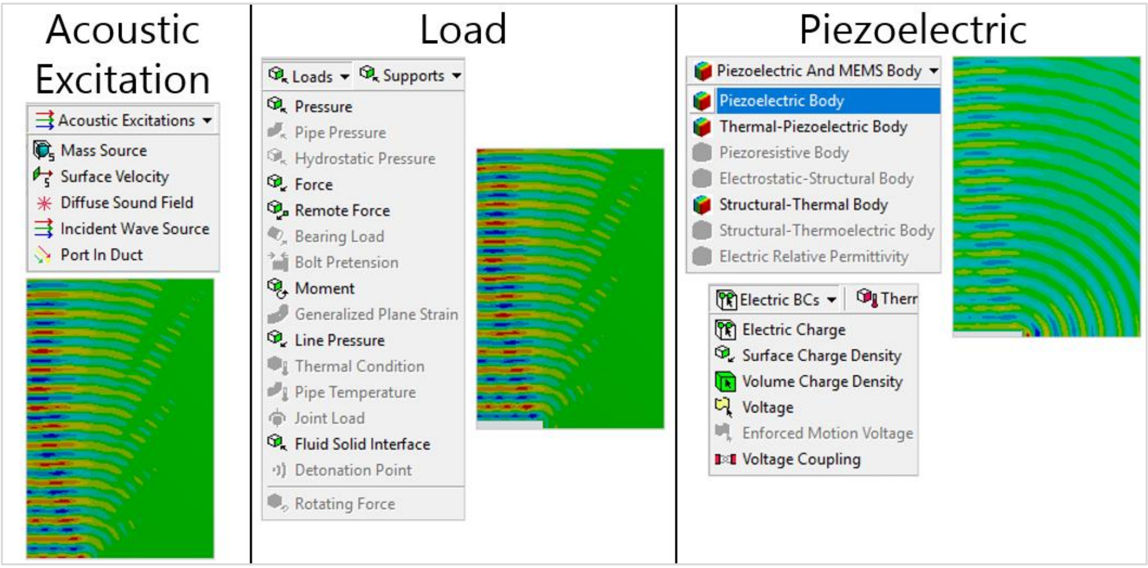

Figure 20: Three main excitation generation methods in ANSYS

Acoustic excitation can only be set on the exterior surface of an acoustic body. Surface Velocity is preferred among the acoustic excitation methods as it can replicate radiation of ultrasonic transducer. Surface Velocity produce excitation normal to the set surface.

Load can only be set on the surface of a structural body. Pressure and Force are preferred in the Load category as it is very straightforward. For Pressure, excitation produced is normal to the set surface. For Force, excitation produced is parallel to the set surface.

For piezoelectric, an ACT extension for ANSYS called Piezo and MEMS is required. The structural body need to be set as piezoelectric body. The piezoelectric body will automatically be made of coupled-field solid elements. Voltage difference is then set to the piezoelectric body using electric boundary condition provided. Side waves shown in Figure 20 indicates the orthotropic behaviour of piezoelectric material.

These methods only provide the magnitude of the excitation rather than the frequency. Excitation frequency is set as shown in Figure 21.

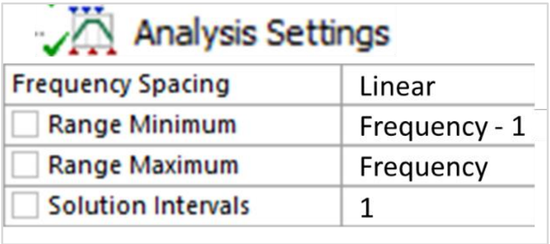

Figure 21: Setting excitation frequency

From Figure 21, frequency spacing is set to linear with solution intervals of 1. Frequency of interest is set to range maximum and frequency – 1 is set to range minimum. This results in solution for only the frequency of interest.

3.8 Solve Model

In this thesis, two variation of acoustic pressure solution is used as shown in Figure 22.

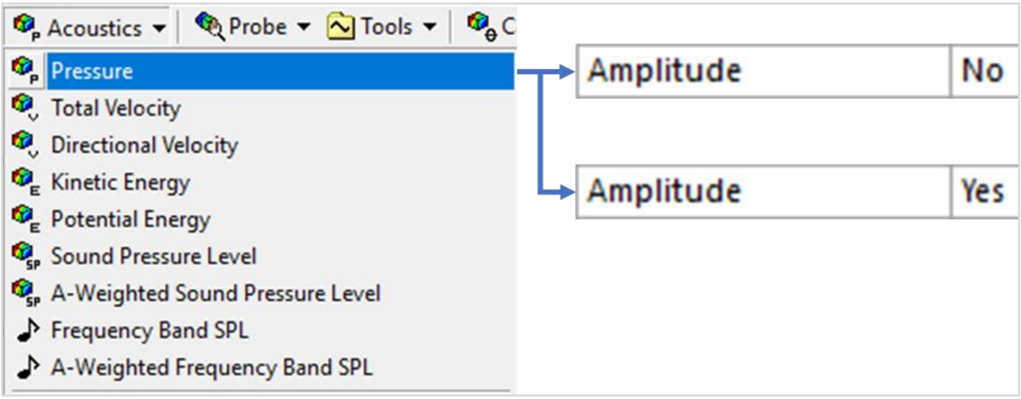

Figure 22:Acoustic pressure solutions

The first one is acoustic pressure with amplitude disabled which is the default setting. For this, the solution shows the positive and negative pressures in the field. The second variation is acoustic pressure with amplitude enabled. The second variation produces acoustic pressure field with pressure amplitude instead of positive and negative pressures. These two solution compliments each other which helps in studying acoustic pressure field.

To study the effect of varying certain parameter in the model to the acoustic pressure field, parameter feature is used to efficiently change the parameter of the model. Figure 23 below shows an arbitrary example of using the parameter feature.

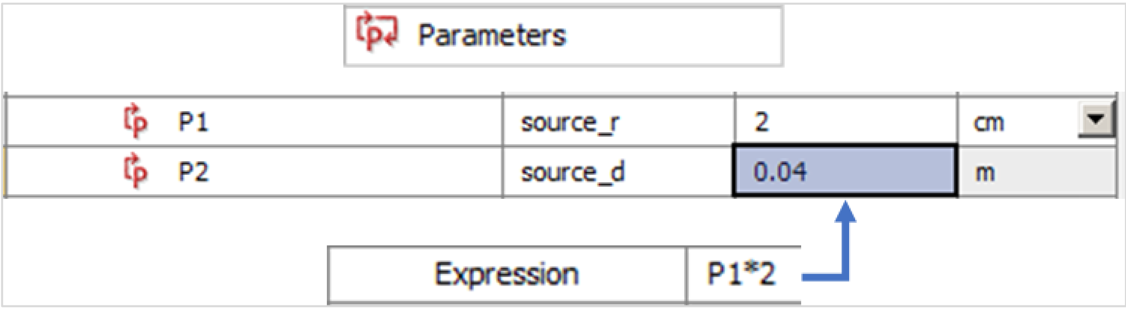

Figure 23: Parameter feature

From Figure 23, source_r is radius of transducer and source_d is diameter of transducer. Using expression, the diameter is made to be twice the radius of the transducer as it should be. By changing source_r, source_d will change as well based on the expression. These changes are reflected on the simulation model. This shows the usefulness of the parameter feature.

3.9 Post-Processing

Post-processing of simulation results is important as it makes the results comprehensible and allows proper comparison between results. In this thesis, post-processing involves:

- Rounding-off results to three significant figures to save space for comparison purpose
- Results shown side-by-side for better comparison
- Tables to summarise and compare results
- Graphs to compare and understand the effect of changes made to simulation model

4 TEST CASE 1: RADIATION OF BAFFLED PISTON

Test case 1 is made to validate the simulation methodology made from literature review by using the established methodology to replicate results from literature. This test case uses information on simulation of radiation produced by a baffled piston from a book on acoustic analysis written by Howard and Cazzolato [40]. Although this case does not involve ultrasonic transducer and excitation in the ultrasonic range, this case is viable since it is about the simulation of acoustic pressure field produced by an excitation source which is essentially what this thesis is about but with lower frequency used.

Howard and Cazzolato [40] provide instructions to produce the baffled piston radiation simulation. They did the simulation model in 2D by incorporating APDL commands (Appendix H). The commands allow 2D elements, material properties, boundary conditions and excitation input of interest be set on a 2D model. The simulation produces acoustic pressure field of up to 1m from the excitation source which is the piston. The main goal is to produce results similar to the acoustic pressure fields produced by them using models with similar methods and other known methods. The other methods involve 2.5D modelling with different approaches in setting the excitation source. 2.5D is just 3D but with relatively small thickness in one axis. Material properties used for all test case 1 models is provided in Appendix I.

4.1 Method and Comparison

In this section, methods used to build the simulation models for test case 1 are simultaneously stated, justified and compared with methods from the book.

4.1.1 2D Simulation Methods

Similar to the book, the 2D simulation model is made without any structural body. The piston model made for the 2D simulation is considered as acoustic body. The actual piston is the horizontal edge of the piston model.

Table 4: Similarities of test case 1 model and book model

Similarity	Comment
Element Type	Howard and Cazzolato [40] made the simulation model without using any structural element. Two 2D acoustic elements are used to simulate this model and the elements are FLUID29 and FLUID129. FLUID129 is placed on the edge of the acoustic body as it is an absorption element. The commands used to set these 2D elements are provided in Appendix H as mentioned previously.
Element Size	For linear elements at least 12 elements per wavelength is required. This is according to the acoustic model meshing guidelines. The element size is set to 2.0833mm via face sizing, edge sizing and all quad multizone method.
Excitation Source and Value Input	From the APDL commands, a harmonic displacement amplitude of 1μm is placed on the horizontal edge of the piston model.
Fluid Structure Interaction (FSI)	From the APDL commands, FSI is set on the horizontal edge of the piston model.
Model Reduction	The model is simplified by half (from semi-circle to a quarter circle). From the APDL commands, the axisymmetric option is enabled for both FLUID29 and FLUID129.
Wave Absorption Condition	FLUID129 is an acoustic absorption element. It is placed on the edge of the acoustic body. It can only be placed on circular edge with FLUID29 as the element used for the circle. This is essentially an Acoustic Boundary Condition (ABC).
Excitation Frequency	The excitation frequency used in the book is 13720Hz. This frequency is set for this test case.

Acoustic Body Size	The model is intended to produce acoustic pressure field of up to 1m. The acoustic body model is a quarter circle with 1m radius
Piston Size	The piston model is a quarter circle with 0.1m radius. The piston model is considered as the acoustic region. The actual piston is the horizontal edge of this model and not the whole 0.1m quarter circle.
Material Properties	The only material involved in this model is air. The sound speed is set to 343 ms^{-1} and the density is set to $1.21kgm^{-3}$.

Table 5: Differences of test case 1 model and book model

Difference	Comment
Software Version	The 2D simulation model for this test case is made by following the instructions provided in the book. However, the book uses ANSYS 14.5 which is a much older version of ANSYS. This test case uses ANSYS 19.1. Some instructions may be irrelevant, and some is just not possible to follow due to changes in the options provided.
Meshing	The meshing method is made by following the instructions. However, there are significant difference for the all quad multizone meshed piston model. This meshed zone for test case model and book model are shown in Figure 25.

Figure 24 shows the meshed 2D simulation model.

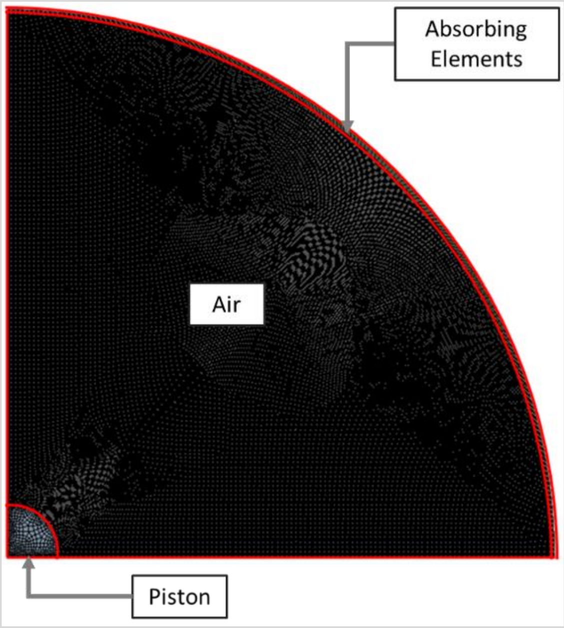

Figure 24: Meshed 2D model of test case 1 with piston, air and absorbing elements labelled

Red lines are used to distinguish the piston model, air model and absorbing elements location. This model has 185721 elements and 186518 nodes.

Figure 25 shows side-by-side comparison of the mesh of 2D piston model of test case 1 and mesh of 2D piston model from the book.

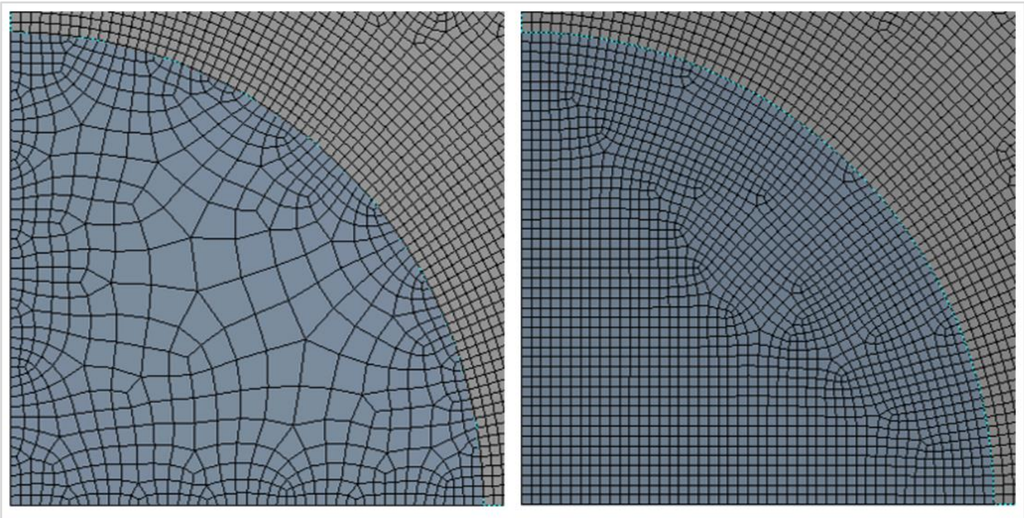

Figure 25: Mesh of 2D piston model of test case 1 (left) and book model (right)

The mesh of piston model of test case 1 is much coarser compared to the book model especially on the middle area even though it is made using the instructions from the book. The mesh should have element size of 2.0833mm throughout the model. The coarser part of the mesh clearly has much bigger element size.

4.1.2 2.5D Simulation Methods

There are three main variations for the 2.5D simulation models. The first one is a model without any structural region (i.e. the piston model is considered as acoustic region and the actual piston is the back horizontal surface of the model with FSI set to it). The second one is a model with the piston model set as a structural region. The third one is a model with the piston model set as a structural region and piezoelectric body. Although piston is not actually made of structural steel nor PZT4, these materials are arbitrarily set to test the produced acoustic pressure field using other excitation methods. The term "acoustic piston", "structural piston" and "piezoelectric piston" refers to these three variations respectively.

Table 6: Similarities of test case 1 model and book model

Similarity	Comment
Model Reduction	The simulation model is rectangular, and the piston model is placed on the middle bottom edge of the whole rectangle. The model is simplified by reducing the model to half. With this, the piston model is at the bottom left corner of the whole rectangle. Symmetry boundary condition is set to faces that lies on plane of symmetry. For acoustic piston, symmetry plane boundary condition is set to the piston, air and perfectly matched layer (PML) model. For structural piston and piezoelectric piston, symmetry region boundary condition is set to the piston model and symmetry plane boundary condition is set to the air model and PML model.
Excitation Frequency	The excitation frequency used in the book is 13720Hz. This frequency is set for this test case.

Table 7: Differences of test case 1 model and book model

Differences	Comment
Element Type	Simulation model from the book uses 2D acoustic elements. The 2.5D test case simulation model uses 3D acoustic and structural elements. The elements are FLUID220 (acoustic fluid), SOLID186 (structural solid) and SOLID226 (coupled-field solid).
Element Size	For quadratic elements, at least 6 elements per wavelength is required. This is according to the acoustic model meshing

	guidelines. The element size is set to 4mm via body sizing and all quad multizone meshing.
Excitation source and Value Input	For acoustic piston, a surface velocity of $1ms^{-1}$ is set on the back horizontal surface of the piston model. For structural piston, a force of 1N is set as the excitation. For piezoelectric piston, excitation is produced by setting potential difference of 1V across PZT4.
Fluid Structure Interaction (FSI)	For structural piston and piezoelectric piston, fluid solid interface boundary condition is set on the piston surfaces which are directly in contact with the air model to enable FSI.
Wave Absorption Condition	PML is used in the 2.5D model. According to acoustic analysis guide provided in ANSYS customer portal, at least 2 layers of PML elements and 2 layers of buffer elements is required to achieve acceptable numerical accuracy. PML thickness is set to 0.02m which means for 4mm element size, there will be 5 layers of PML elements. The 2.5D meshed model in Figure 3 clearly shows that the layers of buffer elements (i.e. elements between excitation source and PML) is much higher than 2.
Acoustic Region Size	The acoustic region is a rectangle with vertical length of 1m and horizontal length of 0.4m (after model reduction). With the PML region, the size increases by 0.02m in both vertical and horizontal length.
Piston Size	The piston model is a rectangle with vertical length of 0.01m and horizontal length of 0.1m (after model reduction).
Thickness (Z-Axis)	For 2.5D simulation model, the thickness of the model needs to be relatively small in one axis. This simulation model is done in XY plane and the thickness in z-axis is set to 0.01m.
Material Properties	For acoustic piston, the only material is air. For structural piston, the materials are structural steel and air. For piezoelectric piston, the materials are PZT4 (y-poling direction) and air. The default material properties of air provided by ANSYS is used and the properties slightly differs from the properties set in the book model. Material properties of air, structural steel and PZT4 are provided in Appendix I.

Figure 26 shows the meshed 2.5D simulation model.

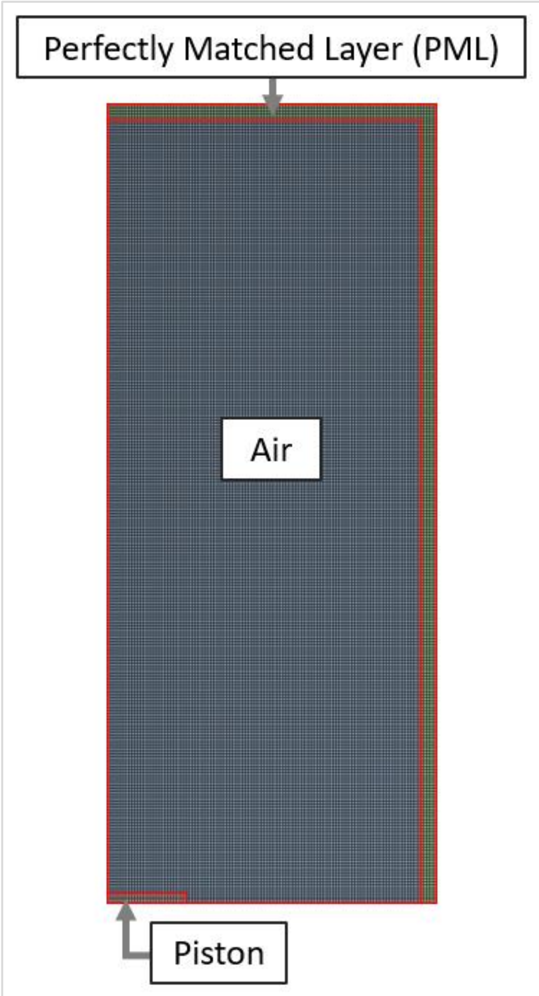

Figure 26: Meshed 2D model of test case 1 with piston, air and PML labelled

Red lines are used to distinguish the piston model, air model and PML model. The element size and shape are uniform throughout the model. This model has 81408 elements and 411029 nodes.

4.2 Results

4.2.1 Initial Results

4.2.1.1 2D Simulation

The resulting acoustic pressure field from the 2D test case model and from the book are shown in Figure 27.

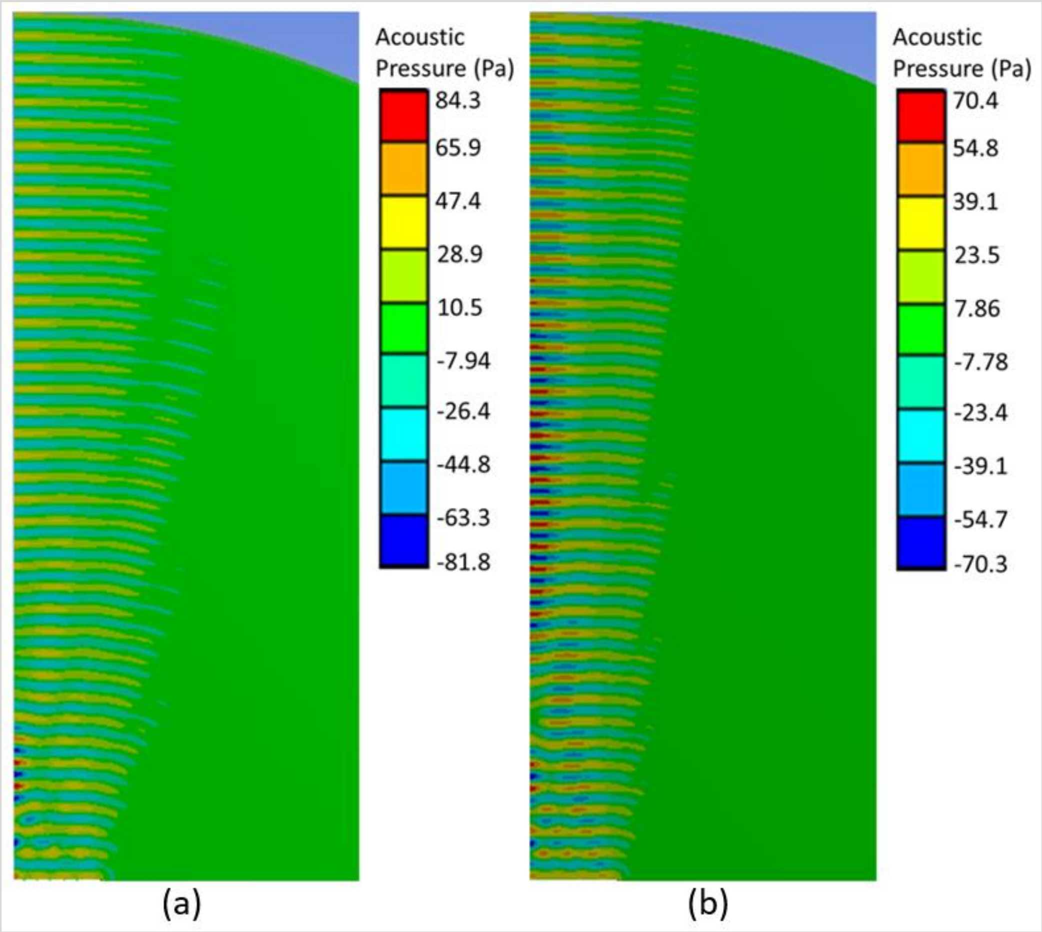

Figure 27: Acoustic pressure field: (a) 2D test case (2D-NU) and (b) book model (2D-BM)

The positive and negative maximum pressure for the test case model is higher compared to the ones from the book model. Acoustic pressure field pattern for the test case slightly differs from the book. The features of the pattern are more visible for the book model. This just means that the area of high pressure and low pressure can be distinguished easily. For test case model, maximum pressure is located near the piston while for the book model, the maximum pressure is located much further from the piston.

4.2.1.2 2.5D Simulation

The resulting acoustic pressure field from the 2.5D test case models are shown in Figure 28.

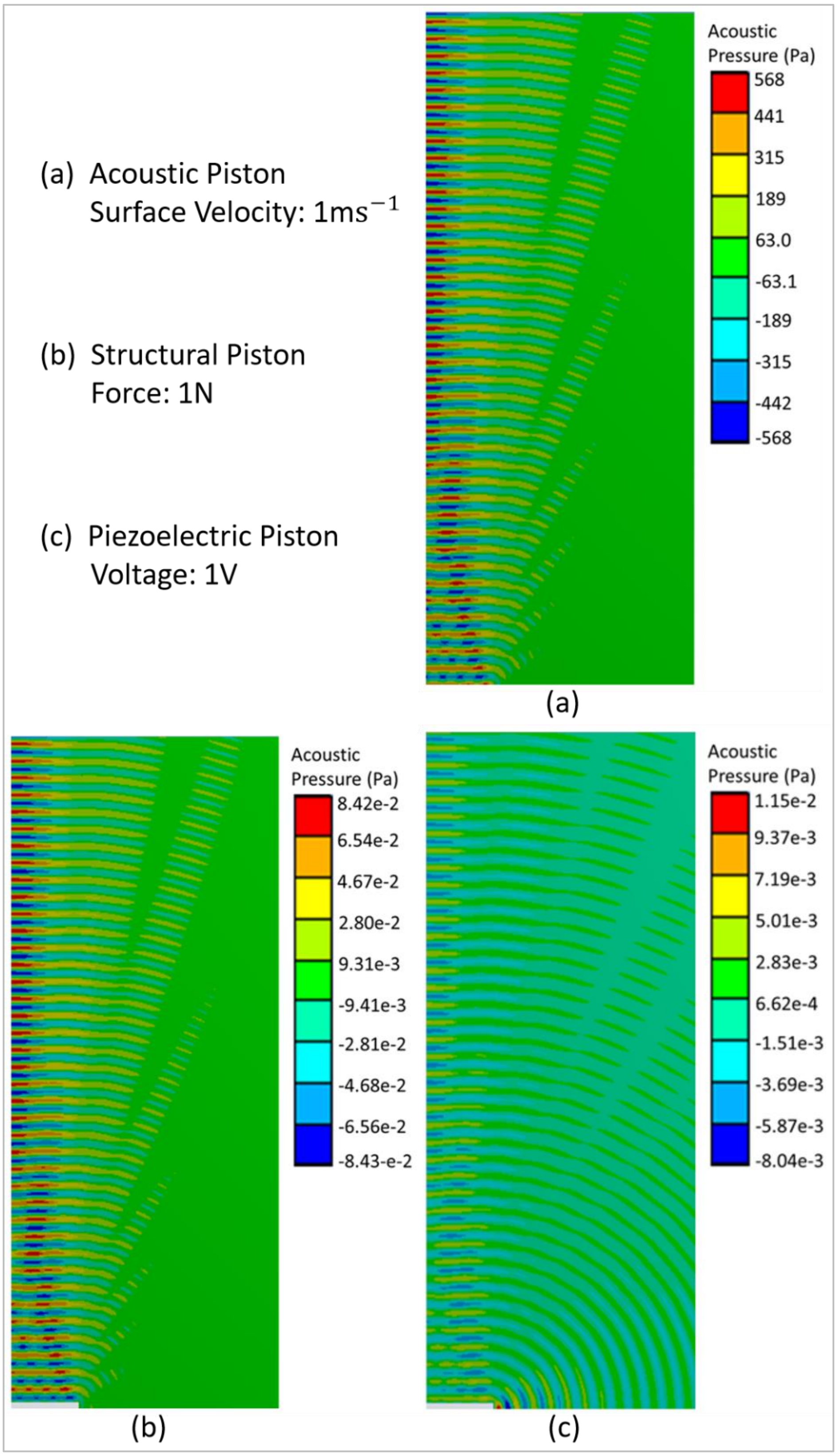

Figure 28: Acoustic pressure field of 2.5D test case models: (a) acoustic piston, (b) structural piston and (c) piezoelectric piston

From Figure 28(a), the acoustic pressure field pattern produced using surface velocity is very similar to the pattern produced by the 2D simulation model from the book. The 2.5D model improves the features of the pattern. The piston model here is visible as it is not considered as acoustic region for this simulation model. From Figure 28(b), the acoustic pressure field pattern produced using force is very similar to the pattern produced by the 2D model from the book and the 2.5D acoustic piston model. Unlike the other 2.5D models, the acoustic pressure field pattern produced using piezoelectric effect results in additional wave propagation on the side of the piston (Figure 28(c)). Disregarding the side waves, the acoustic pressure field pattern produced by this model shows some similarity to the 2D simulation model from the book.

4.2.2 Improvements

4.2.2.1 Uniform Surface Mesh for 2D Model

The 2D test case simulation model is expected to produce identical results with the model from the book as it is made by following the instructions from the book. However, meshing of the test case piston model is non-uniform in size and acoustic pressure field produced by the model differs from the book model. The coarser mesh of the piston model is fixed by setting the surface mesh method of multizone meshing to uniform. Figure 29 shows the new meshed model.

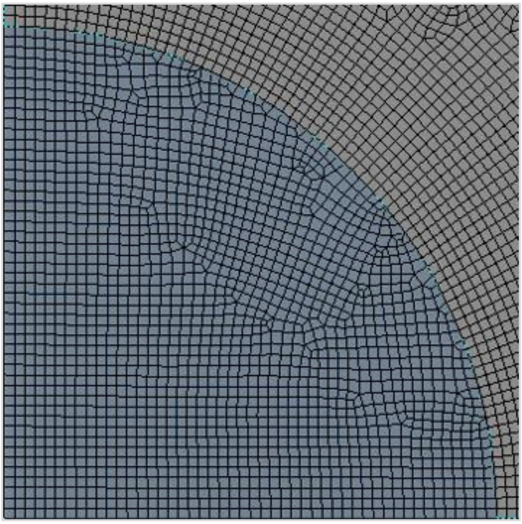

Figure 29: Mesh of 2D piston model after surface mesh method of multizone meshing is set to uniform

The mesh of piston model is now uniform and the set element size of 2.0833mm is maintained. This is very important as all the elements now follows the meshing guidelines for linear elements (i.e. there is at least 12 elements per wavelength). This model has 186886 elements and 187683 nodes.

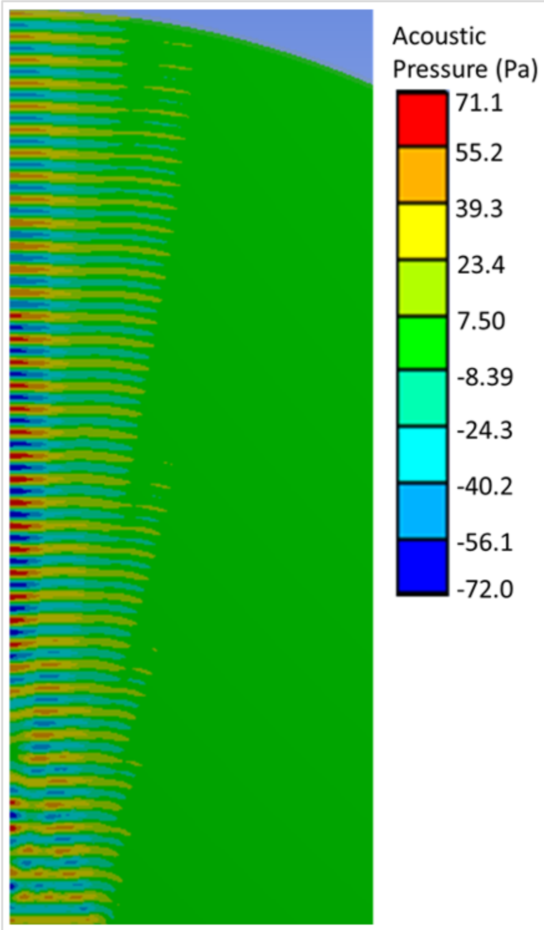

Figure 30: Acoustic pressure field of 2D test case model with uniform meshing (2D-U)

With uniform meshing and adequate element size, the resulting acoustic pressure field is improved in both magnitude and pattern. The positive and negative maximum pressure from this model is very close to the ones from the book model. The acoustic pressure field pattern from this model and the book model is identical.

4.2.2.2 Fixed Support for 2.5D Piezoelectric Piston

To discard the effect of the side piston movement, fixed support is placed on the side of the piston model. The resulting acoustic pressure field from this model is shown in Figure 31.

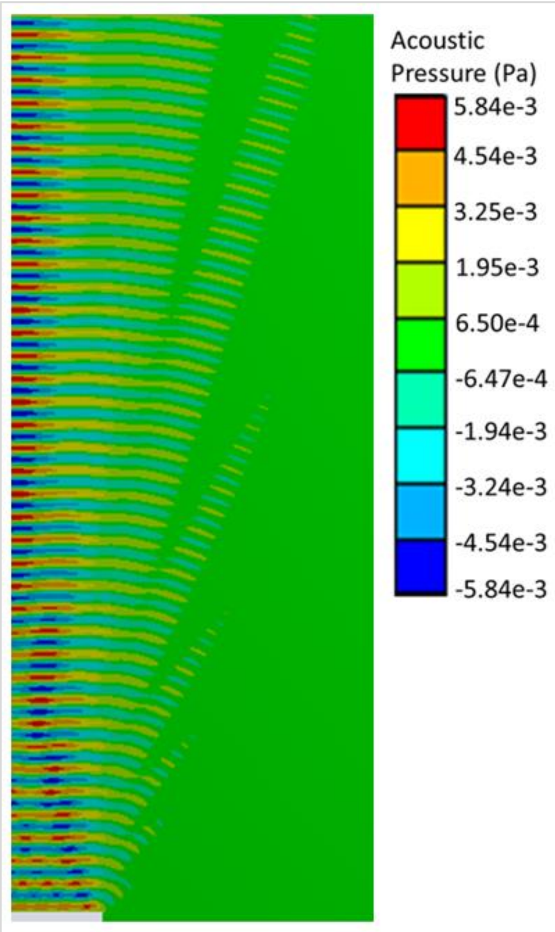

Figure 31: Acoustic pressure field produced by PZT4 with fixed support on the side of the piston model

The addition of fixed support on the side of the piston prevents wave propagation on the side of the piston. The resulting pattern is now very similar to the pattern produced by the 2D model from the book, 2.5D acoustic piston model and 2.5D structural piston model.

4.2.2.3 Scaled Excitation Input Value for All 2.5D Models

Acoustic pressure magnitude of previous 2.5D models cannot be compared properly with the acoustic pressure magnitude from the book model due to excitation inputs that are inequivalent to a harmonic displacement amplitude of 1μm. To fix this, it is important to know that the magnitude of acoustic pressure produced is directly proportional to the excitation input value. Therefore, the excitation input can be scaled to a value that can produce acoustic pressure with similar magnitudes to the acoustic pressure from the book model using the following formula:

$$scaled\ input\ value = \frac{referred\ pressure}{actual\ pressure} \times input\ value \tag{16}$$

The scaled input value for all 2.5D models are provided in Table 9. Maximum pressure from the book model and the 2.5D models are set as the referred pressure and actual pressure respectively. Figure 34 shows the acoustic pressure field of all 2.5D models after scaled input value is set.

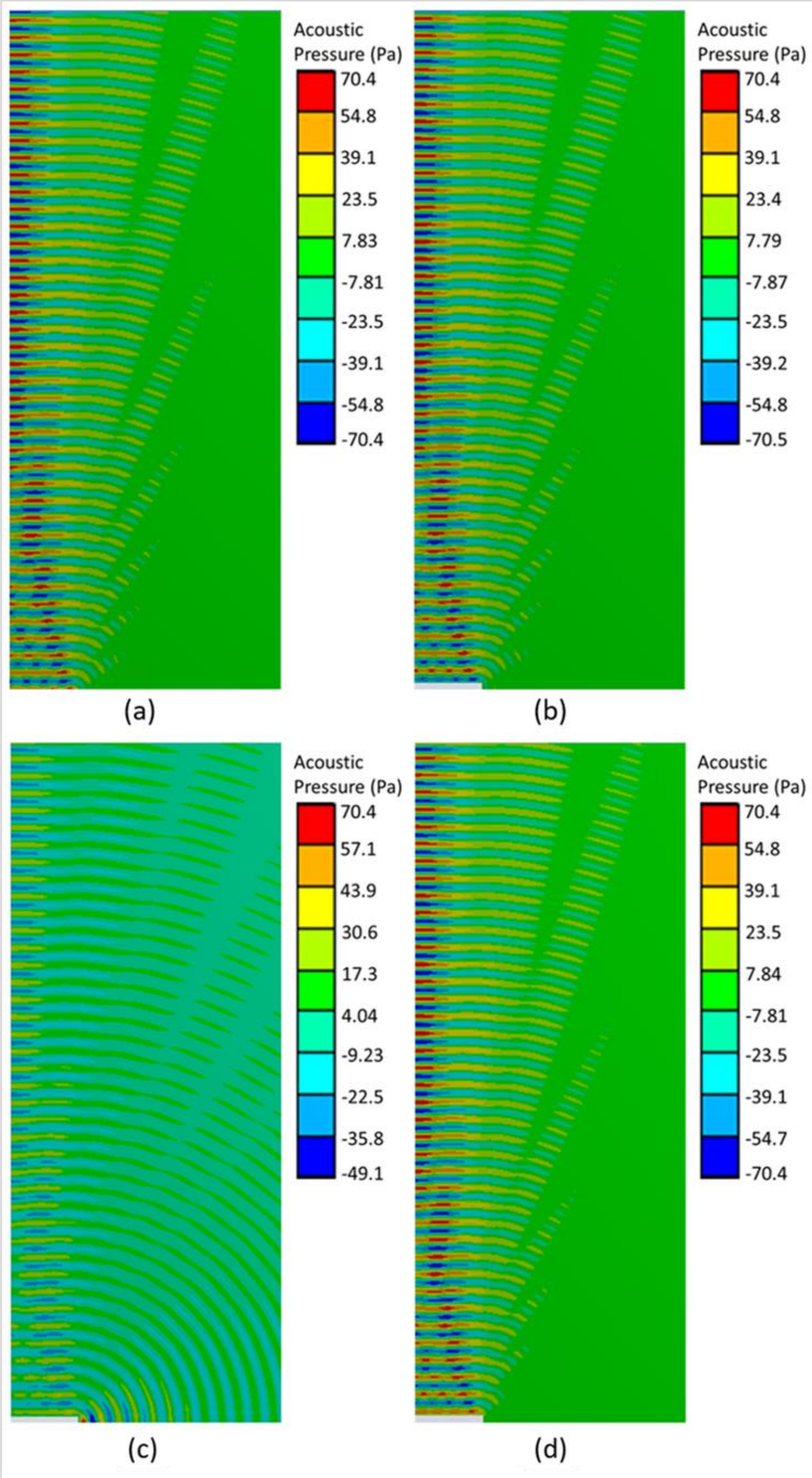

Figure 32: Acoustic pressure field after input value change: (a) surface velocity (2.5D-A), (b) force (2.5D-SS), (c) voltage (2.5D-PZT4) and (d) voltage (model with side fixed support) (2.5D-PZT4-S)

The positive maximum positive pressure should be the same for all 2.5D models which are shown in Figure 32. The negative maximum pressure for all 2.5D models is very close to the book model except the piezoelectric piston model without fixed support (Figure 32(d)).

4.2.3 Data Tabulation and Plotting

The data from initial results, improvements and computational information of 2D and 2.5D baffled piston radiation simulation models are tabulated below.

Table 8: Data from 2D baffled piston radiation simulation models including the simulation model from referred book

Simulation Model	2D-BM (Book Model)	2D-NU	2D-U
Piston Model Material	Air	Air	Air
Element Size, mm	2.0833	2.0833	2.0833
Number of Elements	N/A	185721	186886
Number of Nodes	189213	186518	187683
Wave Absorption Method	Absorption elements	Absorption elements	Absorption elements
Mesh	Uniform	Non-uniform (piston)	Uniform
Excitation Type	Harmonic displacement	Harmonic displacement	Harmonic displacement
Input Value	1µm	1µm	1µm
Max Pressure, Pa	70.419	84.337	71.066
Min Pressure, Pa	-70.344	-81.754	-71.951
Acoustic Pressure Field Similarity	N/A	High	Very high
MAPDL Elapsed Time	N/A	12 s	12 s
MAPDL Memory Used, GB	N/A	1.2705	1.2764
MAPDL Result File Size, GB	N/A	0.16406	0.16531

Table 9: Data from all variations of 2.5D baffled piston radiation simulation model

Simulation Model	2.5D-A	2.5D-SS	2.5D-PZT4	2.5D-PZT4-S
Piston Model Material	Air	Structural Steel	PZT4	PZT4
Element Size, mm	4	4	4	4
Number of Elements	81408	81408	81408	81408
Number of nodes	411029	411029	411029	411029
Wave Absorption Method	PML	PML	PML	PML
Mesh	Uniform	Uniform	Uniform	Uniform
Piston Fixed Support	N/A	N/A	N/A	Side
Excitation type	Surface velocity	Force	Voltage	Voltage
Input Value	$1ms^{-1}$	1N	1V	1V
Max Pressure, Pa	567.50	0.084163	0.011542	0.0058399
Min Pressure, Pa	-567.66	-0.084267	-0.0080425	-0.0058373
Scaled Input Value	$0.12409ms^{-1}$	836.670N	6101.1V	12058V
New Max Pressure, Pa	70.419	70.419	70.422	70.420
New Min Pressure, Pa	-70.399	-70.506	-49.068	-70.387
Acoustic Pressure Field Similarity	Very high	Very high	Medium	Very high
MAPDL Elapsed Time	29 s	32 s	40 s	41 s
MAPDL Memory Used, GB	3.5645	3.7568	6.416	6.3496
MAPDL Result File Size, GB	0.12394	0.14275	0.14900	0.14906

Graph of maximum acoustic pressure against baffled radiation piston simulation models is shown in Figure 33.

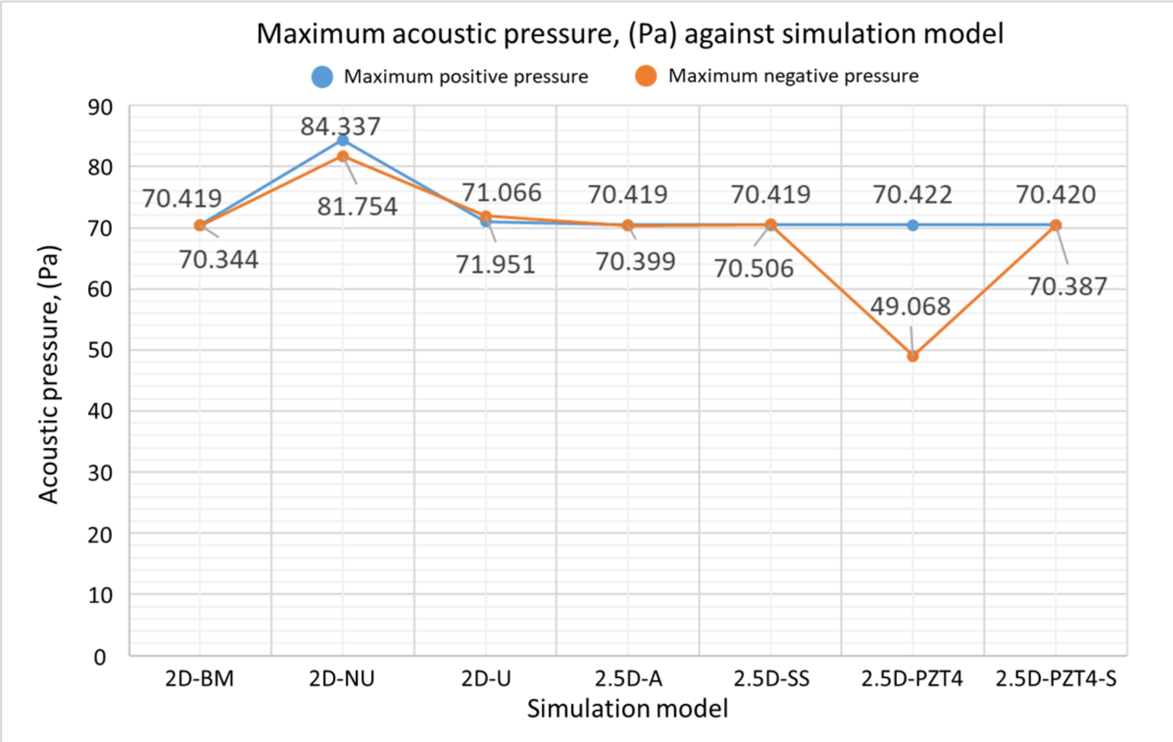

Figure 33: Graph of maximum acoustic pressure, (Pa) against 2D/2.5D simulation model

From the graph, the maximum pressures of 2D-NU are much higher than 2D-BM. With surface mesh set to uniform (2D-U), the maximum pressures almost converge to the pressures from 2D-BM. This is because of the slight difference between meshing of 2D-U and 2D-BM. This difference can be seen by comparing Figure 29 and Figure 25 and also by comparing node counts provided in Table 8. For 2.5D models, the maximum positive pressure should be the same value as 2D-BM since the scaled input values used are obtained using maximum positive pressure values as the pressure input. However, 2.5D-PZT4 and 2.5DPZT4-S produces slightly higher maximum acoustic pressure than 2D-BM. This is assumed to be caused by computational roundoff errors. Since the scaled input values are designed to obtain similar maximum positive pressure, the maximum negative pressure should be compared between the models. Maximum negative pressure of 2.5DPZT4-S is the closest to 2D-BM followed by 2.5D-A, 2.5D-SS and 2.5D-PZT4. 2.5DPZT4 shows significant difference in maximum negative pressure when compared to other 2.5D models and 2D-BM.

Graph of computational resource against baffled radiation piston simulation models is shown in Figure 34.

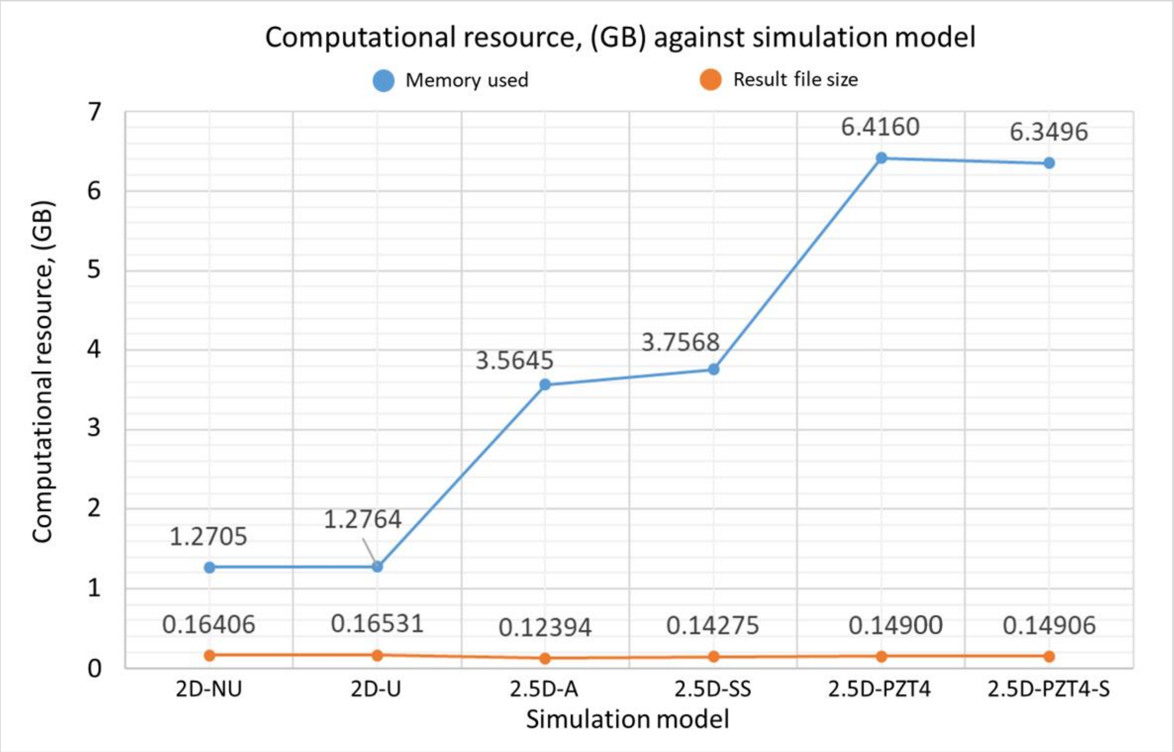

Figure 34: Graph of computational resource, (GB) against 2D/2.5D simulation model

From the memory used plot, the memory required slightly increases from 1.2705GB to 1.274GB when uniform meshing is used. This is because of the increase in number of elements and nodes of the 2D meshed model. There is significant increase (3.5645GB) in memory usage when 2.5D model is used. When structural region is introduced along with FSI on the structural surface, the memory usage slightly increases to 3.7568GB. This is because there are more nodes that have both displacement and pressure DOF from larger FSI enabled surface. Another notable increase (6.4160GB) in memory usage occur when piezoelectric body and voltage-applied surface are included in the model. This is because of the addition of volt in the DOF of coupled nodes. The memory usage slightly drops to 6.3496GB with addition of side fixed support. The fixed support restricts movement of the side nodes of the piston model which made the effect of the side nodes excluded during solving process leading to less resource required.

From the result file size plot, the file size for 2D models is more than 2.5D models. The file size also increases with element and node counts. For 2.5D models, there is relatively high increase (from 0.12394GB to 0.14275GB) of file size when structural region is introduced along with FSI on the structural surface. The addition of piezoelectric body and voltage-applied surface slightly increase the file size to (0.14900GB). Unlike the memory used plot, the result file size plot shows very small increase in computational resource required when side fixed support is added. This shows that the trend of result file size plot does not necessarily follows the memory used plot. From both plots, the overall computational resource required for 2D models is less than 2.5D models.

Graph of computation time against baffled radiation piston simulation models is shown in Figure 35.

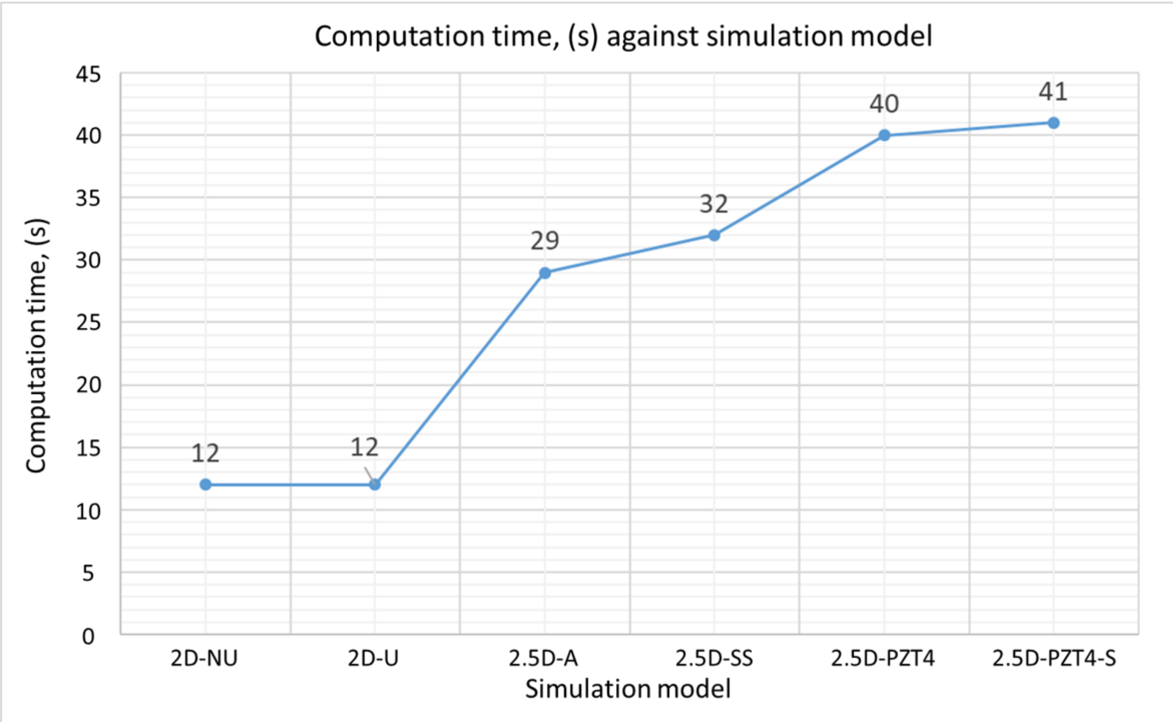

Figure 35: Graph of computation time, (s) against 2D/2.5D simulation model

From the computation time plot, 2D models is computed much faster compared to 2.5D models. When this plot is compared to memory used plot in Figure 34, there is similarity in the plot trend except when side fixed support is added. The computation time plot shows behaviour of a mix between the memory used plot and result file size plot.

4.3 Discussion and Recommendation

Although the 2D test case simulation model is made according to the instructions in the book, the results obtained from the 2D test case model differs from the book model due to large difference in the software version used. The initial 2D simulation produces piston model with non-uniform meshing instead of uniform meshing and this affects the acoustic pressure field produced by the model. The middle area of the piston model has coarse mesh which means that the area is filled with elements with larger size than 1/12 wavelength and acoustic meshing guideline is not followed. The number of elements in that area is insufficient to properly capture and transfer the effect of harmonic load at 13720Hz in air. This is evident in Figure 4 where the maximum pressure is located near the piston while for the book model, the maximum pressure is located much further from the piston. To ensure uniform mesh size for this model, the surface mesh method for multizone meshing is then set to uniform. With uniform meshing and adequate element size, the resulting acoustic pressure field is improved in both magnitude and pattern. It is recommended to check the mesh and improve it if the model is not meshed as intended to ensure satisfactory results.

For 2.5D simulation, the acoustic piston and structural piston model produces similar acoustic pressure field pattern to the pattern produced by book model. The 2.5D models also improves the features of the pattern making the wave propagations, area of high pressures and area of low pressures more distinctive. The piezoelectric piston model produces acoustic pressure field with additional wave propagation on the side of the piston model. This is caused by the piezoelectric effect on PZT4 which is orthotropic. The PZT4 piston vibrate in a way that the length in the propagation axis extends and the length in the other two axes contracts and vice versa. Due to this, the side of the piston also produces wave. Fixed support is then placed on the side of the piston model to restrain the side nodes from moving. With the fixed support, the acoustic pressure field pattern is identical to the pattern from all other 2.5D models. Based on the three main variations of 2.5D simulation models, it is recommended to simulate radiation of baffled piston or most generic case with simple excitation source on one end by modelling the case with full acoustic body with harmonic excitation that can be set on acoustic body such as surface velocity. This method is the simplest and yet it requires the least computational resource and computation time to produce satisfactory result.

In the improvement section, it is demonstrated that scaled input value can be calculated and used to obtain similar acoustic pressure value (Figure 32). It is recommended to do this to allow proper comparison of the magnitude and pattern of acoustic pressure field from simulation model to results from referred work when the excitation source and input value set is not similar to the referred work. When comparing 2D simulation with 2.5D simulation, 2D simulation uses less memory and storage size and is simulated faster compared to 2.5D simulation. However, 2.5D simulation is easier to make compared to 2D since 2D simulation requires APDL commands. If the user is experienced with using APDL commands, then 2D can be the definite better choice.

5 TEST CASE 2: ULTRASONIC CLEANING TANK

Test case 2 is another section made to validate the simulation methodology made from literature review by using the established methodology to replicate results from literature. This test case uses information provided in research articles by Tangsopha, Thongsri and Busayaporn [25] on ultrasonic cleaning simulation to study ways to improve cleaning efficiency. They did this by varying excitation frequency and power input of transducer in the simulation to obtain and compare the resulting acoustic pressure fields. They validate their result by comparing their acoustic pressure field from simulation with an experiment result that yields erosion pattern (due to ultrasonic cavitation) on an aluminium foil plate placed in the middle of ultrasonic cleaning tank where the tank is made to operate with similar settings to the simulation. For this test case, the main goal is to obtain acoustic pressure field pattern similar to the pattern from simulation done by them.

There are three research articles by Tangsopha et al [25] on the same theme which are published in 2017, 2018 and 2019 respectively. The newer version covers transducer configuration from 2017 as well as several other proposed transducer configurations and excitation frequency. Transducer configuration here means the placement of transducer on the ultrasonic cleaning tank. This test case uses material properties, excitation frequency, transducer configuration and results provided in their 2017 research article (Appendix J). Size of the tank, plate, transducer and distances between transducers for the model are taken from 2019 research article (Appendix K) as the 2017 research article did not provide this. For clarity, "research article" or "article" in this section refers to the 2017 research article.

5.1 Method and Comparison

In this section, methods used to build the simulation model for test case 2 are simultaneously stated, justified and compared with methods from research article.

Table 10: Similarities of test case 2 model and research article model

Similarity	Comment
Element Type	It was stated by Tangsopha et al [25] that hexahedral mesh is used for their simulation model. This means that their model consists of FLUID220/FLUID221 for fluid, SOLID186/SOLID187 for solid and SOLID226/SOLID227 for piezoelectric solid. FLUID221, SOLID187 and SOLID227 are the 10-node tetrahedral variation which are used instead of FLUID220, SOLID186 AND SOLID226 (20-node brick) when the part to be modelled have insufficient volume to surface area ratio for set element size. The model for this test case uses hexahedral mesh where 20-node brick element is used for tank and transducer while 10-node tetrahedral element is used for the plate.
Excitation Source	Since this simulation model involves excitation done by transducer with plate in between it and the acoustic region, acoustic excitation source option which must be set on the acoustic region itself is not viable. In the research article, the transducer model is made with minor simplification and most material properties of PZT4 are provided in the research article. Therefore, the model in the research article most likely use piezoelectric excitation source which requires a solid body set as piezoelectric body and an electricity input across the body to excite it. The model for this test case utilised piezo and MEMS ACT extension to create piezoelectric excitation source.
No Model Reduction	For a symmetrical model, model reduction is highly recommended especially for a relatively simple simulation model as it produces identical result with less computation time. However, the ultrasonic cleaning tank model is considered complex enough that there may be large difference in the pressure output between the reduced model variation and the full model. Therefore, just like

	the research article model, the model for this test case is not reduced.
Wave Absorption Condition	There is no PML layer set in the research article model, it is not stated whether other wave absorption method is used. It is assumed that no wave absorption method is used. This will cause reflection on the boundary of acoustic domain which is most likely intended since waves in water in the tank would be reflected due to high impedance difference. For this reason, no wave absorption method is used for this test case model.
Excitation Frequency	The excitation frequency used in the research article model is 28kHz, 48kHz and 68kHz. Higher excitation frequency requires smaller element size according to meshing guideline for acoustic model. Due to this, the test case only focuses on obtaining similar acoustic pressure field pattern for 28kHz and 48kHz to minimise overall computation time required for this test case. To obtain similar acoustic pressure field pattern, the excitation frequency used in this test case should be 28kHz and 48kHz.
Tank Size (Inside)	The research article stated that their model is based on an ultrasonic tank with the size of 244mm x 340mm x 290mm (width x length x depth). However, the measurement of the inside of the tank is not given in the 2017 research article. This measurement along with plate size, transducer quantity, transducer placement and transducer contact surface diameter is provided in the 2019 research article. Appendix K shows the provided measurements. The tank size is made according to Appendix K.
Transducer Quantity and Placement	According to Appendix K.
Plate Size	According to Appendix K.
Transducer Contact Surface Diameter	According to Appendix K.
Material Properties	Properties of water at 45°C, stainless steel, aluminium alloy and PZT4 follows the research article. The properties are provided in Appendix J. There is a slight variation made to the PZT4

	properties which will be discussed in the differences section below.

Table 11: Differences of test case 2 model and research article model

Difference	Comment
Element Size	Tangsopha et al [25] did not provide the element size set to their model. However, it is stated that their model has 6 elements per wavelength indicating that they follow the meshing guideline for 3D acoustic model which uses quadratic elements. The model for this test case also follows the same guideline by ensuring that the element size is set where there are at least 6 elements per wavelength. The element size is set to 5mm.
Boundary Conditions (Support)	The support type and location are not stated in the research article. For this test case, fixed support is placed on the bottom of the transducer (opposite direction of ultrasonic wave propagation of interest).
Transducer Model	A typical transducer used in ultrasonic cleaning consists of 2 piezoelectric ceramic which are stacked together and is sandwiched between 2 metal with bolts used to keep those materials intact. The transducer model in the research article slightly simplifies this by making the stacked piezoelectric ceramic as 1 piezoelectric ceramic. Also, in the research article, there is a ring-shaped part in between the plate model and the transducer model which is assumed to be the epoxy adhesive to stick them together. However, the material properties of the adhesive are not provided. For simplicity, the transducer model used for this test case is cylinder with 5.8cm diameter and 0.8cm height.
Material of Plate and Transducer	The material assigned to the plate and transducer components are not stated in the research article. However, ultrasonic cleaning setup generally uses stainless steel ultrasonic cleaning tank and aluminium alloy transducer. The first few simulation models for this test case are made before this was known. It is assumed that

	the plate is made of aluminium alloy. Since the transducer model for this test case is just a cylinder, PZT4 is assigned to it.
Electricity Input	Tangsopha et al [25] done their simulation with 300W, 350W and 400W. It is not known how to set Power (W) as the input. Change in electricity input value causes change in vibration magnitude of piezoelectric ceramic. This affect the acoustic pressure magnitude and therefore, contouring intensity of the acoustic pressure field. Since the aim for this test case is to obtain similar acoustic pressure field pattern, an arbitrary non-extreme voltage input is set. The voltage input is set to 150V for all transducers used in this test case.
C33 Value (Elasticity Matrix – Z Poling Direction)	The C33 value is not provided in the research article. Therefore, the exact C33 value of the PZT4 is assumed to be 1.15E+11Pa.

Figure 36 shows simple representation of the model.

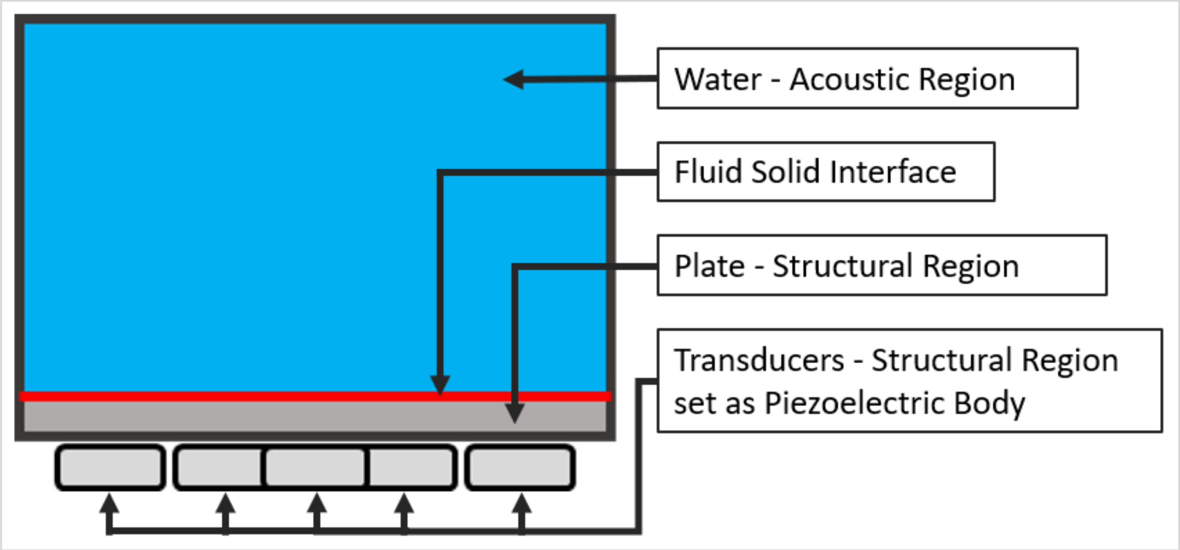

Figure 36: Simple representation of test case 2 model with region and fluid solid interface specification

Figure 37 shows side-by-side comparison of meshed model of test case 2 and meshed model from research article.

Figure 37: Meshed model of test case 2 (left) and meshed model from research article (right)

The meshed model of test case 2 have a simplified excitation source with contact diameter of 5.8cm which is based on the research article model. The element size for test case 2 is smaller compared to research article model. Total number of elements and nodes for test case 2 model are 179369 and 688224 respectively.

5.2 Results

5.2.1 Initial Results

The resulting acoustic pressure field from the test case model is shown alongside acoustic pressure field from research article in Figure 38.

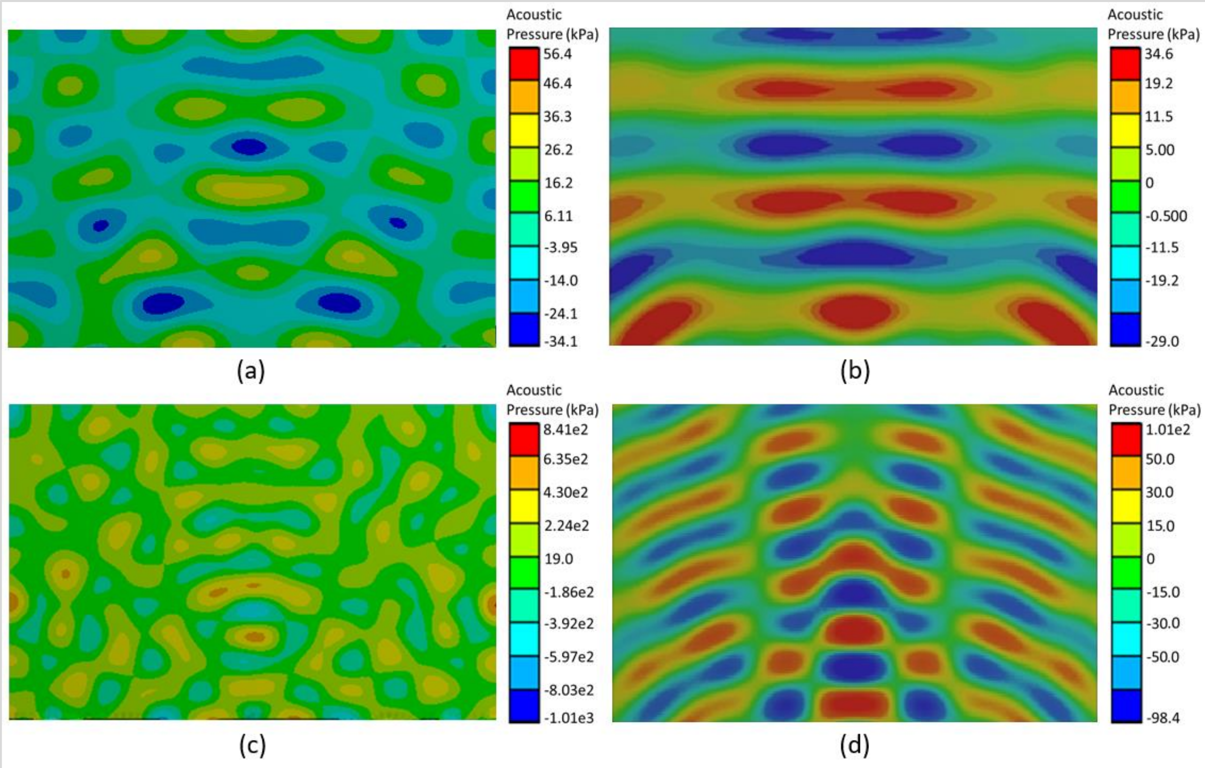

Figure 38: Acoustic pressure field: (a) test case 28kHz (28kHz-1), (b) research article 28kHz, (c) test case 48kHz (48kHz-1) and (d) research article 48kHz

Area of pressures close to maximum pressure (indicated by red and orange colour) are barely present in the middle of the pressure field for test case1. Disregarding this however, there is some pattern similarity between the acoustic pressure field of test case 2 and acoustic pressure field from research article especially for 28kHz result. Improvements on the simulation method are necessary to increase the similarity of acoustic pressure field pattern.

5.2.2 Improvements

5.2.2.1 Fixed Support on Edges of Plate

To improve pattern similarity of acoustic pressure field from test case with acoustic pressure field from research article, boundary conditions used in the test case requires revision. It is found that the edges of the plate are not supposed to move since the plate is a direct representation of the bottom part of the ultrasonic tank instead of being another separate plate placed at the bottom on the inside of the tank. The movement of the edges of the plate are constrained by the tank wall that is connected to it. To translate this into the simulation, fixed supports are set on the edges of plate model to prevent axial movement of the edges. Figure 39 below shows the resulting acoustic pressure field.

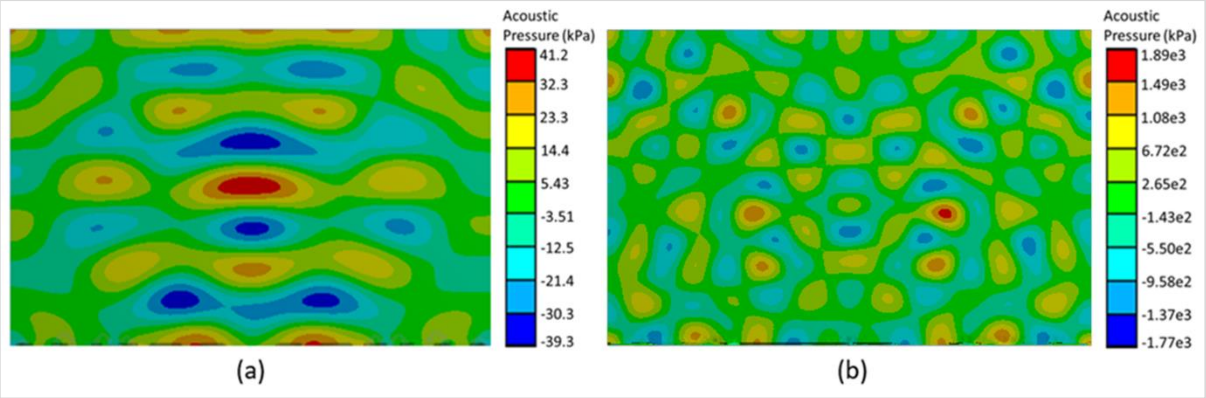

Figure 39: Acoustic pressure field after addition of fixed support: (a) test case 28kHz (28kHz-2) and (b) test case 48kHz (48kHz-2)

With the addition of fixed supports, the resulting acoustic pressure field pattern of test case 2 for 28kHz looks more similar to the acoustic pressure field pattern from research article. Area of pressures that are close to maximum pressure are also present in the middle of the pressure field. For 48khz, there is improvement in the pattern similarity especially on the middle part. However, the area with highest pressure deviates slightly from the middle.

5.2.2.2 Reduce Element Size

Element size is reduced as an attempt to improve pattern similarity for 48kHz simulation model. Figure 40 shows the acoustic pressure field after reduction of element size.

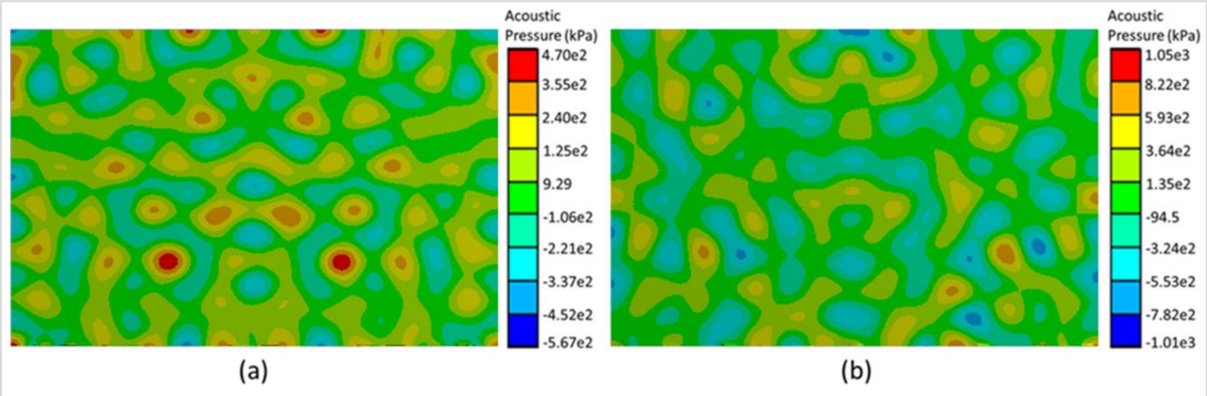

Figure 40: Acoustic pressure field after element size reduction: (a) test case 48kHz with 4.5mm element size (48kHz-3) and (b) test case 48kHz with 4 mm element size (48kHz-4)

The first attempt (Figure 40(a)) is made using element size of 4.5mm which produces meshed model with 245147 elements and 943885 nodes. The pressure field is symmetrical, but it barely resembles the pressure field from the research article. Another attempt (Figure 40(b)) is made using element size of 4mm which produces meshed model with 354724 elements and 1365949 nodes. The pressure field gets less symmetrical and less similar to the pressure field from research article. This improvement method is not used due to poor result.

5.2.2.3 Transducer Model and Material Switch

Previous simulation model uses flat cylinder as the transducer. To improve the simulation model, the transducer is made to resemble the actual transducer used in the research article and the material is set based on information on commercial ultrasonic cleaning tank setup. Since the research article only provide contact surface diameter of the transducer, other measurements of the transducer are obtained by enlarging the picture of transducer to scale and measuring the perimeter of the transducer using a ruler. Although this method will not give accurate transducer measurements, this is the best method for the situation. Figure 41 shows the transducer measurement found using this method and the material assigned to the transducer.

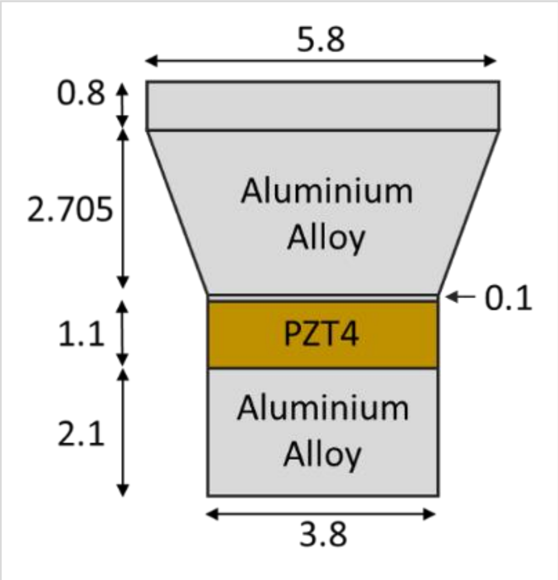

Figure 41: Transducer measurements and material

Following the commercial ultrasonic cleaning tank setup, the plate material is changed to stainless steel and transducer horn metal and back metal is set to aluminium alloy. Figure 42 shows the meshed model which incorporates these changes.

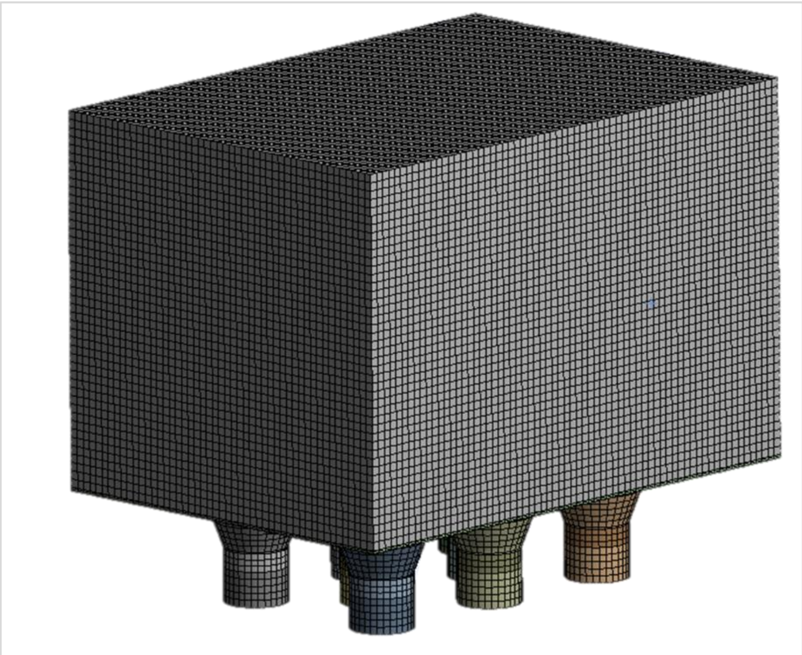

Figure 42: Meshed model of test case 2 with new transducer model

With this transducer model, there is 195964 elements and 762859 nodes. Fixed support is still placed at the bottom of the transducer to represent the bolts that keeps the piezoelectric ceramic and the metals that sandwiched it together as well as to represent the adhesive that allows the transducer to stick and be in contact with the plate. The acoustic pressure field when this model is used is shown in Figure 43.

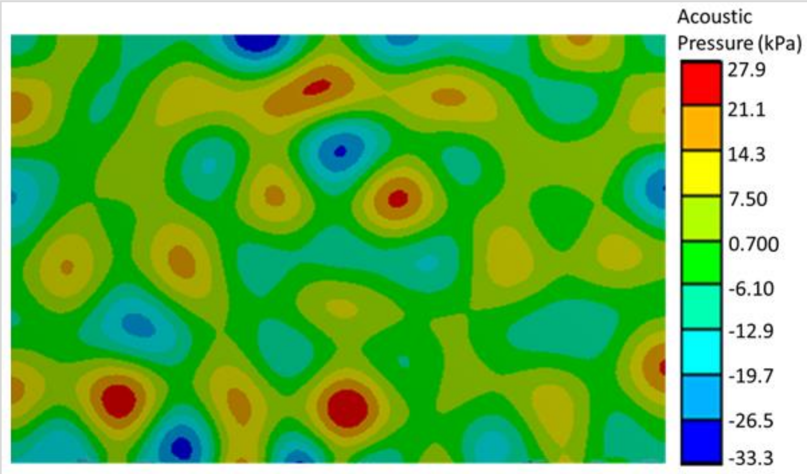

Figure 43: Acoustic pressure field of test case 28kHz with new transducer model and material switch (28kHz-3)

With the new transducer model, the resulting acoustic pressure field is less symmetrical and less similar to the pressure field in the research article. When comparing the left side and the right side of the acoustic pressure contour, it is found that the left side generally have higher positive and negative pressure compared to the right side. This indicates that at least some of the transducer on the left side vibrates with higher amplitude. The deformation of the transducers is shown in Figure 44.

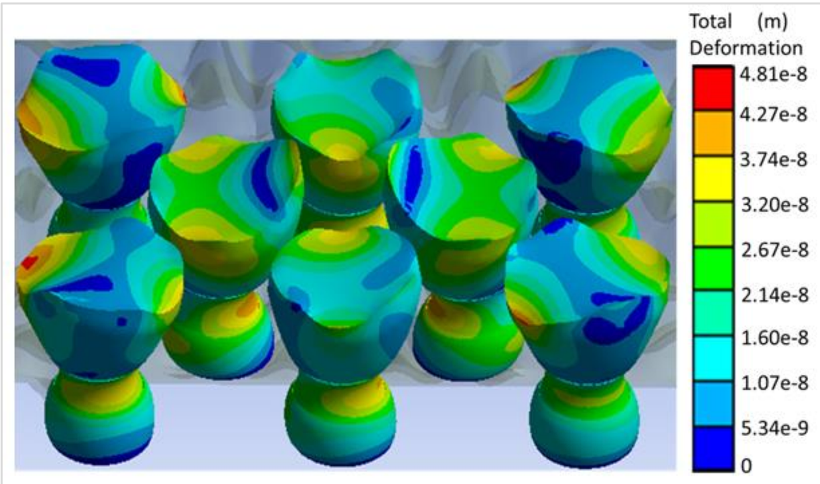

Figure 44: Deformation of transducers (new model)

From the deformation figure above, transducers on the left side generally have higher deformation compared to the transducers on the right side. Also, the deformation contour of the middle transducers is not symmetrical. These should not occur since the simulation model is symmetrical and the voltage input is the same for all transducers.

5.2.2.4 Cylindrical Support on Lateral Surface of Transducer

To solve the non-symmetrical deformation issue. Cylindrical supports are set on the lateral surface of the transducers. Figure 45 shows the resulting acoustic pressure field.

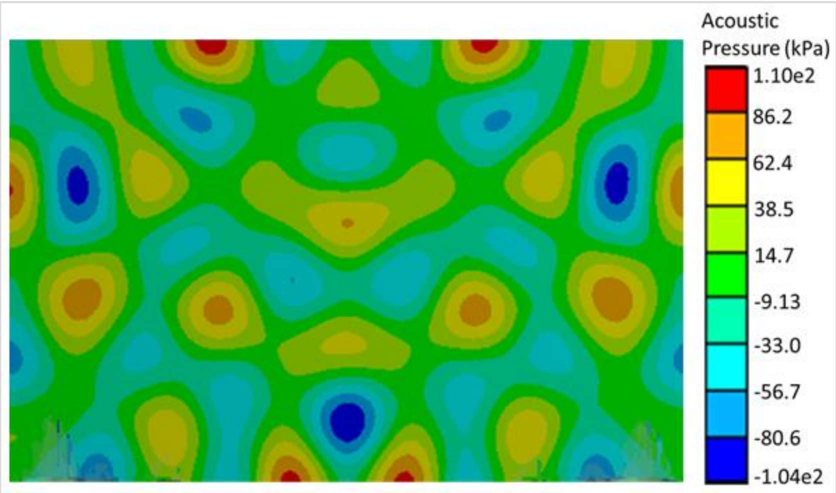

Figure 45: Acoustic pressure field of test case 28kHz with cylindrical supports (28kHz-4)

The addition of cylindrical supports results in a symmetrical acoustic pressure field. However, the pressure field is not similar to the pressure field from research article and there is mesh distortion at the bottom. Compared to all other variation of test case for 28kHz, the maximum positive and negative pressure is much higher. Due to unsatisfactory result, the simulation model is reverted to the simpler version with fixed support.

5.2.2.5 Model Reduction via Plane of Symmetry

From the established method, the ultrasonic cleaning tank simulation model is considered complex enough making model reduction not viable. When the model is simplified to half or quarter, there may be large difference in the pressure output between the reduced models and the full model. However, the acoustic pressure field pattern is expected to be the same as when doing full model. To put it simply, model reduction can be viable for a symmetrical ultrasonic cleaning tank simulation if only the pattern (and not the pressure magnitude) of the acoustic pressure field is of interest. For this reason, this option is explored for simulation efficiency. The meshed half model has 90728 elements and 353491 nodes. The quarter model has 44880 elements and 177252 nodes. Figure 46 shows the meshed model when reduced.

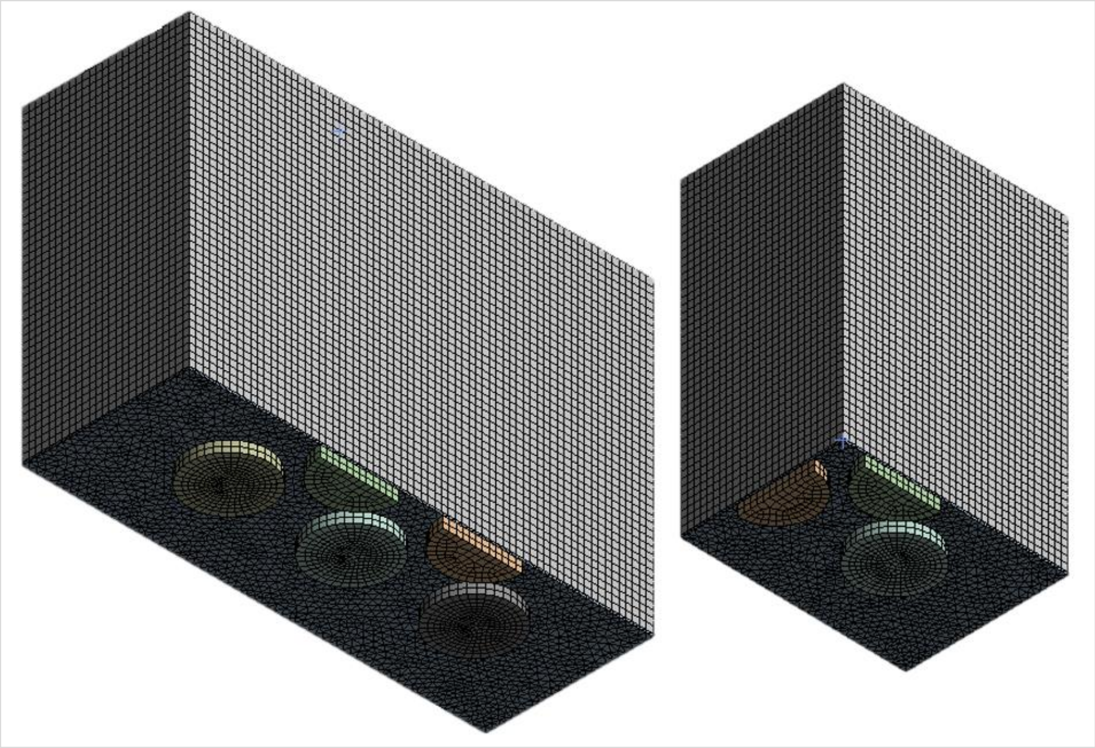

Figure 46: Meshed model of test case 2 simplified to half (left) and quarter (right)

For this to work properly, symmetry region and symmetry plane boundary condition is set to the exposed area (from model reduction) of structural region and acoustic region respectively. This is shown in the simple representation below:

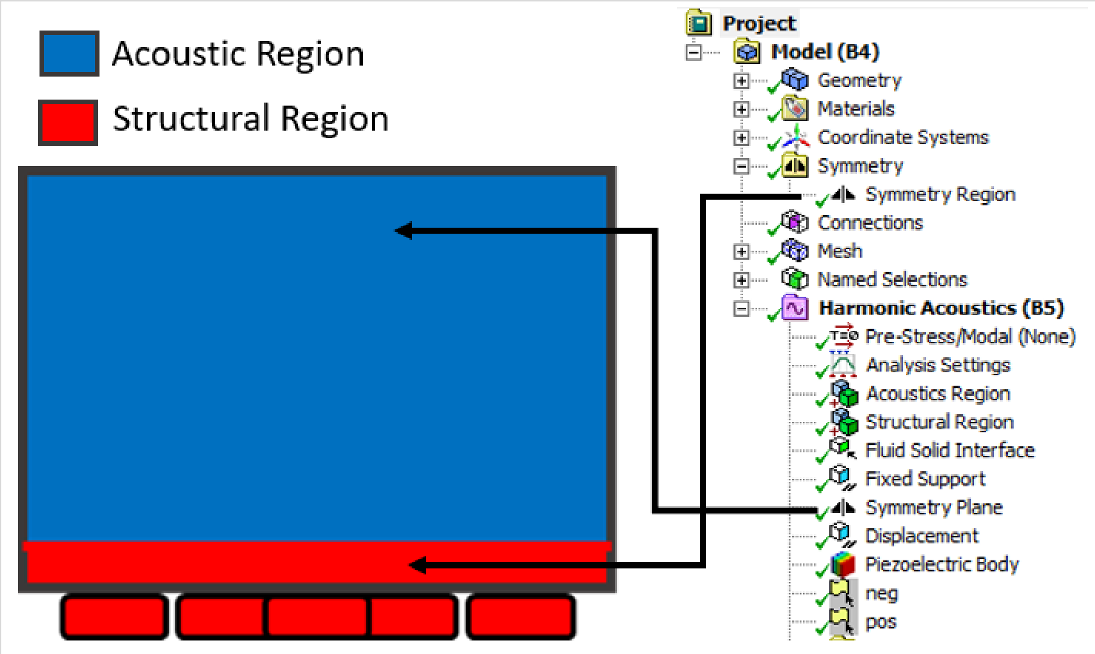

Figure 47: Simple representation of reduced model with symmetry boundary conditions

The resulting acoustic pressure fields for both 28kHz and 48kHz reduced models are shown in Figure 48.

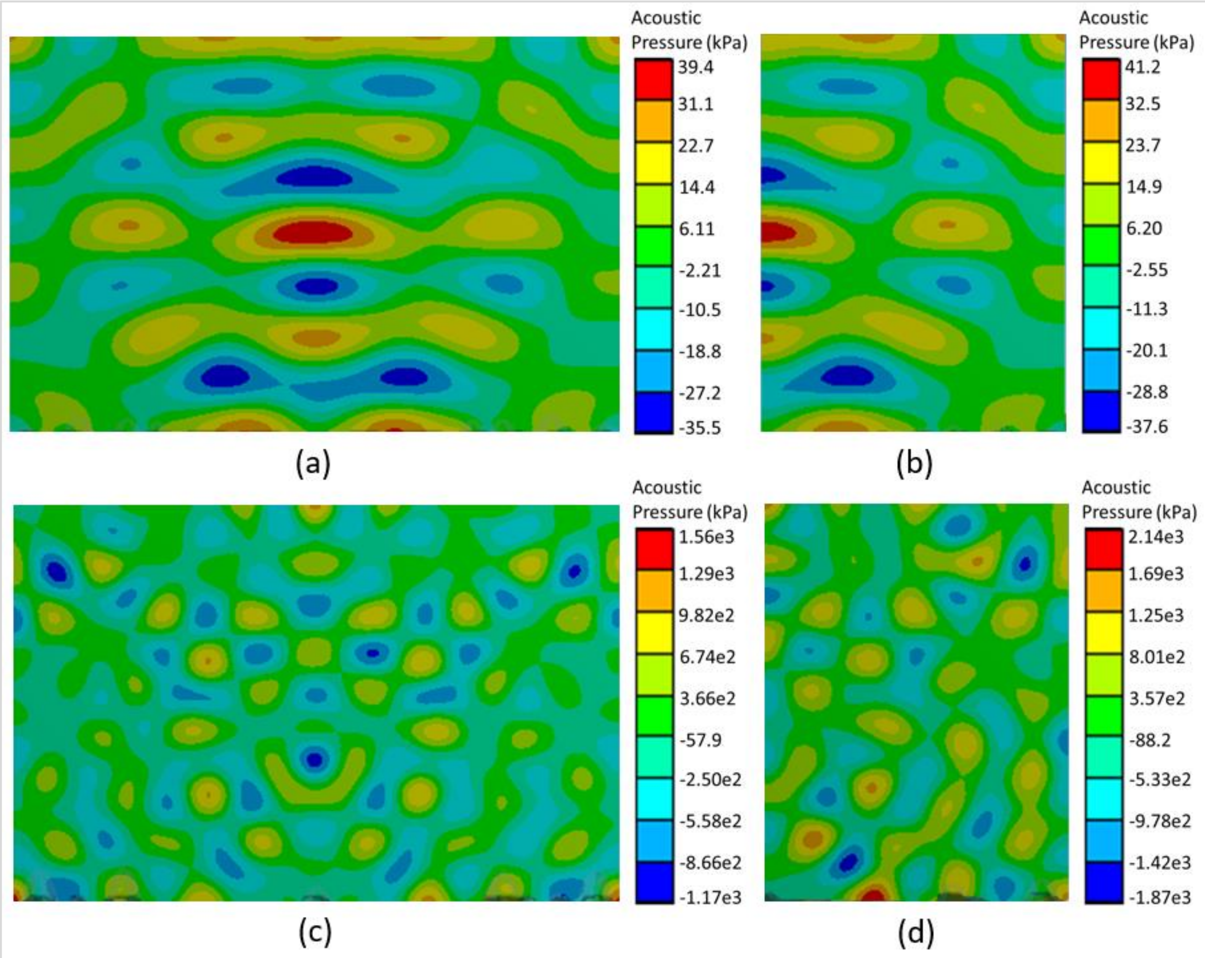

Figure 48: Acoustic pressure field after model reduction: (a) test case 28kHz half (28kHz-2-H) (b) test case 28kHz quarter (28kHz-2-Q), (c) test case 48kHz half (48kHz-2-H) and (d) test case 48kHz quarter (48kHz-2-Q)

For 28kHz, the acoustic pressure field pattern of the reduced models is identical to the full model. For 48kHz, the pattern from the reduced models is almost identical to the full model.

5.2.3 Data Tabulation and Plotting

5.2.3.1 28kHZ Ultrasonic Cleaning Tank Model

The data from initial results, improvements and computational information of 28kHz ultrasonic cleaning tank simulation models are tabulated below.

Table 12: Data from 28kHz ultrasonic cleaning tank simulation models

Simulation Model	28kHz-1	28kHz-2	28kHz-3	28kHz-4
Model Reduction	N/A	N/A	N/A	N/A
Transducer Model	Simple	Simple	Complex	Complex
Transducer Material	PZT4	PZT4	PZT4 and Aluminium Alloy	PZT4 and Aluminium Alloy
Plate Material	Aluminium Alloy	Aluminium Alloy	Stainless Steel	Stainless Steel
Element Size, mm	5	5	5	5
Number of Elements	179369	179369	195964	195964
Number of Nodes	688224	688224	762859	762859
Fixed Support	N/A	Plate edges	Plate edges	Plate edges
Cylindrical Support	N/A	N/A	N/A	Transducer shell
Max Pressure, kPa	56.422	41.200	27.899	110.02
Min Pressure, kPa	-34.143	-39.274	-33.292	-104.45
Pattern Symmetry	High	High	Low	High
Pattern Similarity	Medium	High	Low	Low
MAPDL Elapsed Time	2 h 8 m	2 h 10 m	3 h 3 m	2 h 47 m
MAPDL Memory Used, GB	5.2813	7.5498	8.9346	8.7998
MAPDL Result File Size, GB	1.8088	1.8119	1.9500	1.9672

Table 13: Comparison of full, half and quarter 28kHz ultrasonic cleaning tank simulation model

Simulation Model	28kHz-2	28kHz-2-H	28kHz-2-Q
Model Reduction	N/A	Half	Quarter
Transducer Model	Simple	Simple	Simple
Transducer Material	PZT4	PZT4	PZT4
Plate Material	Aluminium Alloy	Aluminium Alloy	Aluminium Alloy
Element Size, mm	5	5	5
Number of Elements	179369	90728	44880
Number of Nodes	688224	353491	177252
Fixed Support	Plate edges	Plate edges	Plate edges
Cylindrical Support	N/A	N/A	N/A
Max Pressure, kPa	41.200	39.381	41.202
Min Pressure, kPa	-39.274	-35.482	-37.559
Pattern Symmetry	High	High	N/A
Pattern Similarity	High	High	High
MAPDL Elapsed Time	2 h 10 m	27 m 32 s	7 m 51 s
MAPDL Memory Used, GB	7.5498	10.366	4.2930
MAPDL Result File Size, GB	1.8119	0.94313	0.46881

Graph of computational resource against 28kHz ultrasonic cleaning tank simulation models is shown in Figure 49.

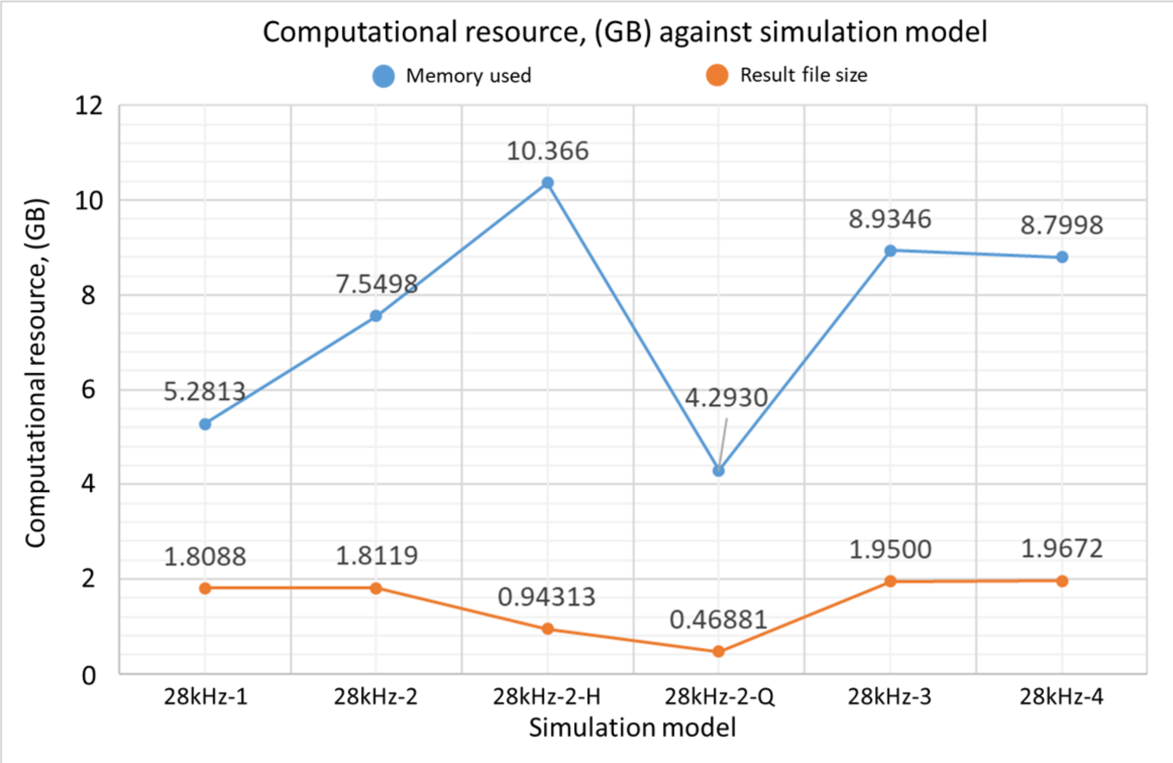

Figure 49: Graph of computational resource, (GB) against 28kHz simulation model

From the memory used plot, the memory required increases from 5.2813GB to 7.5498GB when fixed support is set on the edges of the plate. It increases further to 10.366GB when the simulation model is reduced to half and symmetry boundary condition is set. The increase in memory usage is unexpected since the half model have approximately half the elements and nodes from the full model which should require less memory usage. It is assumed that the symmetry boundary condition requires relatively large memory. If the model is reduced to quarter instead, the memory required decrease to 4.2930GB. For the quarter model, the large memory usage from symmetry boundary condition is compensated by the relatively low element and node counts making the overall memory usage much lower. When new transducer model is used, the memory required increases from 7.5498GB to 8.9346GB. This is because of the increase of elements and nodes of the model and also, there is more components involved in load transmission. When the new transducer model has cylindrical support set to it, the memory required decreases from 8.9346GB to 8.7998GB.

Comparing 28kHz-1 with 28kHz-4, the addition of support results in more memory usage when its set on the plate and less memory usage when its set on the transducer. Recalling results from Figure 34 of Test Case 1: Radiation of Baffled Piston, the model with side fixed support on the piston (excitation source) uses slightly lower memory than the one without the support. This applies to 28kHz-4 since the support is set on the excitation source as well. For 28kHz-1, the support is set on a component that is affected by the excitation source instead. This means that the model has to solve a more computationally complicated setup instead of having a setup that have an excitation source with limited node movements.

From the result file size plot, models with added support requires slightly larger file size compared to models without support. This is further confirmed by comparing this behaviour to the 2.5D-PZT4-S model from Test Case 1: Radiation of Baffled Piston. The file size required for reduced models is significantly less than full model. Unlike the memory used plot, the result file size plot shows significant decrease in computational resource when model is reduced.

Graph of computation time against 28kHz ultrasonic cleaning tank simulation models is shown in Figure 50.

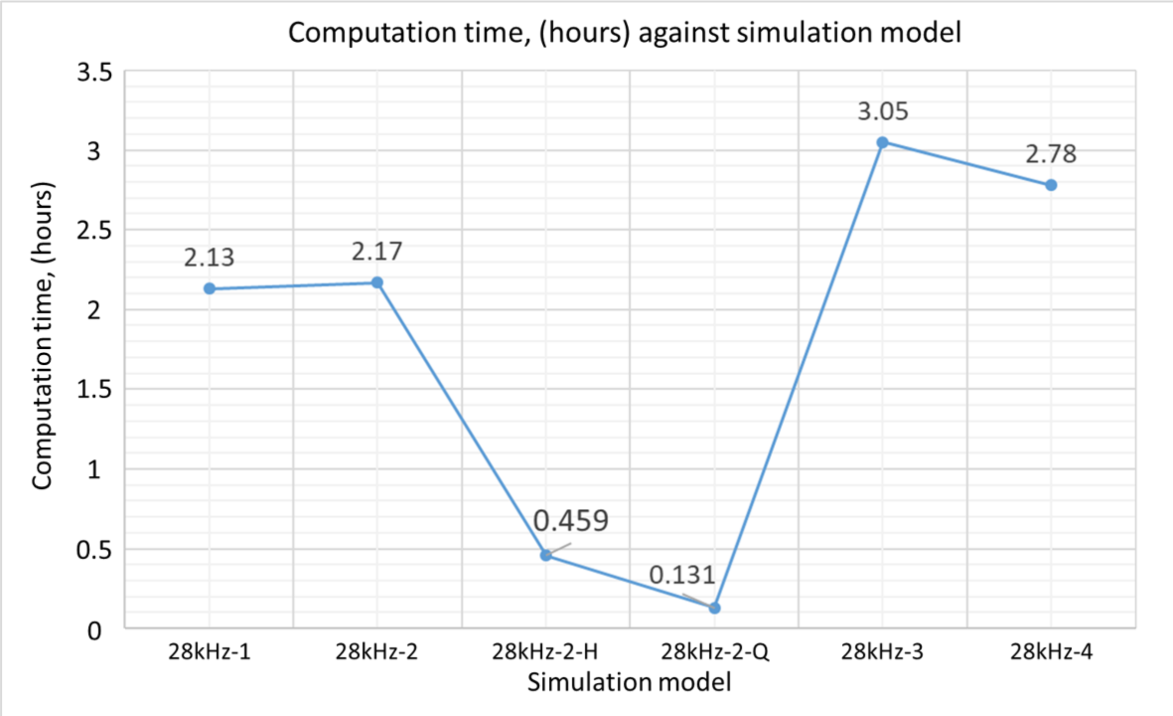

Figure 50: Graph of computation time, (hours) against 28kHz simulation model

From the computation time plot, reduced models are computed substantially faster compared to full models. When this plot is compared to the graph in Figure 49, results of 28kHz-2-H shows that large memory usage does not necessarily mean larger file size and longer computational time. The computation time plot shows behaviour of a mix between the memory used plot and result file size plot.

5.2.3.2 48kHZ Ultrasonic Cleaning Tank Model

The data from initial results, improvements and computational information of 48kHz ultrasonic cleaning tank simulation models are tabulated below.

Table 14: Data from 48kHz ultrasonic cleaning tank simulation models

Simulation Model	48kHz-1	48kHz-2	48kHz-3	48kHz-4
Model Reduction	N/A	N/A	N/A	N/A
Transducer Model	Simple	Simple	Simple	Simple
Transducer Material	PZT4	PZT4	PZT4	PZT4
Plate Material	Aluminium Alloy	Aluminium Alloy	Aluminium Alloy	Aluminium Alloy
Element Size, mm	5	5	4.5	4
Number of Elements	179369	179369	245147	354724
Number of Nodes	688224	688224	943885	1365949
Fixed Support	N/A	Plate edges	Plate edges	Plate edges
Max Pressure, kPa	840.63	189.89	470.40	105.10
Min Pressure, kPa	-100.80	-177.28	-567.09	-101.10
Pattern Symmetry	Medium	High	High	Medium
Pattern Similarity	Low	Medium	Low	Low
MAPDL Elapsed Time	2 h 7 m	1 h 59 m	3 h 57 m	9 h 18 m
MAPDL Memory Used, GB	5.2813	7.3877	7.7881	12.613
MAPDL Result File Size, GB	1.8088	1.8119	2.4824	3.6006

Table 15: Comparison of full, half and quarter 48kHz ultrasonic cleaning tank simulation model

Simulation Model	**48kHz-2**	**48kHz-2-H**	**48kHz-2-Q**
Model Reduction	N/A	Half	Quarter
Transducer Model	Simple	Simple	Simple
Transducer Material	PZT4	PZT4	PZT4
Plate Material	Aluminium Alloy	Aluminium Alloy	Aluminium Alloy
Element Size, mm	5	5	5
Number of Elements	179369	90728	44880
Number of Nodes	688224	353491	177252
Fixed Support	Plate edges	Plate edges	Plate edges
Max Pressure, kPa	189.89	159.80	213.60
Min Pressure, kPa	-177.28	-117.41	-186.75
Pattern Symmetry	High	High	N/A
Pattern Similarity	Medium	Medium	Medium
MAPDL Elapsed Time	1 h 59 m	25 m 2 s	8 m 12 s
MAPDL Memory Used, GB	7.3877	10.366	4.2930
MAPDL Result File Size, GB	1.8119	0.94313	0.46881

Graph of computational resource against 48kHz ultrasonic cleaning tank simulation models is shown in Figure 51.

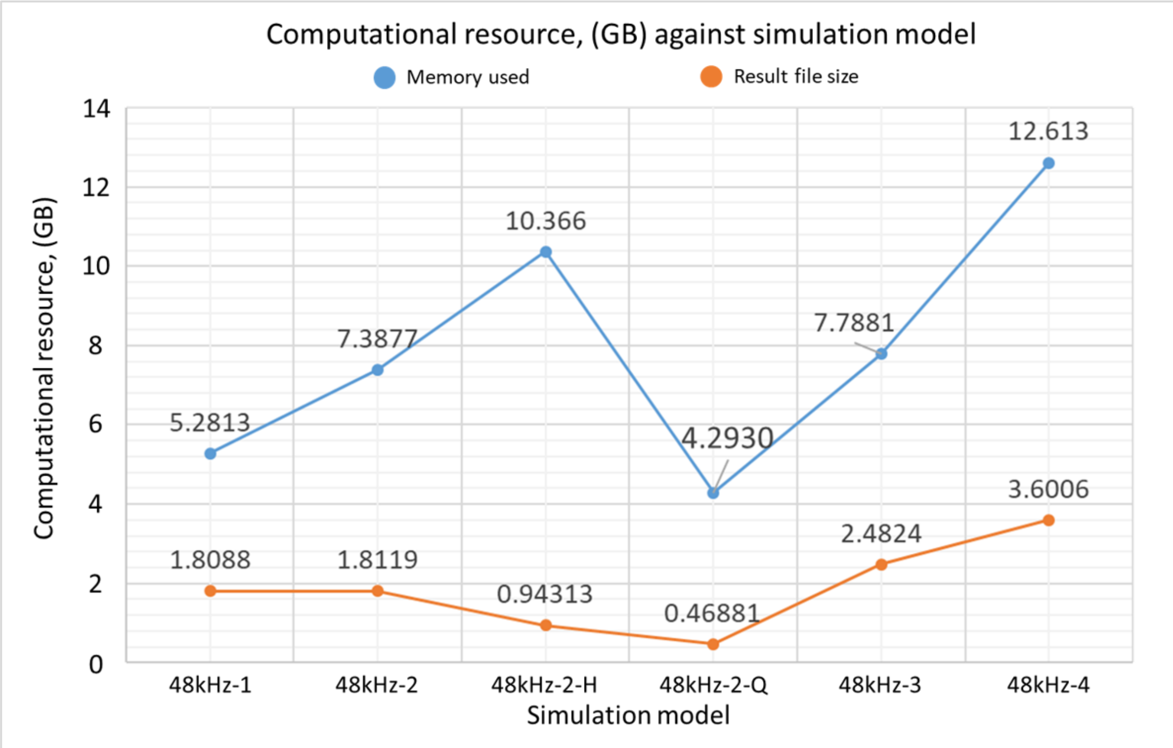

Figure 51: Graph of computational resource, (GB) against 48kHz simulation model

Computational resource for 48kHz-1, 48kHz-2, 48kHz-2-H and 48kHz-Q is similar to its 28kHz counterparts since it uses the same meshed model with only the analysis frequency changed from 28kHz to 48kHz. Looking at both the memory used plot and result file size, the computational resource required increases when element size is changed from 5mm to 4.5mm. The computational resource required notably increase when the element size is further reduced to 4mm.

Graph of computation time against 48kHz ultrasonic cleaning tank simulation models is shown in Figure 52.

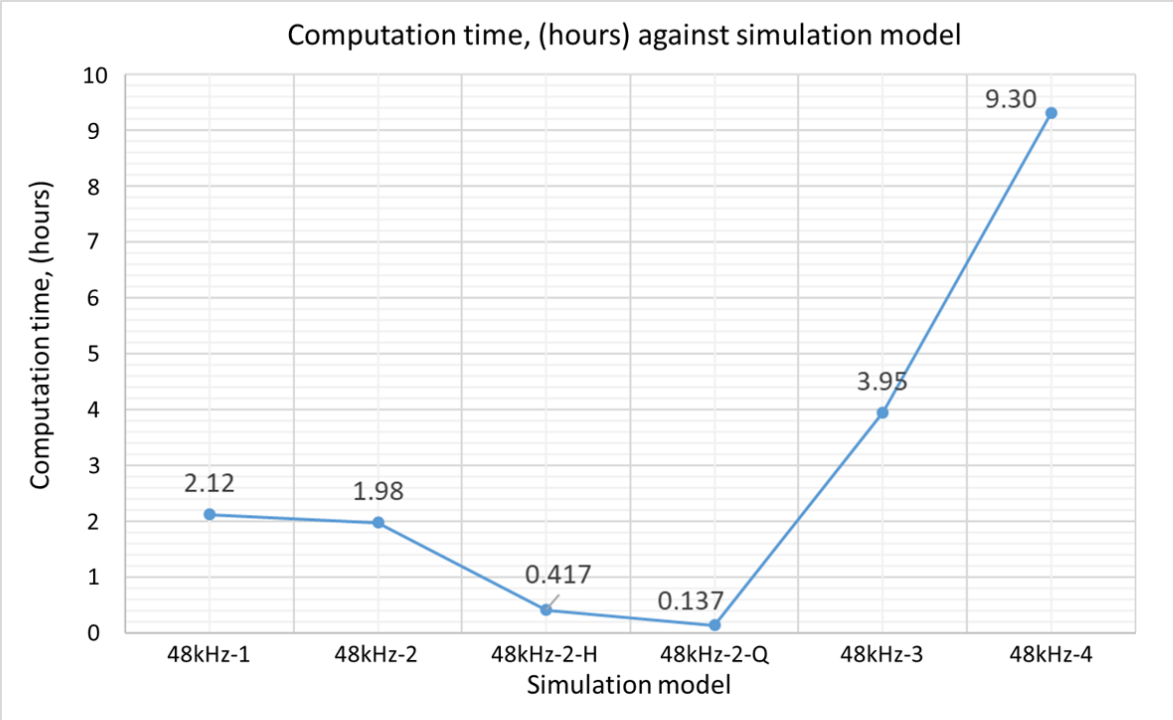

Figure 52: Graph of computation time, (hours) against 48kHz simulation model

From the computation time plot, the computation time decreases when support is added which contradicts the results from 28kHz models. Model reduction reduces computation time which is consistent with previous results. There is extremely large increase in computation time when the element size is reduced. This is because size reduction by 0.5mm and 1mm is relatively significant because the model is already large compared to the size of one 5mm element. This causes the decrease in element size to increase the element and node counts of the model substantially.

5.3 Discussion and Recommendation

From the results, the acoustic pressure field pattern obtained from the simulation models are unable to completely replicate the pattern from the research article due to lack of information and finite element modelling skill. Most of the improvements attempt ended up producing unsatisfactory results. Fixed support is a great addition to the ultrasonic cleaning tank simulation model as it increases the acoustic pressure field similarity to the pressure field in the research article. This shows the importance of understanding the mechanism of the acoustic problem before modelling it and the skill to translate the mechanism into the simulation model.

Element size reduction always increases solution computation time, but it does not always improve the result especially when thoughtlessly used. For example, the 48kHz model with element size reduction to 4mm substantially increase the computation time to 9 hours 18 minutes but produces acoustic pressure field pattern that is less symmetrical and less similar to the pattern from research article. To ensure optimal simulation model, it is recommended to refine mesh on area with high load and stress concentration. For area with minimal load and stress concentration, the mesh should be coarsened instead with element size up to 1/6 of wavelength (acoustic model meshing guideline).

When the transducer model and material of transducer and plate are changed, the acoustic pressure field shows obvious uneven pressure distribution even though the simulation model is symmetrical. This may be due to the meshing plate and transducer being non-symmetrical. With the addition of cylindrical support, the acoustic pressure field become symmetrical, but the pattern has low similarity to the pattern in research paper. The acoustic pressure also greatly increases indicating that the addition of cylindrical support to force pattern symmetry is not a suitable approach in ensuring credible results. The non-symmetrical mesh should be made symmetrical instead.

The acoustic pressure field pattern of the half model and quarter model is identical to the pattern of its full model counterpart. The computation time to simulate these reduced models are very short as well. Although the acoustic pressure magnitude is not focused for this test case, referring to Table 13, it is worth mentioning that the reduced models of test case 28kHz especially the quarter model produces very close pressure values to its full model counterpart. From Table 15, reduced models of test case 48kHz produces pressure values with noticeable difference when compared to its full model. With improved modelling and meshing method, model reduction for the ultrasonic cleaning tank model can be viable to produce accurate acoustic pressure field in both magnitude and pattern with minimal computation effort and time.

6 CASE STUDY: EFFECT OF PLATE TO ACOUSTIC PRESSURE FIELD

Case study is made to gauge the effectiveness of simulation made based on established simulation methodology by investigating acoustic pressure field produced by ultrasonic transducer for an arbitrary simple case. The chosen setup involves placing a structural steel plate in the near field radiation of ultrasonic transducer. Figure 53 shows the graphical representation of the setup to be simulated.

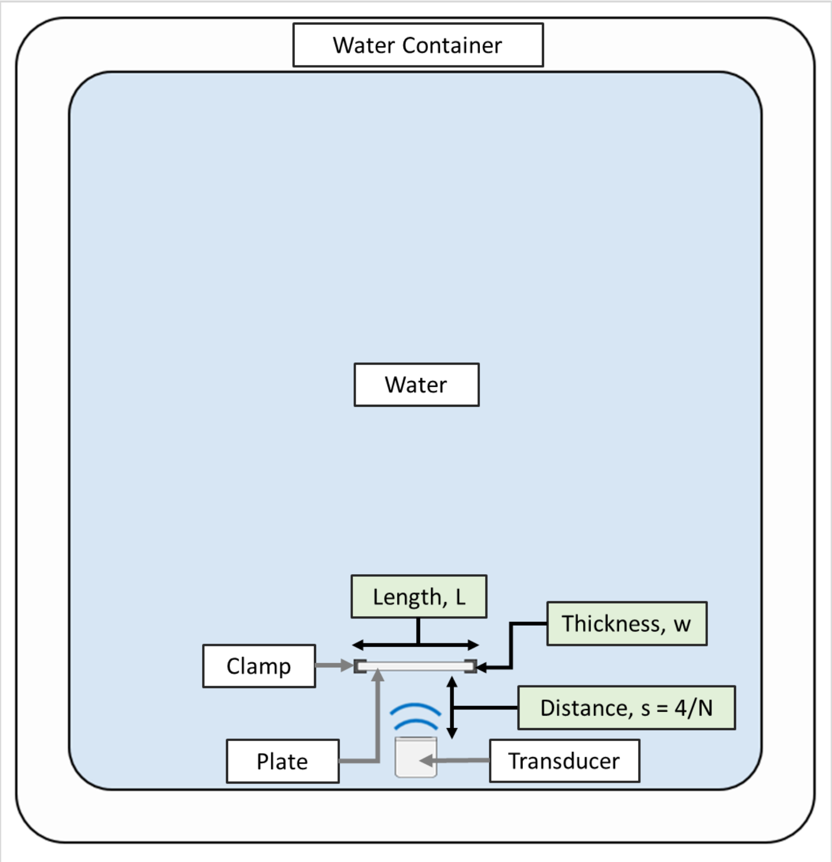

Figure 53: Analysis case setup

From the figure, the transducer is placed close to the edge of the rectangular container filled with water and the structural steel plate is placed close to the transducer. Diameter of the transducer is 4cm and the excitation frequency is 500kHz. The distance, s of the plate to the transducer is a quarter of the theoretical near field radiation, N. Since this setup is simulated in ANSYS, the default speed sound provided in ANSYS (Appendix L) is used in calculating the near field radiation, N. Value of N obtained is 13.5cm and therefore, the distance, s of plate to the transducer is 3.375cm. The varied parameters for this setup are the plate thickness, w and the plate length, L. The simulation model is described in the following model description section.

6.1 Model Description

Simulation model for this case study is made in 2.5D to ensure low computational resource and computation time required to run it without the need to use APDL commands. The features of this model are described in Table 16.

Table 16: Model description of case study simulation model

Features	Description
Model Reduction	The simulation model is reduced to half for further reduction in computation time and resource. Symmetry boundary condition is set to the symmetry cut surface to ensure that ANSYS takes the model reduction into consideration when solving for results. For this case study, when describing the measurements of the model, the value before model reduction is used.
Material	Only water and structural steel material is used for this model. Structural steel is set to the plate and water is set to all other sub-model. ANSYS default structural steel and water properties is used (Appendix L).
Wave Absorption Condition	Perfectly matched layer (PML) is used to absorb outgoing waves. PML thickness is set to 0.12cm.
Size of Water Model	The acoustic pressure field of interest is up to the end of theoretical near field radiation, N. The water model is a rectangle with vertical length of 13.5cm and horizontal length of 20cm. With PML, the size increases by 0.12cm in vertical length and 0.24 cm in horizontal length (0.12cm left, 0.12cm right). Since the model is reduced to half, only 0.12cm increase in horizontal length can be observed.
Transducer Size	The transducer is a rectangle with vertical length of 1cm and horizontal length of 4cm.
Plate Size (Varied Parameter)	The default plate thickness and length are set to 0.4cm and 4cm respectively.
Thickness (Z-Axis)	For 2.5D simulation model, the thickness of the model needs to be relatively small in one axis. This simulation model is done in XY plane and the thickness in z-axis is set to 0.12cm.
Element Size	For quadratic elements (used in 3D acoustic simulation), at least 6 elements per wavelength is required. This is according to the

	acoustic model meshing guidelines. The element size is set to 0.04cm via body sizing and all quad multizone meshing.
Physics Region	Acoustic region is set to the transducer, water and PML. Structural region is set to the plate.
Element Type	Only 2D brick elements are used in this model. FLUID220 is used for transducer, water and PML. SOLID186 is used for plate.
Support	Fixed support is set on the side of the plate to represent the clamp that puts the plate in place.
Excitation Source	Acoustic excitation is used for this model. Surface velocity of an arbitrary magnitude of $1ms^{-1}$ is set on the back horizontal surface of the transducer model.

Figure 54 shows the meshed model of case study.

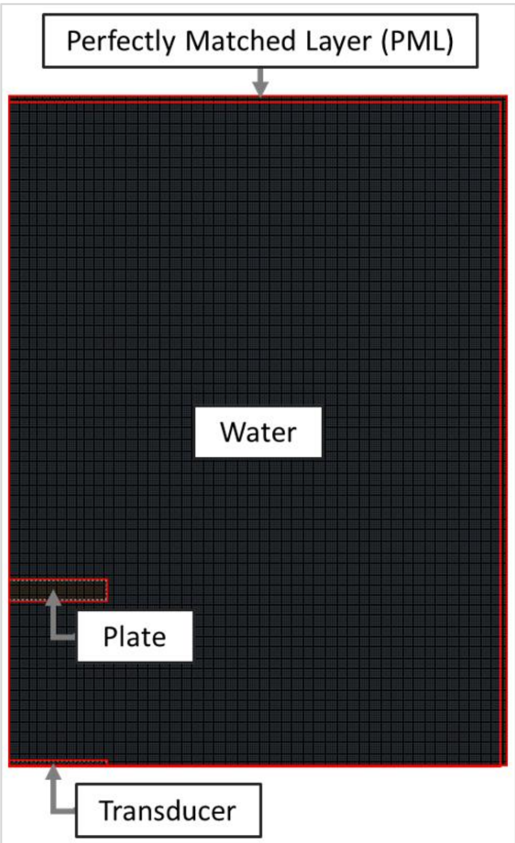

Figure 54: Meshed case study model with transducer, plate, water and PML labelled

Since relatively small element size is used, the meshed model appears to be black. red lines are used to distinguish the transducer model, water model, PML model and plate model. The element size and shape are uniform throughout the model. This model has 252000 elements and 1266453 nodes.

6.2 Analysis Procedure

1. The simulation model described above is made without plate model.
2. The model is then solved for acoustic pressure when the amplitude option is turned off (default setting) and on. With amplitude option turned on, acoustic pressure amplitude is shown instead of positive and negative acoustic pressures.
3. The acoustic pressure (amplitude: off) and acoustic pressure (amplitude: on) results are saved.
4. Steps 1 to 3 are repeated using simulation model with default plate size (length of 4cm and thickness of 0.4cm).
5. Steps 1 to 3 are repeated using simulation model with plate length adjusted to 2cm, 8cm and 16cm.
6. Graph of maximum acoustic pressure against plate length is plotted.
7. Steps 1 to 3 are repeated using simulation model with plate thickness adjusted to 0.2cm, 0.8cm and 1.6cm.
8. Graph of maximum acoustic pressure against plate thickness is plotted.

6.3 Results

Figure below and all other subsequent acoustic pressure field figures have a grey line placed at the bottom left to indicate the length of the transducer. Red ring is used to indicate location of maximum positive pressure and maximum pressure amplitude. Blue ring is used to indicate location of maximum negative pressure.

6.3.1 Near Field Radiation

Simulation model without plate is used to verify near-field radiation produced by the model. Figure 55 shows acoustic pressure field for model without plate.

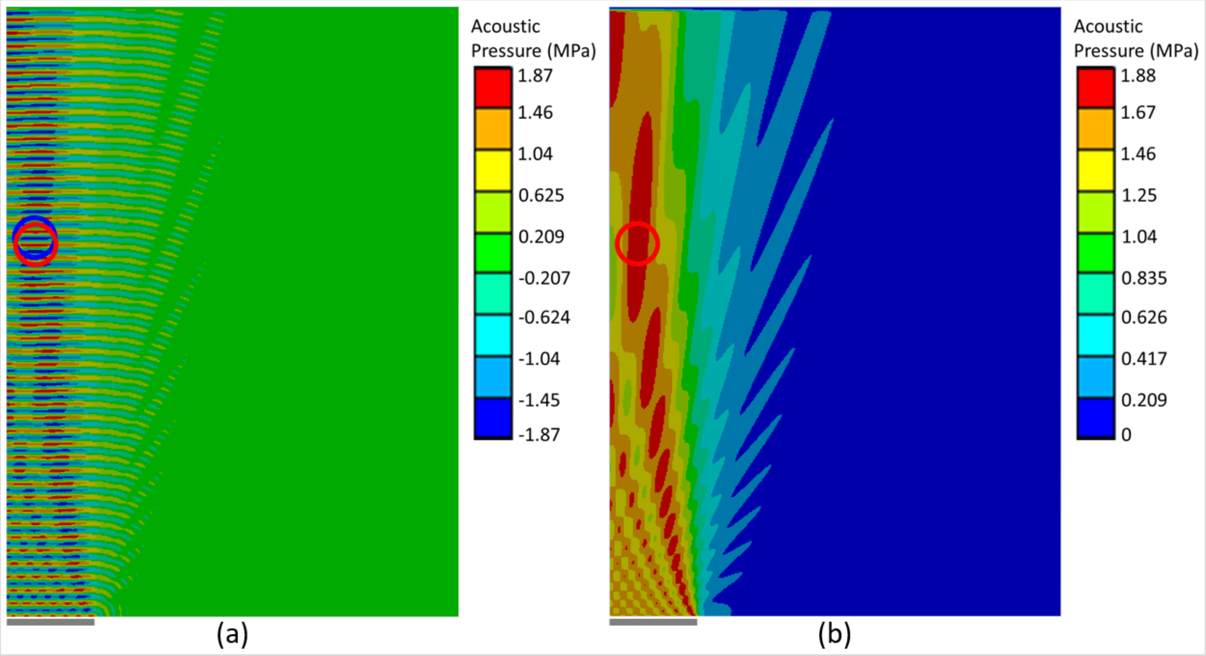

Figure 55: Acoustic pressure field for model without plate: (a) amplitude: off and (b) amplitude: on

The maximum positive and negative pressure from Figure 55(a) is very close to the maximum pressure amplitude from Figure 55(b). Pressure waves on the transducer surface shows that the wave is produced from most of the surface of the transducer rather than from a single point which is similar to the theory in literature. The acoustic pressure field shows reduction in the number of areas of amplified pressure waves (from constructive interference) and increase in the intensity of amplification as it reaches the end of the vertical length of the model which is made according to the theoretical near field radiation, 13.5cm. The maximum pressure location is at the red pressure area before the fully converged red pressure area. The acoustic pressure field shows characteristics of near field radiation. Therefore, if a plate is introduced inside this model, it is indeed in the near field radiation as intended.

6.3.2 Default Plate Size

This simulation has a plate of 4cm length and 0.4cm thick and is placed 3.375cm in front of the transducer. The size of this plate is regarded as the default size and other subsequent simulation will either have the length or thickness of the plate changed. Figure 56 shows acoustic pressure field for model with default plate.

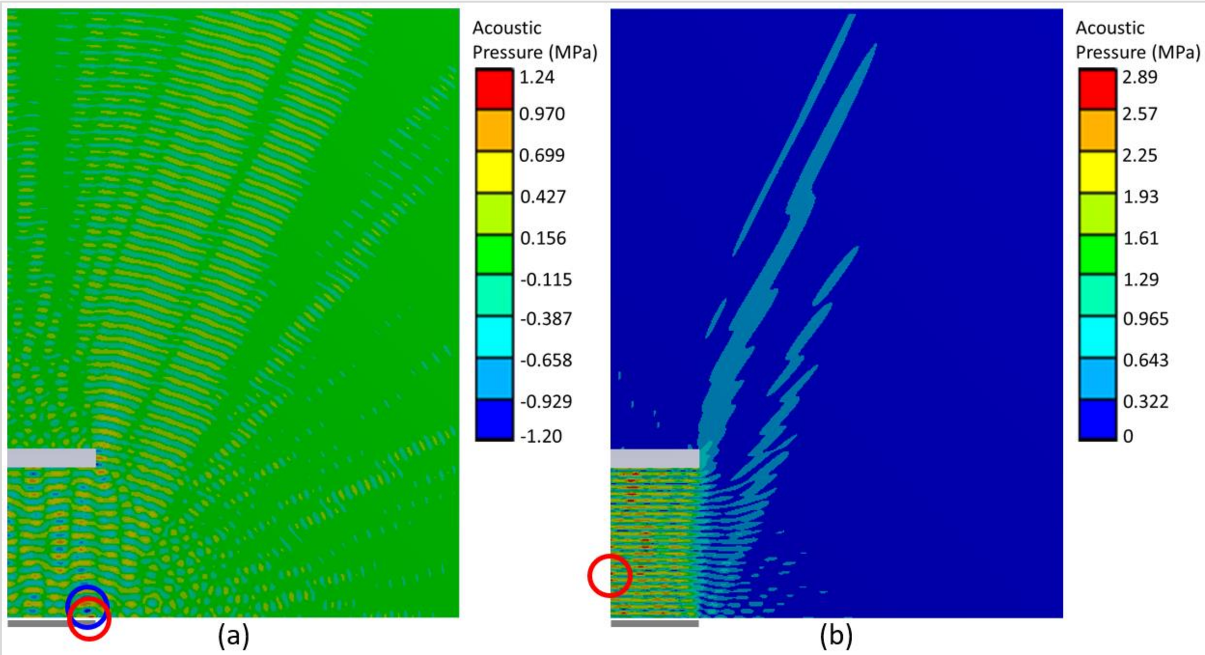

Figure 56: Acoustic pressure field for model with default plate: (a) amplitude: off and (b) amplitude: on

The maximum positive and negative pressure are located on the outermost transducer radiation surface. Maximum pressure amplitude is located at a short distance in front of the centre of transducer. Most of the waves are reflected and some of the waves are transmitted through the centre area of the plate and continue to propagate back into the water in front of the plate. Wave transmission becomes less across the plate length. There is little wave diffracted by the plate side.

6.3.3 Plate with Adjusted Length

Plate length is set to half the default length. Figure 57 shows acoustic pressure field for model with plate length of 2cm.

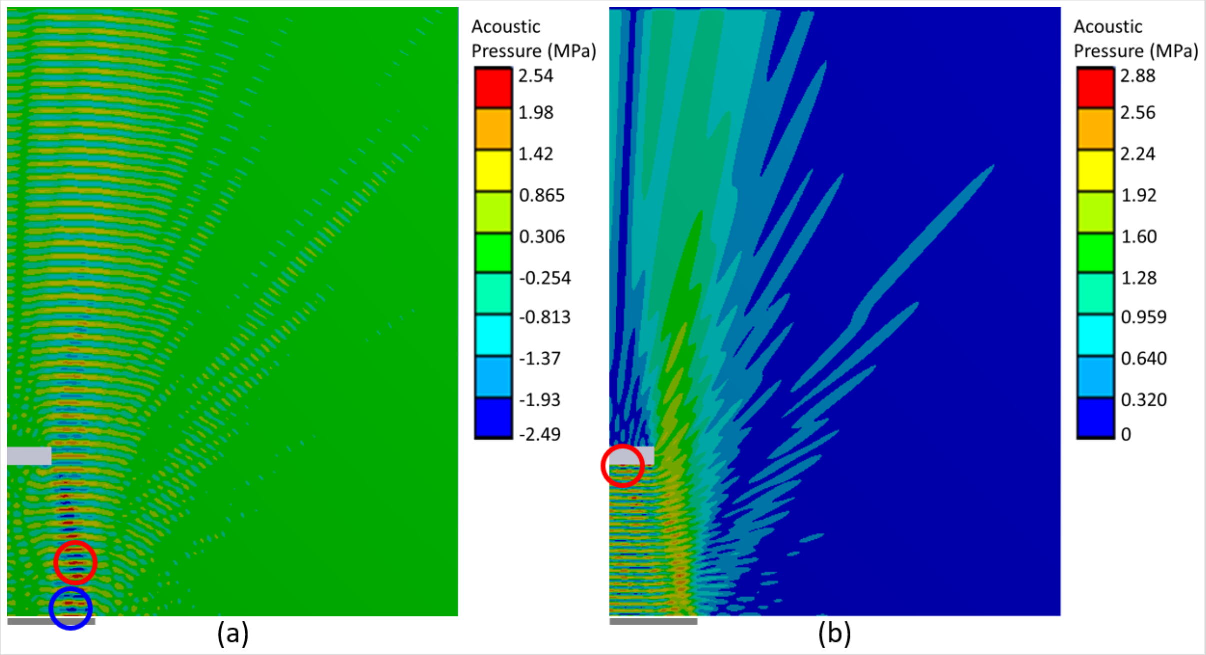

Figure 57: Acoustic pressure field for model with plate length of 2cm: (a) amplitude: off and (b) amplitude: on

This model shows higher maximum positive and negative pressure compared to models with longer plate length. The maximum positive and negative pressure are located close to the side edge of transducer radiation surface. Maximum pressure amplitude is located at a short distance to the side of the centre of plate reflecting surface. With plate length that is half the transducer diameter, there is more wave diffraction and the waves managed to converge into a radiation beam.

Plate length is set to twice the default length. Figure 58 shows acoustic pressure field for model with plate length of 8cm.

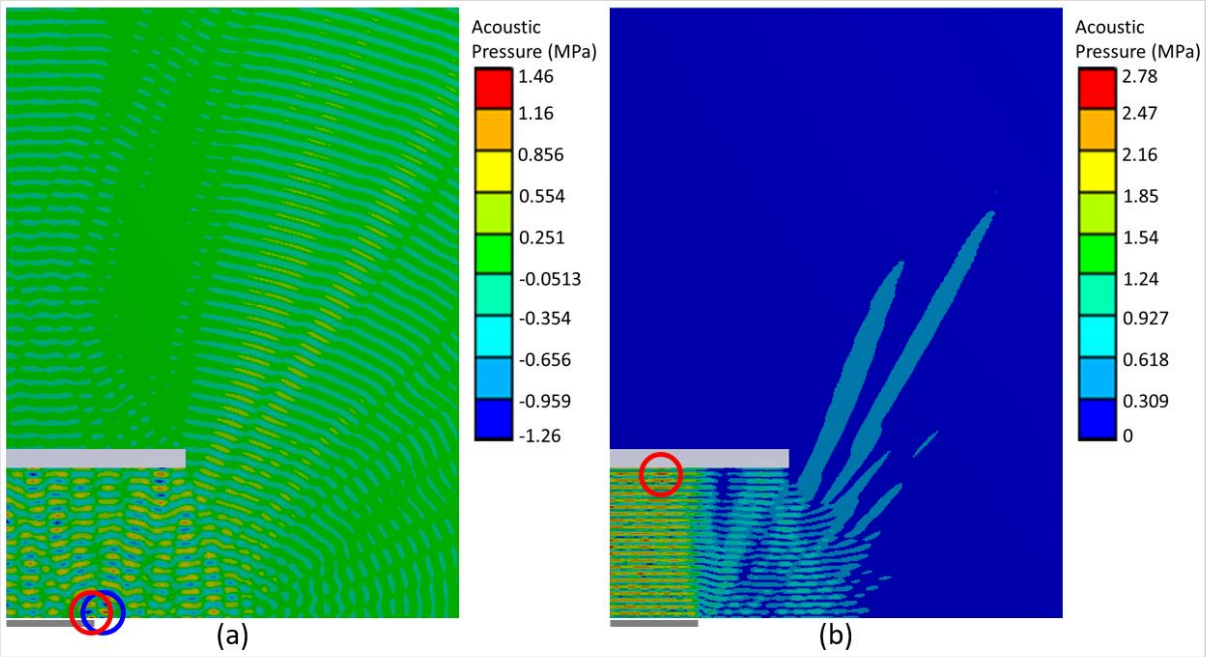

Figure 58: Acoustic pressure field for model with plate length of 8cm: (a) amplitude: off and (b) amplitude: on

The maximum positive and negative pressure located close to the side edge of transducer radiation surface. Maximum pressure amplitude is located on the outermost transducer radiation surface. Wave transmission through the plate becomes less across the plate length. With plate length that is twice the transducer diameter, there is an apparent area of negligible wave transmission in between plate centre area and plate side edge which is the shadow zone. There is less wave diffracted by the plate side compared to when default plate length is used.

Plate length is set to four times the default length. Figure 59 shows acoustic pressure field for model with plate length of 16cm.

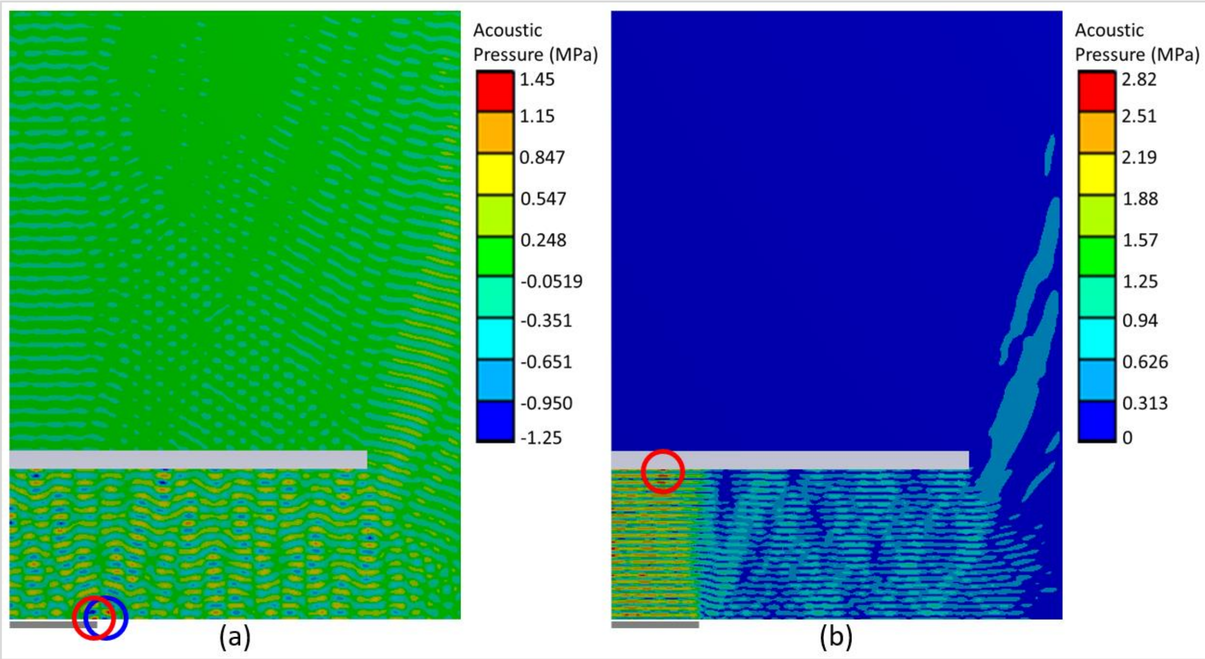

Figure 59: Acoustic pressure field for model with plate length of 16cm: (a) amplitude: off and (b) amplitude: on

The maximum positive and negative pressure are located close to the side edge of transducer radiation surface. Maximum pressure amplitude is located on the outermost transducer radiation surface. Wave transmission through the plate becomes less across the plate length. This model has the largest shadow zone and least wave diffraction.

Figure 60 shows graph of maximum acoustic pressure against plate length.

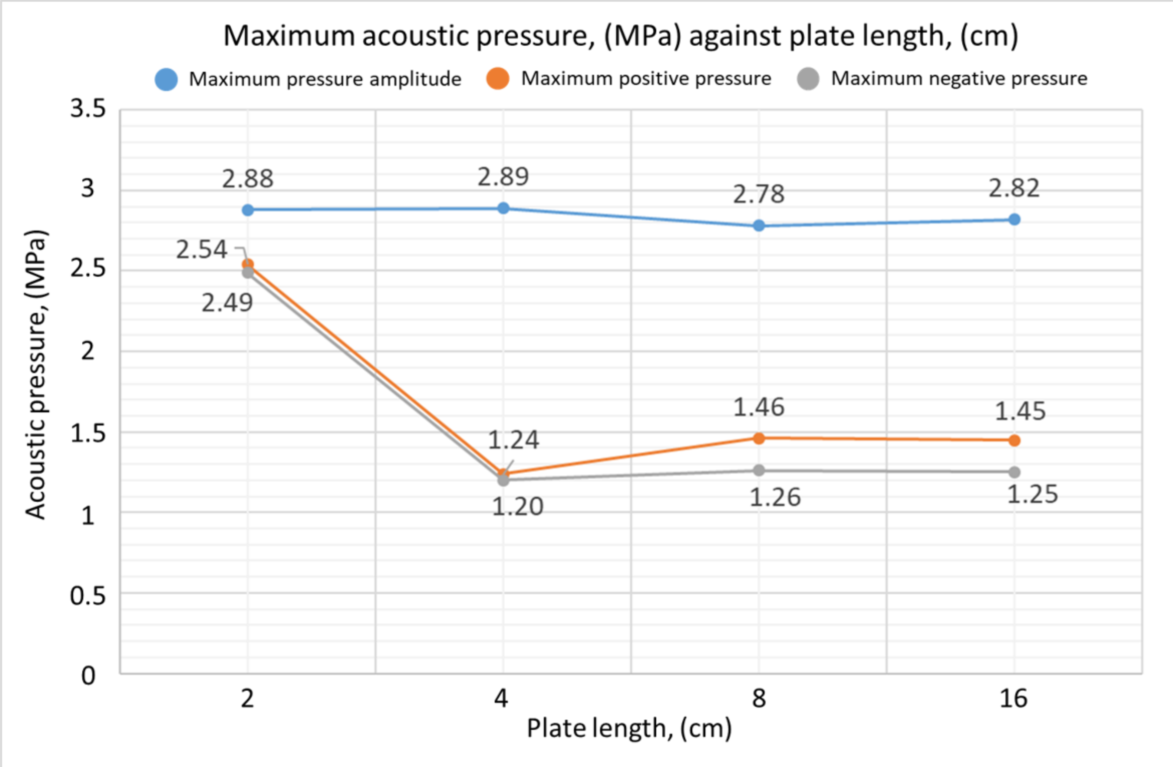

Figure 60: Graph of maximum acoustic pressure, (MPa) against plate length, (cm)

From the graph, the maximum pressures in between the plate and transducer for plate length of 2cm shows different behaviour compared to the general trend of this graph. The maximum positive and negative pressure are substantially higher. Disregarding results for plate length of 2cm, the maximum positive and negative pressure increases with longer plate and converges to an approximate pressure of 1.45MPa and 1.25MPa respectively. The maximum pressure amplitude shows a decrease from 2.89MPa to 2.78MPa followed by a slight increase to 2.82MPa.

6.3.4 Plate with Adjusted Thickness

Plate thickness is set to half the default thickness. Figure 61 shows acoustic pressure field for model with plate thickness of 0.2cm.

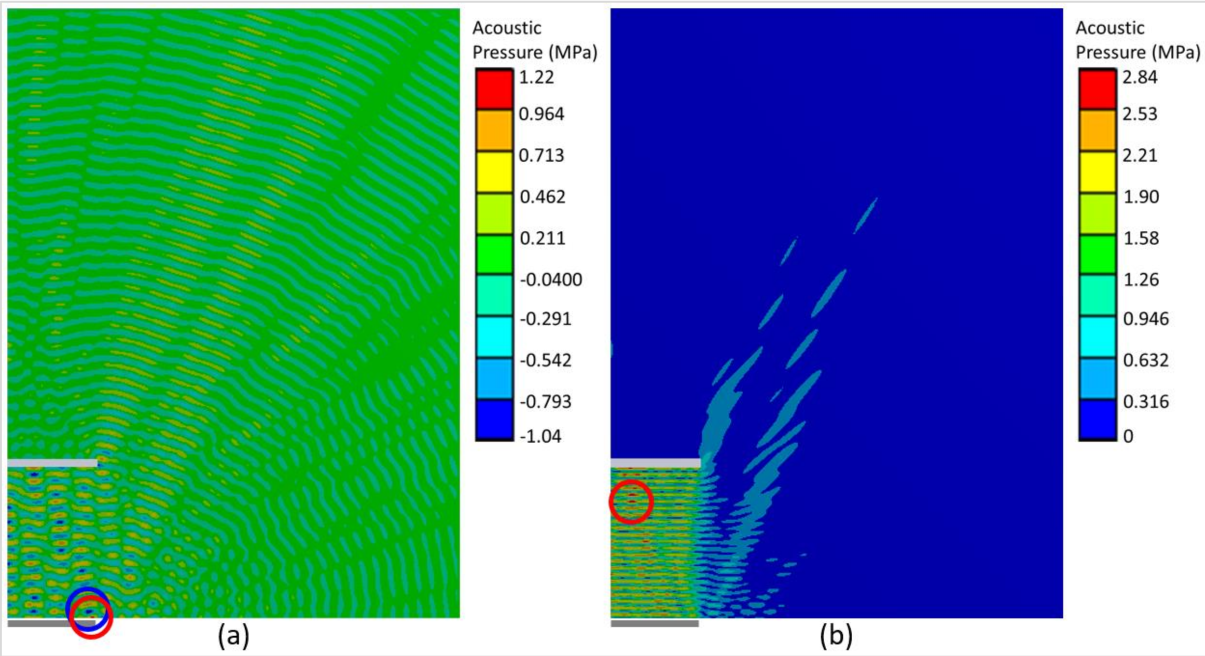

Figure 61: Acoustic pressure field for model with plate thickness of 0.2cm: (a) amplitude: off and (b) amplitude: on

The maximum positive and negative pressure located on the outermost transducer radiation surface. Maximum pressure amplitude is located at a short distance in front of the plate reflecting surface. The acoustic pressure past the plate from transmitted wave and diffracted wave is less apparent compared to when 0.4cm thick plate is used.

Plate thickness is set to twice the default thickness. Figure 62 shows acoustic pressure field for model with plate thickness of 0.8cm.

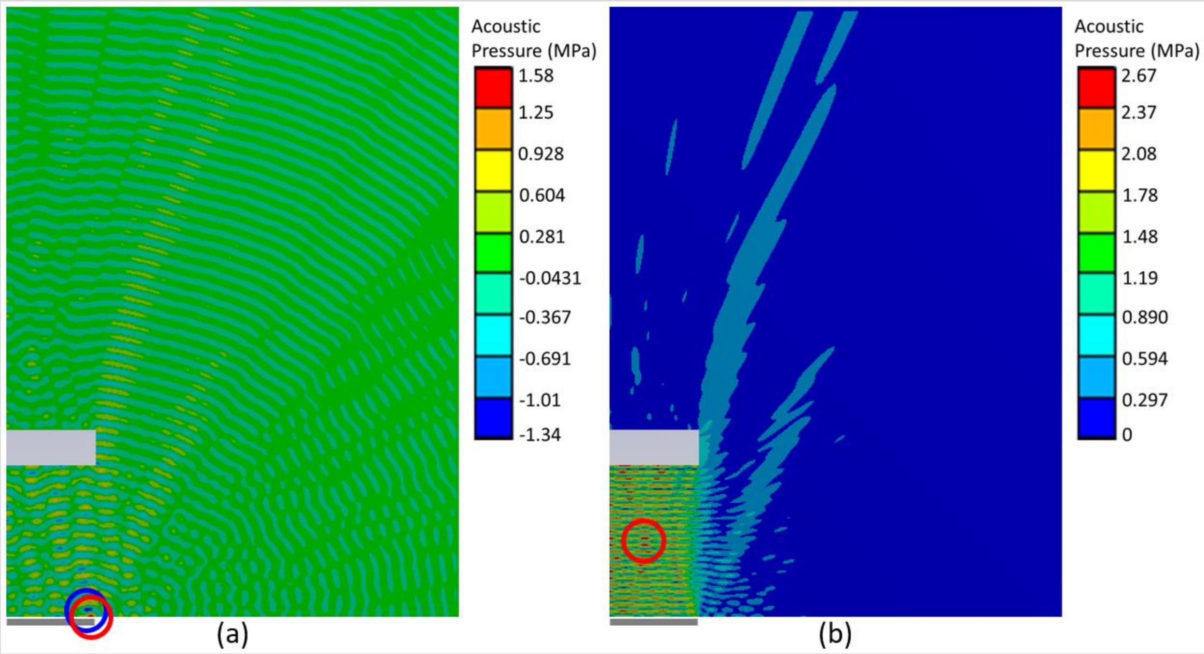

Figure 62: Acoustic pressure field for model with plate thickness of 0.8cm: (a) amplitude: off and (b) amplitude: on

The maximum positive and negative pressure are located on the outermost transducer radiation surface. Maximum pressure amplitude is located in between the plate and transducer at an approximately equal distance. The acoustic pressure past the plate from transmitted wave and diffracted wave is more apparent compared to when 0.4cm thick plate is used.

Plate thickness is set to four times the default thickness. Figure 63 shows acoustic pressure field for model with plate thickness of 1.6cm.

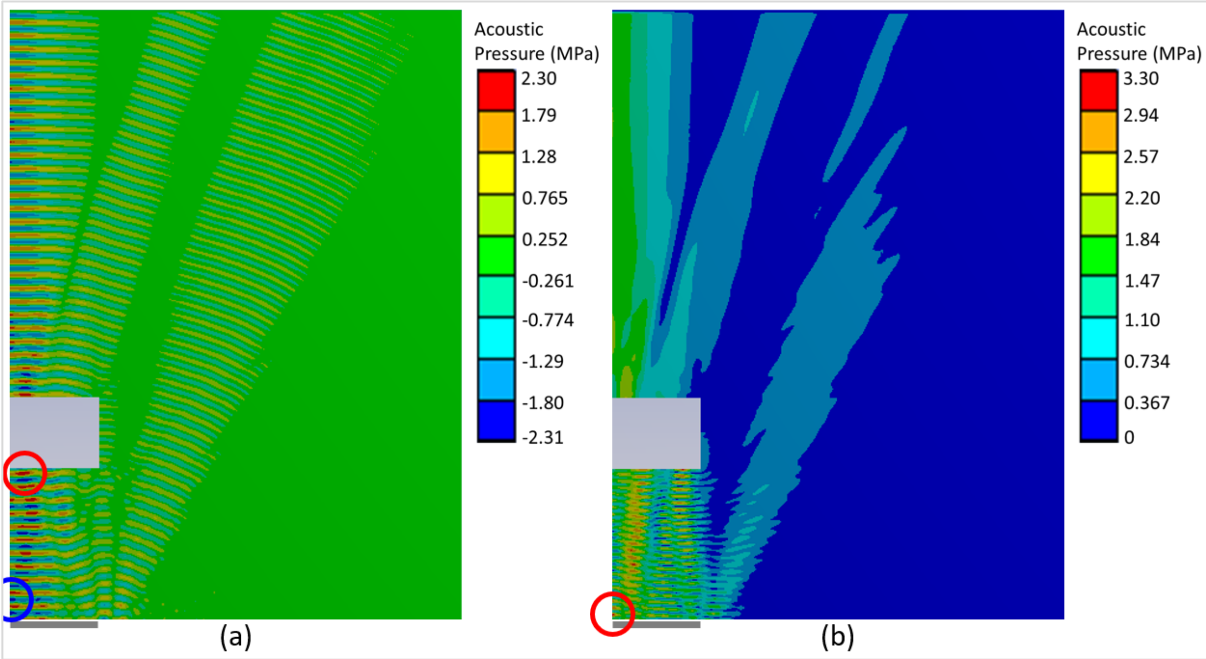

Figure 63: Acoustic pressure field for model with plate thickness of 1.6cm: (a) amplitude: off and (b) amplitude: on

This model shows distinct behaviour compared to models with thinner plate. The maximum pressures are notably higher. The maximum positive pressure is located at the middle area of plate reflecting surface while the maximum negative pressure is located at the middle and in front of transducer. Large portion of the waves are transmitted through the plate and produces radiation beam.

Figure 64 shows graph of maximum acoustic pressure against plate thickness.

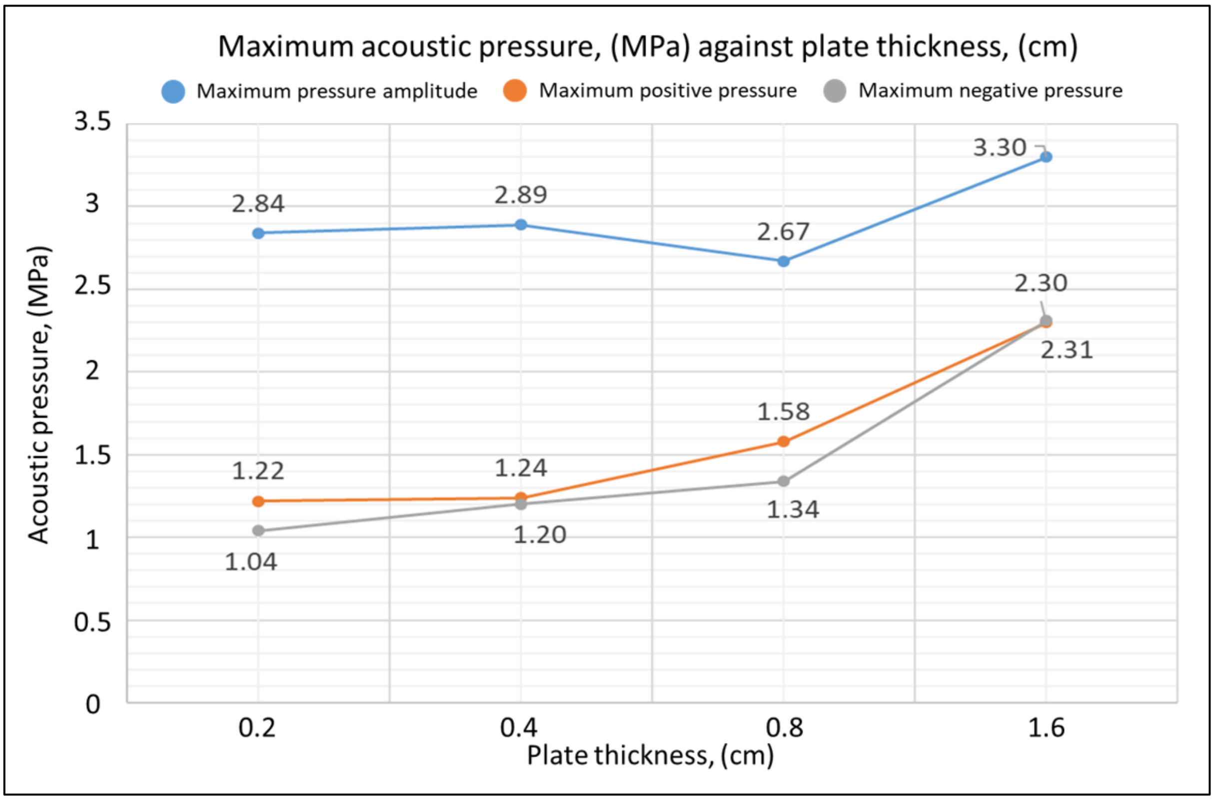

Figure 64: Graph of maximum acoustic pressure, (MPa) against plate thickness, (cm)

From the graph, the maximum positive and negative pressure increases with thicker plate. For maximum pressure amplitude, the pressure initially increases slightly from 2.84MPa to 2.89MPa. When the plate thickness is increased to 0.8cm, the maximum pressure amplitude decreases to 2.67MPa. When the plate thickness is increased to 1.6cm, the maximum pressure amplitude rose to 3.30MPa.

6.4 Discussion and Recommendation

Acoustic pressure field obtained by the model without plate shows that pressure wave is generated from most of the surface of the transducer and it produces areas of high pressures via constructive interference. The number of areas of amplified pressure waves reduces and the intensity of pressure amplification increases as it reaches the end of the vertical length of the model. This shows that it produces near-field radiation according to theoretical near-field radiation calculation. The maximum pressure amplitude is located at a high-pressure area before the pressure waves fully converged. If the model is slightly extended, the maximum pressure is expected to be in the fully converged high pressure area. This is because the location of maximum pressure is right after the near-field radiation distance according to the near field radiation theory.

With plate added into the simulation model, the wave from the transducer is reflected. Since the bottom of the model does not have PML to absorb the wave, it is then reflected back to the plate and this continues until the wave spreads beyond the plate length. This situation reproduces the case setup shown in Figure 1 to a certain extent since the transducer is placed very close to the water container and the container does reflects wave due to impedance difference.

For the model without plate, the acoustic pressure field produced when amplitude option is turned off and turned on shows similarity in the maximum pressure magnitude and location between the two acoustic pressure field results. This is not the case for models with plate since there is noticeable difference between magnitude and location of the maximum pressures. The location of the maximum pressure amplitude in particular is unpredictable which makes the process to produce a proper conjecture for this situation challenging.

Most of the results shows maximum positive and negative pressure on the outermost transducer radiation surface. The reflection of waves disrupts the waves convergence process. Therefore, the area of maximum positive and negative pressure should be on the radiation surface where the effect of wave disruption is negligible since it is where the wave is produced. Along the radiation surface, the outermost area produces the highest pressure, and this can be confirmed by inspecting the acoustic pressure on the outermost transducer radiation surface in Figure 3. For this reason, the maximum positive and negative pressure are located on or at least close to the outermost transducer radiation surface.

When plate length is set to half the default length, the plate length is also half of the transducer diameter. The result shows diffracted waves that converge and forms radiation beam. For models with plate of equal length or longer than the transducer diameter, there is wave diffraction, but the waves does not converge to form radiation beam. For plate of at least equal length to the transducer diameter, wave transmission through the plate becomes less across the plate length and there is less wave diffraction with longer plate. For plate that is twice the length of transducer diameter, there is an apparent area of negligible wave transmission in between plate centre area and plate side edge which is the shadow zone. When plate of 16cm length is set, the shadow zone is larger. This means that the shadow zone area increases with longer plate.

Comparing plate with 0.2cm, 0.4cm and 0.8cm thickness, acoustic pressure field obtained shows that the wave diffraction caused by these plates are similar. The pressure field also shows that acoustic pressure past the plate from transmitted wave and diffracted wave is more apparent with increasing plate thickness. This means that there is more area of relatively high pressure when only the area past the plate is considered. This is indicated in the acoustic pressure field (amplitude: on) results with light blue. When a plate of 1.6cm thickness is set, the acoustic pressure field obtained is very different to all other models in this case study. Large portion of the waves are transmitted through the plate and produces radiation beam. Maximum positive and negative pressure are not located on the outermost transducer radiation surface because of this. From the result of this model, it is conjectured that waves transmission through the plate increases with plate thickness.

From this case study, it is recommended to do the analysis with more models with varied length and thickness to better analyse the waves and pressure behaviour. With more data, transition point of discussed behaviours can be determined. Two notable transition point that can be analysed is when wave diffraction starts to converge to form radiation beam and when wave transmission through the plate is enough to form radiation beam and notably change the wave behaviour between the plate and transducer. Another transition point to be considered is when shadow zone is effectively formed. It is also recommended to do the analysis with plate in the far-field radiation so that it can be compared with results of plate in the near-field radiation to provide insights on discussed behaviour.

7 CONCLUSION AND RECOMMENDATION

7.1 Conclusion

The aim for this thesis was to develop simulation of acoustic pressure field generated by ultrasonic transducers using ANSYS Workbench to obtain accurate data of the resulting flow and pressure fields for steady state ultrasonic excitations. Simulation methodology that focuses on producing accurate and efficient simulation was developed from reviewing literatures and was used to replicate results from literatures for validation purpose. An arbitrary experimental setup is then simulated to investigate acoustic pressure field. Through these processes, the following deductions are made regarding accuracy and efficiency of simulation:

- Computational resource usage and computation time increases with higher number of degrees of freedom (DOF) of nodes involved in solving process. This means that both increase of elements and coupled elements of a model increases computational resource and computation time required to solve it.
- Mesh quality should be prioritised, and the element size should follow the meshing guidelines to ensure accurate results. Quality of a mesh is governed by the shape and size of meshed elements. If there is distortion and non-uniformity of the shape of meshed elements, accuracy of results is compromised even with further reduction of element size.
- Boundary conditions of experimental setup should be identified or assumed correctly before translating it to simulation using the right method to ensure feasibility of simulation results. This shows the importance of understanding the experiment and knowing the right simulation methods.
- Simple simulation model is better than complex model in both result accuracy and computation time when there is insufficient information on the case to be simulated. Model should be designed to only have the boundary of interest and excitation source instead of the whole system.
- Model reduction via plane/axis of symmetry and use of 2D/2.5D models should be prioritised as it can produce accurate result but with substantially lower computation time as opposed to full 3D model. However, viability of these models should always be tested by comparing it to experimental result before proceeding with the intended research.

Overall, the simulation methodology made is beneficial to produce efficient simulation that can be used for investigation of acoustic pressure field generated by ultrasonic transducers. From the deductions, meshing techniques to ensure good mesh quality should be incorporated into the simulation methodology. With proper improvisation, the simulation methodology can potentially be used as a basis to simulate acoustic pressure field of a more complex setting.

7.2 Recommendation for Future Work

Recommendations on project executions and simulation improvements are made for future work related to acoustic simulation involving ultrasonic excitations. When beginning the project, learn using the chosen simulation software and the simulation methods for the software by referring to books on acoustic analysis that uses the same software and tutorials provided by the software company. Research papers is not a suitable platform to learn simulation. It is useful for discovering and comparing simulation methods when there is adequate knowledge on simulation. When doing simulation, ensure that the software license allows adequate nodes use. It is preferable to have license that allows unlimited nodes since simulation involving ultrasonic frequency uses large number of nodes. In doing research, consider doing simulation and experiment simultaneously. This helps in understanding the boundary condition of the experiment and translating it to simulation. This also allows two-way verification that can improve both the experiment and the simulation. To ensure optimum simulation model, meshing technique should be improved for better mesh quality and mesh optimisation. Mesh optimisation is made by refining mesh on area with high load and stress concentration. For area with minimal load and stress concentration, the mesh should be coarsened instead whilst still ensuring that it is within the size recommended by the meshing guidelines. Convergence test can be considered, to find optimum element size and result accuracy ratio. Convergence test can be done by incrementally increasing the element size and observing the result of interest converges to an approximate value. With this thesis used as the foundation, the scope can be broadened by considering transient analysis and extensive use of APDL commands. Transient excitation is closer to most real-life ultrasonic transducer application and APDL commands offers more simulation options and better simulation control.

REFERENCES

[1] J. F. Tressler, "Piezoelectric Transducer Designs for Sonar Applications," in *Piezoelectric and Acoustic Materials for Transducer Applications*, Washington, Springer Science & Business Media, 2008, p. 217.

[2] M. Toda and M. Thompson, "Novel Multi-Layer Polymer-Metal Structures For Use in Ultrasonic Transducer Impedance Matching and Backing Absorber Applications," *IEEE Transactions on Ultrasonics, Ferroelectrics, and Frequency Control*, vol. 57, no. 12, pp. 2818-2827, 2010.

[3] "Radiated Fields of Ultrasonic Transducers," [Online]. Available: https://www.nde-ed.org/EducationResources/CommunityCollege/Ultrasonics/EquipmentTrans/radiatedfields.htm. [Accessed 2018].

[4] V. Natarajan, R. Padmakumar and J. C. Vinod, "Calibration Of Underwater Electro-Acoustic Transducers In The Nearfield," in *Proceedings of the International conference on SonarSensors of Systems*, Thrikkakara, 2002.

[5] K. G. Foote:, "Discriminating between the nearfield and the farfield of acoustic transducers," *The Journal of the Acoustical Society of America*, vol. 136, no. 4, pp. 1511-1517, 2014.

[6] M. V. Brook, "Straight Beam Spherical Focused Probe Design," in *Ultrasonic Inspection Technology Development and Search Unit Design*, New Jesey, John Wiley & Sons, 2012, p. 231.

[7] A. Nowicki, T. Kowalewski, W. Secomski and J. Wojcik, "Estimation of acoustical streaming: theoretical model, Doppler measurements and optical visualisation," *European Journal of Ultrasound*, vol. 7, pp. 73-81, 1998.

[8] L. K. Zarembo, "Acoustic Streaming: Introduction," in *High-Intensity Ultrasonic Fields*, New York, Springer Science & Business Media, 1971, pp. 137-140.

[9] K. Rajdeo, C. Ashish, G. M. Kumar, K. K. Kumar and B. Jitendra, "Screening the Effect of Ultrasonic Wave on Effluent Treatment," *Journal of Bioremediation & Biodegradation*, 2015.

[10] F. Yu, Y. Takuya and K. Sergey, "Cavitation and acoustic streaming generated by different sonotrode tips," *Ultrasonics - Chemistry,* vol. 48, pp. 79-87, 2018.

[11] M. G. Sirotyuk, "Experimental Investigations of Ultrasonic Cavitation," in *High-Intensity Ultrasonic Fields,* New York, Springer Science & Business Media, 1971, pp. 260-284.

[12] H. Lais, P. S. Lowe, T. Gan and L. C. Wrobel, "Numerical modelling of acoustic pressure fields to optimize the ultrasonic cleaning technique for cylinders," *Ultrasonics - Sonochemistry,* vol. 45, pp. 7-16, 2018.

[13] K. Yasui, "Acoustic Cavitation," in *Acoustic Cavitation and Bubble Dynamics,* Cham, Springer International Publishing, 2018, pp. 1-35.

[14] C. E. Brenne, Cavitation and Bubble Dynamics, Pasadena: Cambridge University Press, 2013.

[15] K. Yasui, Y. Iida, T.Tuziuti, T.Kozuka and A.Towata, "Strongly interacting bubbles under an ultrasonic horn," *Physical Review E,* vol. 77, 2008.

[16] W. Joe, "What is acoustic impedance and why is it important?," [Online]. Available: https://newt.phys.unsw.edu.au/jw/z.html. [Accessed 2019].

[17] L. M. Brekhovskikh and O. A. Godin, "Reflection at the Interface of Two Homogenous Media," in *Acoustics of Layered Media I: Plane and Quasi-Plane Waves,* New York, Springer Science & Buiness Media, 2012, pp. 19-24.

[18] Olympus Australia Pty Ltd, "Ultrasonic Transducers Technical Notes," Olympus NDT, 2006.

[19] ANSYS, Inc., "2.1. Elements Used in an Acoustic Analysis," [Online]. Available: https://ansyshelp.ansys.com/account/secured?returnurl=/Views/Secured/corp/v191/ans_acous/acous_tools_elements.html. [Accessed 2019].

[20] C. Q. Howard and B. S. Cazzolato, "2.7 Element Types in ANSYS for Acoustic Analyses," in *Acoustic Analyses Using MATLAB and ANSYS*, Boca Raton, CRC Press, 2015, pp. 22-31.

[21] C. Q. Howard and B. S. Cazzolato, “8.2 Wave-Absorbing Conditions,” in *Acoustic Analyses Using MATLAB and ANSYS*, Boca Raton, CRC PRESS, 2015, pp. 431-438.

[22] J. Kim and H. S. Kim, “Finite element analysis of piezoelectric underwater transducers for acoustic characteristics,” *Journal of Mechanical Science and Technology*, vol. 23, pp. 452-560, 2009.

[23] ANSYS, Inc., “7.2. Absorbing Boundary Condition (ABC),” [Online]. Available: https://ansyshelp.ansys.com/account/secured?returnurl=/Views/Secured/corp/v191/ans_acous/acous_bc_abc.html. [Accessed 2019].

[24] ANSYS, Inc., “7.3. Artificially Matched Layers,” [Online]. Available: https://ansyshelp.ansys.com/account/secured?returnurl=/Views/Secured/corp/v191/ans_acous/acous_artificial.html. [Accessed 2019].

[25] W. Tangsopha, J. Thongsri and W. Busayaporn, “Simulation of Ultrasonic Cleaning and Ways to Improve the Efficiency,” in *5th International Electrical Engineering Congress*, Pattaya, 2017.

[26] G. Massimino, A. Colombo, L. D. Alessandro, F. Procopio, R. Ardito, M. Ferrera and A. Corigliano, “Multiphysics modelling and experimental validation of an air-coupled array of PMUTs with residual stresses,” *Journal of Micromechanics and Microengineering*, vol. 28, 2018.

[27] M. W. Nygren, “Finite Element Modeling of Piezoelectric Ultrasonic Transducers,” Norwegian University of Science and Technology Department of Electronics and Telecommunications, 2011.

[28] ANSYS, Inc., “9.1. Matrix-Coupled FSI Solutions,” [Online]. Available: https://ansyshelp.ansys.com/account/secured?returnurl=/Views/Secured/corp/v191/ans_acous/matrixcoupfsi.html. [Accessed 2019].

[29] C. Q. Howard and B. S. Cazzolato, “2.4 Fluid-Structure Interaction,” in *Acoustic Analyses Using MATLAB and ANSYS*, Boca Raton, CRC Press, 2015, pp. 13-17.

[30] C. Q. Howard and B. S. Cazzolato, “2.3 Pressure-Formulated Acoustic Elements,” in *Acoustic Analyses Using MATLAB and ANSYS*, Boca Raton, CRC Pres, 2015, p. 13.

[31] ANSYS, Inc., “Introduction to Acoustics,” 2017.

[32] C. Q. Howard and B. S. Cazzolato, “2.11 Mesh Density,” in *Acoustic Analyses Using MATLAB and ANSYS*, Baco Raton, CRC Press, 2015, pp. 87-90.

[33] P. Langer, M. Maeder, C. Guist, M. Kraust and S. Marburg, “More Than Six Elements Per Wavelength: The Practical Use of Structural Finite Element Models and Their Accuracy in Comparison with Experimental Results,” *Journal of Computational Acoustics*, vol. 25, no. 4, 2017.

[34] C. Q. Howard and B. S. Cazzolato, “2.12 Use of Symmetry,” in *Acoustic Analyses Using MATLAB and ANSYS*, Boca Raton, CRC Press, 2015, pp. 90-99.

[35] E. Madenci and I. Guven, The Finite Element Method and Applications in Engineering Using ANSYS, Boston: Springer, 2015.

[36] J. Kim and E. J, “Finite element analysis for acoustic characteristics of a magnetostrictive transducer,” *Smart Materials and Structures*, vol. 14, 2005.

[37] M. Odabaee, M. Odabaee, M. Pelekanos, G. Leinenga and J. Gotz, “Modeling ultrasound propagation through material of increasing geometrical complexit,” *Ultrasonics*, vol. 90, pp. 52-62, 2018.

[38] ANSYS, Inc., “Chapter 33: Analysis of a Piezoelectric Flextensional Transducer in Water,” [Online]. Available: https://ansyshelp.ansys.com/account/secured?returnurl=/Views/Secured/corp/v191/ans_tec/tecxducer.html. [Accessed 2019].

[39] I. ANSYS, “ANSYS Piezoelectric material data for the Piezoelectric and MEMS ACT Extension,” 2017.

[40] C. Q. Howard and B. S. Cazzolato, “8.4 Example: Radiation of a Baffled Piston,” in *Acoustic Analyses Using MATLAB and ANSYS*, Baco Raton, CRC Press, 2015, pp. 459-510.

[41] W. Tangsopa and J. Thongsri, “Development of an industrial ultrasonic cleaning tank based on harmonic response analysis,” *Ultrasonics*, vol. 91, pp. 68-76, 2019.

APPENDIX

A. Comparison between results of reduced models and experiment by Massimino et al [26].

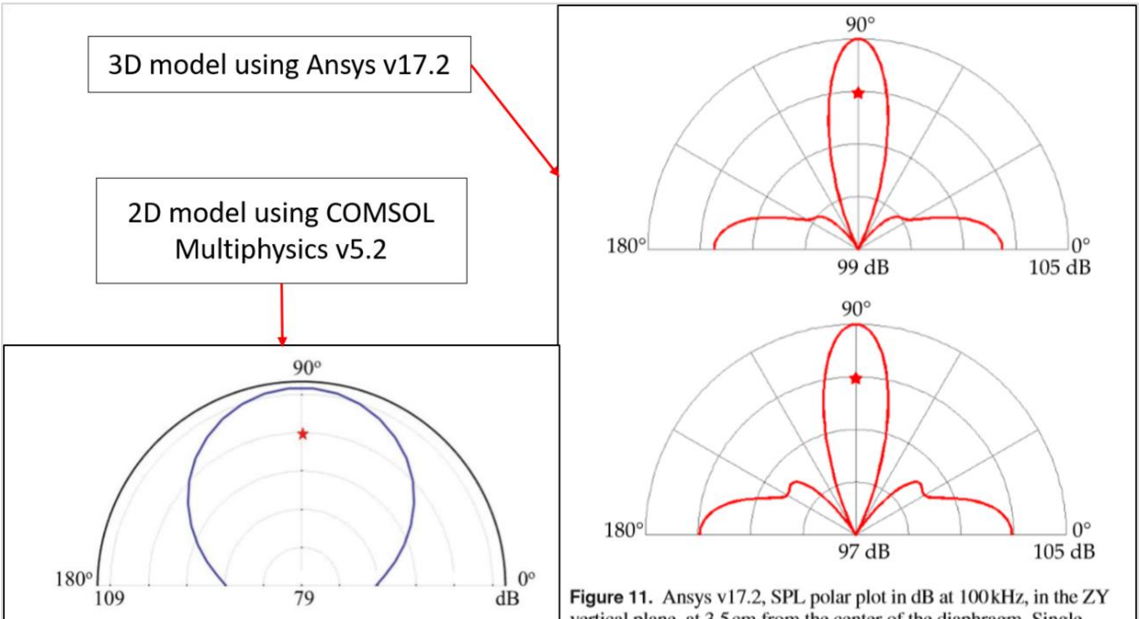

Figure 10. COMSOL Multiphysics v5.2, SPL polar plot in dB at 100 kHz, in the vertical plane, at 3.5 cm from the center of the diaphragm. The experimental result is highlighted (red star).

Figure 11. Ansys v17.2, SPL polar plot in dB at 100 kHz, in the ZY vertical plane, at 3.5 cm from the center of the diaphragm. Single transducer belonging to the silicon dye surrounded by the fluid (above), single transducer belonging to the silicon dye in the operating configuration (below); the experimental result is highlighted (red star).

B. Comparison between results of model using unsymmetrical FSI matrix equation and model using symmetrical FSI matrix equation by Howards and Cazzolato [29].

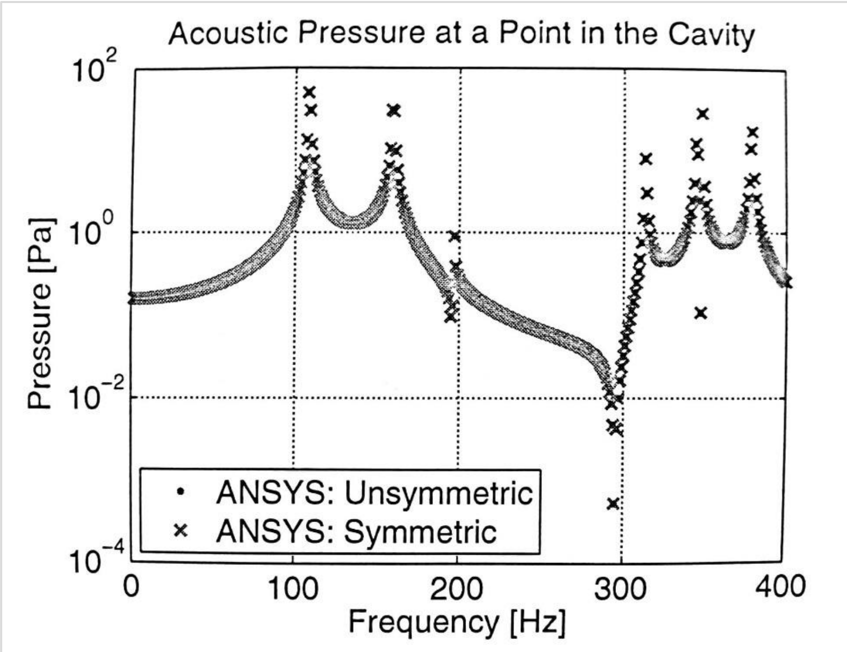

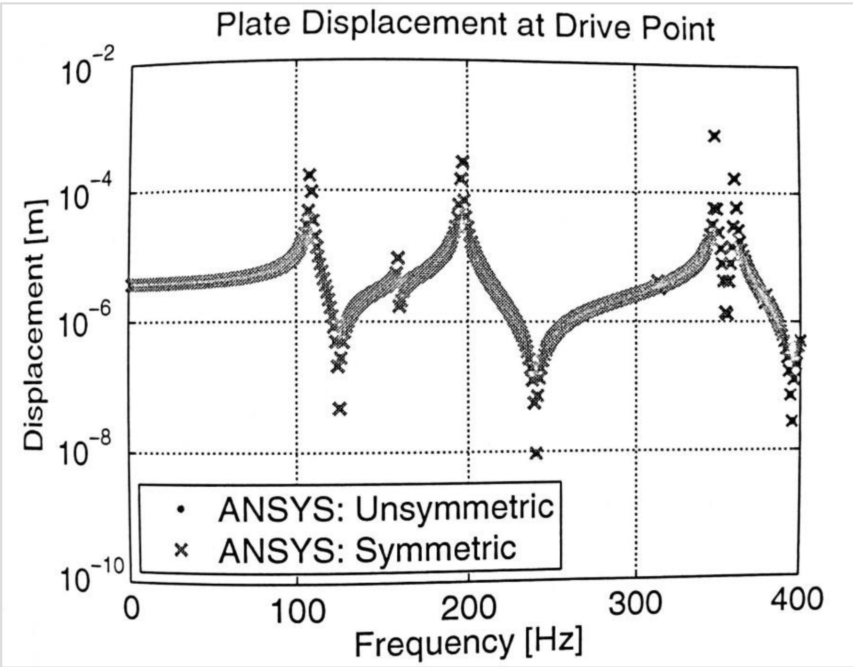

C. Validity test of recommended EPW by Nygren [27].

S	w [μm]	t_{load} [μm]	m1,max [μm]	m1,min [μm]	m2,max [μm]	m2,min [μm]	El	DOF
1	2500	2000	20	0.04	40	0.08	21018	56282
2	1000	1000	20	0.04	40	0.08	5039	15861
3	500	500	20	0.04	40	0.08	1734	6416
4	200	200	20	0.04	40	0.08	485	2213
5	100	100	20	0.04	40	0.08	222	1120
6	50	50	20	0.04	40	0.08	161	879
7	50	50	10	0.02	20	0.04	382	2152
8	50	50	5	0.01	10	0.02	1317	7397
9	50	50	2	0.005	5	0.01	7405	41989
10	50	50	5	0.01	5	0.01	1638	8060

Table 4.3: Parameters that are varied in the simulations and their values. S = simulation number, w = width of model, $t_{load} = t_{PML}$ = thickness of load layer or PML, m1,max & m1,min = maximum and minimum element sizes for mesh in domain 1 and 2, m2,max & m2,min = maximum and minimum element sizes for mesh in domain 3 and 4, El = number of elements, DOF = degrees of freedom.

S	MAE_{Yreal} [S/m^2]	MAE_{Yimag} [S/m^2]	MAE_{Httabs} [μm/(s*V)]	$MAE_{Httangle}$ [degrees/1000]
1	2.383	1.817	22.36	258.3
2	2.372	1.856	24.34	310.6
3	2.347	1.767	22.30	279.0
4	3.362	2.900	34.76	274.2
5	6.364	5.972	62.87	333.7
6	9.404	8.902	90.06	403.8
7	9.386	8.814	88.77	395.6
8	2.313	1.689	21.27	222.8
9	2.161	1.557	10.98	206.4
10	2.161	1.558	10.97	206.4

Table 4.4: Mean average errors for the simulations listed i 4.3.

D. Validity test of recommended EPW by Langer et al [33].

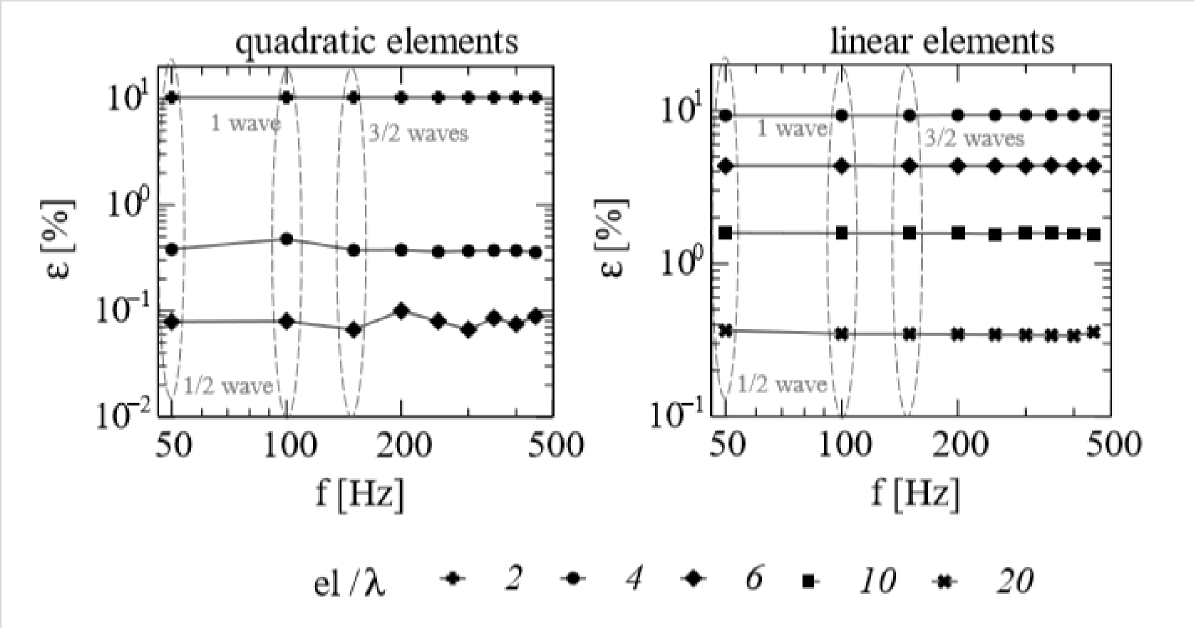

E. Comparison between results of full model and quarter model made using ANSYS 14.5 by Howard and Cazzolato [34].

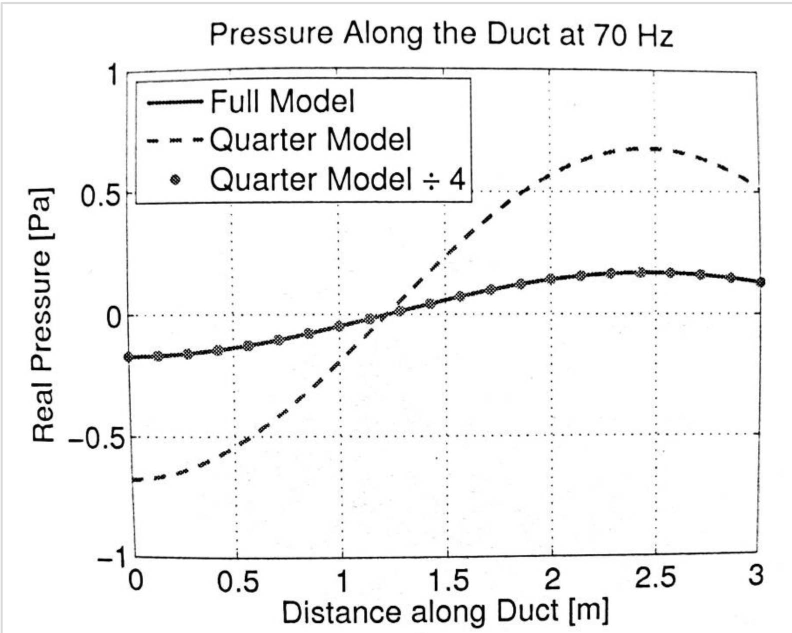

F. Comparison between results of full model, half model and quarter model made using ANSYS 19.1.

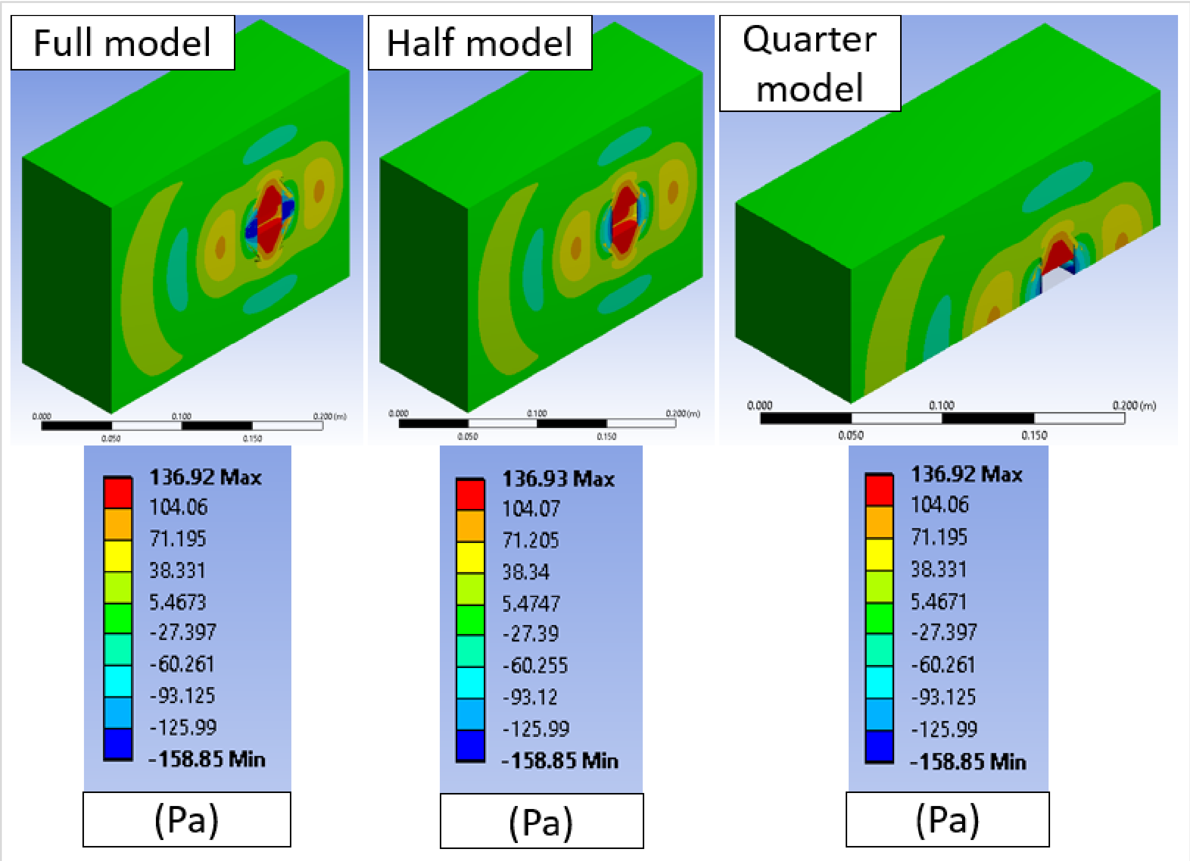

G. Interface of engineering data in ANSYS Workbench.

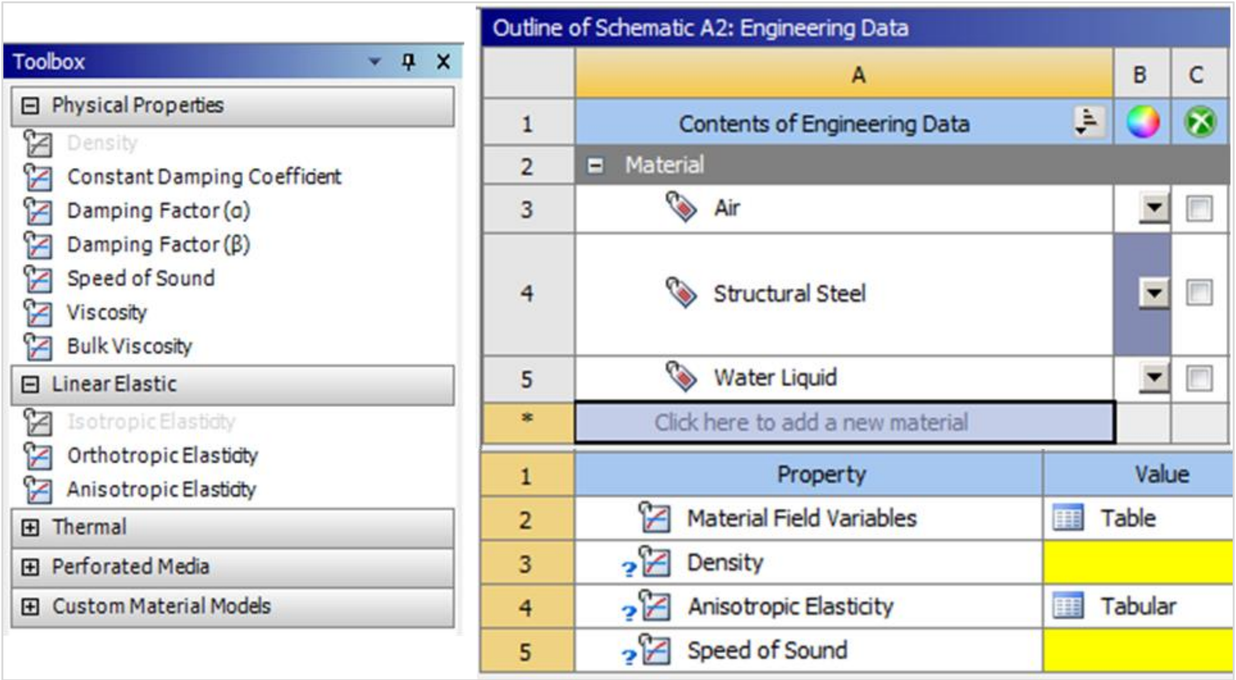

H. APDL Commands and argument inputs used in baffled piston model by Howard and Cazzolato [40].

```
! Attach these commands to the solid part under geometry
! where the freefield_body is the large semi-infinite region.


!------------------------------------------------
! Units are m, kg
!
! In the Details view, under "Input Arguments",
! please enter the following:
!
! ARG1 = density
! ARG2 = speed of sound
!------------------------------------------------

!------------------------------------------------
! change to acoustic element (purely acoustic)
!------------------------------------------------
! Standard acoustic element, no structure
ET,MATID,FLUID29
KEYOPT,MATID,2,1          ! 1= structure absent, 0=structure present
KEYOPT,MATID,3,1          ! 1=axi symmetric, 0=planar


!------------------------------------------------
! define material properties
!------------------------------------------------
MPDELE,ALL,MATID
MP,DENS,MATID,ARG1
MP,SONC,MATID,ARG2
MP,MU  ,MATID,1
```

Input Arguments	
ARG1	1.21
ARG2	343.

```
! Attach these commands to the solid part under geometry
! where the piston_body is the small piston region.

!-----------------------------------------------------
! Units are m, kg
!
! In the Details view, under "Input Arguments",
! please enter the following:
!
! ARG1 = density
! ARG2 = speed of sound
!-----------------------------------------------------

!-----------------------------------------------------
! change to acoustic element (with displacement DOFs)
!-----------------------------------------------------
! Standard acoustic element, no structure
ET,MATID,FLUID29
KEYOPT,MATID,2,0        ! 1= structure absent, 0=structure present
KEYOPT,MATID,3,1        ! 1=axi symmetric, 0=planar

!-----------------------------------------------------
! define material properties
!-----------------------------------------------------
MPDELE,ALL,MATID
MP,DENS,MATID,ARG1
MP,SONC,MATID,ARG2
MP,MU  ,MATID,1
```

Input Arguments	
ARG1	1.21
ARG2	343.

```
! Attach these commands to the geometry
! where the radiation_boundary for the outer infinite edge
! on the circumference of the circle.

!-----------------------------------------------------
! Units are m, kg
!
! In the Details view, under "Input Arguments",
! please enter the following:
!
! ARG1 = density
! ARG2 = speed of sound
! ARG3 = baffle_r: Radius of the baffle
!-----------------------------------------------------

!-----------------------------------------------------
! change to infinite acoustic elements
!-----------------------------------------------------
! Infinite element for the circumference
ET,MATID,FLUID129
KEYOPT,MATID,3,1        ! 1=axi symmetric, 0=planar

! Infinite element for the circumference
R,MATID,ARG3,0,0

!-----------------------------------------------------
! define material properties
!-----------------------------------------------------
MPDELE,ALL,MATID
MP,DENS,MATID,ARG1
MP,SONC,MATID,ARG2
MP,MU  ,MATID,1
```

Input Arguments	
ARG1	1.21
ARG2	343.
ARG3	1.

```
! Define these parameters in the Input Arguments
! ARG1 = piston_r

! Select the nodes for the piston only
ALLS
NSEL,S,LOC,Y,0
NSEL,R,LOC,X,0,ARG1      ! ARG1 = piston_r
SF,ALL,FSI,1             ! turn on the FSI flag

! Make the piston move with 1e-6 harmonic amplitude
! If calculating the radiated power, you can define a
! displacement for the piston.
D,ALL,UY,1e-6

! Constrain the U motion so that only UY is allowed
D,ALL,UX

ALLS
```

Input Arguments	
ARG1	0.1

```
!------------------------------------------
! Export the pressure on axis of piston
!------------------------------------------

FINISH

! Change the format of the output listings
! to get rid of header information.
/HEADER,OFF,OFF,OFF,OFF,OFF,OFF
/PAGE,,,100000,1000


! Enter the post-processor
/POST1

!------------------------------------------
! Export the REAL pressure
!------------------------------------------
! Select the first set of results
! and look at the REAL values
SET,     1, 1    ,     ,REAL
NSEL,S,LOC,X,0
/OUTPUT,axis,p_re.txt
PRNSOL,PRES
/OUTPUT

!------------------------------------------
! Export the IMAGINARY pressure
!------------------------------------------
! Select the first set of results
! and look at the IMAGINARY values
SET,     1, 1    ,     ,IMAG
/OUTPUT,axis,p_im.txt
PRNSOL,PRES
/OUTPUT

!------------------------------------------
! write the nodal coordinates
!------------------------------------------
FINISH
/PREP7
NWRITE,axis,node.txt
FINISH
/POST1

ALLS                        ! Select all nodes and elements

FINISH                      ! Exit the post processor
!------------------------------
! End of script
!------------------------------
```

I. Material properties for Test Case 1: Radiation of Baffled Piston.

For 2D, Air (From Book)

$$Density = 1.21kg/m^3$$

$$Speed\ of\ Sound = 343ms^{-1}$$

For 2.5D, Air (ANSYS Default)

	A	B	
1	Property	Value	
2	Material Field Variables	Table	
3	Density	1.225	kg m^-3
4	Isotropic Thermal Conductivity	0.0242	W m^-1 K^-1
5	Specific Heat, C_p	1006.4	J kg^-1 K^-1
6	Speed of Sound	346.25	m s^-1
7	Viscosity	1.7894E-05	kg m^-1 s^-1

For 2.5D, Structural Steel (ANSYS Default)

	A	B	
1	Property	Value	
2	Material Field Variables	Table	
3	Density	7850	kg m^-3
4	Isotropic Thermal Conductivity	60.5	W m^-1 C^-1
5	Specific Heat, C_p	434	J kg^-1 C^-1

For 2.5D, PZT4 Y-Poling

	A	B	
1	Property	Value	
2	Material Field Variables	Table	
3	Density	7500	kg m^-3
4	Anisotropic Elasticity	Tabular	

Table of Properties Row 4: Anisotropic Elasticity

	A	B	C	D	E	F
1	D[*,1] (Pa)	D[*,2] (Pa)	D[*,3] (Pa)	D[*,4] (Pa)	D[*,5] (Pa)	D[*,6] (Pa)
2	1.39E+11					
3	7.4E+10	1.15E+11				
4	7.8E+10	7.4E+10	1.39E+11			
5	0	0	0	2.56E+10		
6	0	0	0	0	2.56E+10	
7	0	0	0	0	0	3.05E+10

J. Material properties, transducer configuration and acoustic pressure field from research article by Tangsopha et al [25]

Domain	***Type***	***Value***
Water)45 C°(	Water density	990.2 kg/m^3
	Acoustic velocity	1,533.5 m/s
	Dynamic viscosity	5.798x10^{-4} kg/m·s
Aluminum alloy	Density	2,770 kg/m^3
	Young's modulus	7.1x10^{10} Pa
	Poisson's ratio	0.33
	Bulk modulus	6.961x10^{10} Pa
	Shear modulus	2.669x10^{10} Pa
Stainless steel	Density	7,750 kg/m^3
	Young's modulus	1.93x10^{11} Pa
	Poisson's ratio	0.31
	Bulk modulus	1.693 x10^{10} Pa
	Shear modulus	7.366x10^{10} Pa
Piezoelectric)PZT4(	Density	7,500 kg/m^3
	Permittivity constant)ε_0(	8.854 x10^{-12} F/m
	Stiffness matrix [c^E] (x10^{10})	c_{11}=c_{22}=13.9, c_{21}=7.78, c_{31}=c_{32}= 7.43, c_{44}=3.06, c_{55}= c_{66} = 2.56 Pa
	Stress matrix [e]	e_{31}= -5.2, e_{33}= 15.1, e_{15}=12.7 C/m^2
	Relative permittivity [ε_r]	$\varepsilon_{r\,11}$ = $\varepsilon_{r\,22}$ = 1,475, $\varepsilon_{r\,33}$ = 1,300

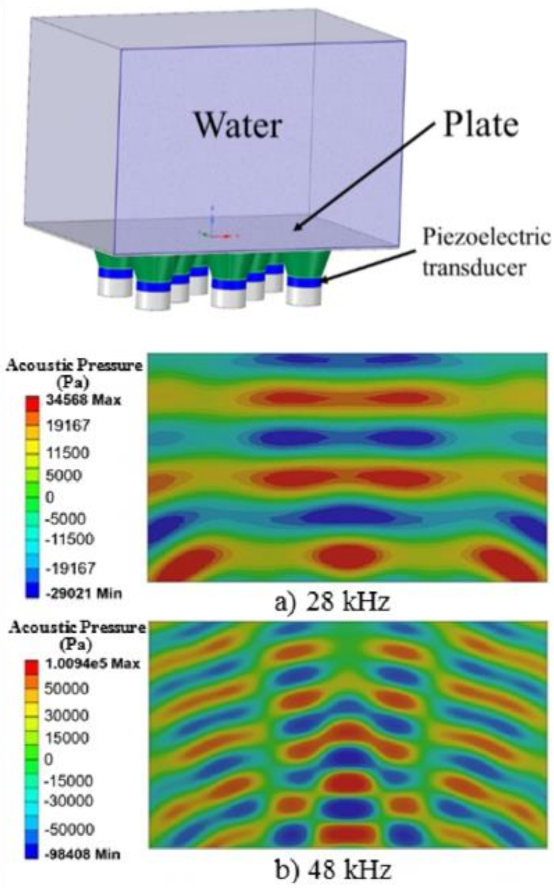

a) 28 kHz

b) 48 kHz

K. Sizing of ultrasonic cleaning tank model by Tangsopa and Thongsri [41].

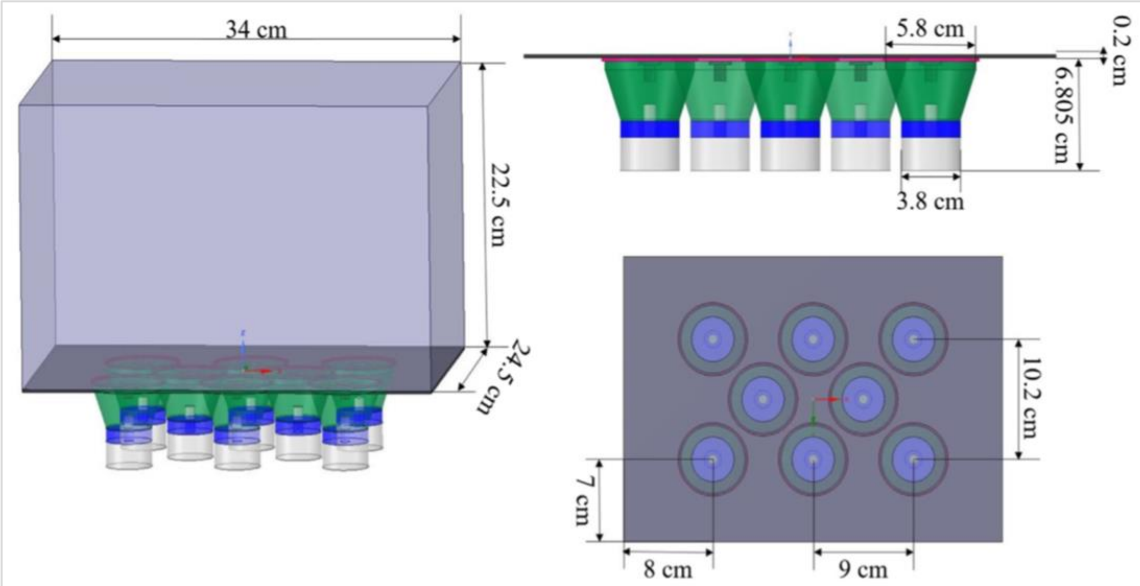

L. Material properties for Case Study: Effect of Plate to Acoustic Pressure Field.

Structural Steel (ANSYS Default)

	A	B	
1	Property	Value	
2	Material Field Variables	Table	
3	Density	7850	kg m^-3
4	Isotropic Thermal Conductivity	60.5	W m^-1 C^-1
5	Specific Heat, C_p	434	J kg^-1 C^-1

Water (ANSYS Default)

	A	B	
1	Property	Value	
2	Material Field Variables	Table	
3	Density	998.2	kg m^-3
4	Isotropic Thermal Conductivity	0.6	W m^-1 K^-1
5	Specific Heat, C_p	4182	J kg^-1 K^-1
6	Speed of Sound	1482.1	m s^-1
7	Viscosity	0.001003	kg m^-1 s^-1